Master's thesis

NTNU
Norwegian University of Science and Technology
Faculty of Engineering
Department of Geoscience and Petroleum

Rashad Nazaraliyev

Numerical Modelling of Liquid-Rich Shale Wells

OGR Oscillations in Highly Undersaturated Fluids

Master's thesis in Petroleum Engineering
Supervisor: Curtis Hays Whitson
June 2020

NTNU
Norwegian University of
Science and Technology

Abstract

The unconventional petroleum resources have attracted significant attention throughout recent years. These resources are estimated to have reserves greater than those of conventional ones. Increasing energy demands and depletion of conventional petroleum have forced the petroleum industry to thoroughly consider these resources.

The shale reservoirs are a common example of unconventional reservoirs. Due to characteristic low permeability, these reservoirs were challenging for production in the past. Advanced hydraulic fracturing and horizontal drilling technologies and techniques, which allowed to increase the conductivity between rock and wellbore, along with associated reduced costs have made these formations develop economically.

Despite the significant attention and interest on shale reservoirs, they have not been fully studied. This work focuses on the characteristic oil-gas ratio behaviour of liquid-rich shale wells that produce liquid-rich fluids (i.e. condensate gas, wet gas, volatile oil). The idea comes from the study SPE155499. In comparison with the analytical solutions, which show constant OGR behaviour for infinite acting period, numerical studies are associated with OGR oscillations. The study analyses the OGR oscillations in highly undersaturated fluids observed in numerical solutions.

This report is divided into several chapters. Section 1 is a literature review for unconventional petroleum resources and, particularly, liquid-rich shale reservoirs. The section introduces definition and classification for unconventional resources and provides general characteristics for the most common unconventional resources. As the liquid-rich shale reservoirs are the focus area of the study, geology and minerology of shales are described in the chapter, which is followed by the detailed discussion about shale reserves (i.e. shale gas and liquid-rich shale reserves). The description of the fluids in LRS reservoirs are also provided. The production challenges in shale reservoirs are also introduced. Finally, a brief explanation of PVT terminology used in the study is given. Section 2 states the objective of the study. Section 3 describes the software tools used in the project. Section 4 is a chapter for the description of the reservoir model. All the necessary data used to create LRS base case well model is provided in this chapter. The results and discussion for the various case studies are given in Section 5. Each case study and associated definition is described in this section. Finally, all the data necessary to set up the simulation is provided in Appendix.

Acknowledgement

This study is the final part of the master's degree program at the department of Petroleum Engineering and Petroleum Geosciences, NTNU, Trondheim, Norway. This work takes the idea from the study SPE155499, PVT in Liquid-Rich Shale Reservoirs by Curtis Hays Whitson, NTNU & Whitson and Snjezana Sunjerga, Whitson to investigate the OGR oscillations in highly undersaturated fluids by modelling of the unconventional ultra-tight liquid-rich shale wells.

As for the study, I would like to express my deep gratitude to my supervisor, Professor Curtis Hays Whitson, who allowed me to have the opportunity of working with him on the project. His knowledge, technical mentorship and most importantly patience, especially during these bizarre days of pandemic Corona, assisted me in understanding the concepts of the study and improve my knowledge in reservoir engineering, specifically unconventional reservoir engineering, in a theoretical and practical aspect. It was my pleasure and honour to have Professor Whitson as my supervisor.

I would like to thank to Coats Engineering Inc. for providing the licence for the Sensor, which is the main tool used throughout the study.

I would like to thank truly to my friend Shamsi who shared such an enjoyable 2-year journey together with me.

Finally, but most importantly, I would like to thank faithfully to my parents, Rauf and Aida, and my brothers, Ravan and Nurlan, for their infinite love, respect and continuous support through the entire life of mine.

Contents

List of Figures

List of Tables

1 Technical Background

1.1 Importance of Unconventional Petroleum Resources

The terminology world energy consumption is defined as the total energy that is produced and exploited by the whole human population. It is normally measured on a year base and covers all energy derived from any energy source. Figure 1.1 summarizes the energy consumption globally from 1990 and the predictions until 2040 in quadrillion BTUs[1]. As the figure shows, the energy consumption has risen from between 1990 and 2020. Hydrocarbons maintain the top levels for energy consumption by source throughout the period analysed. (1) (2)

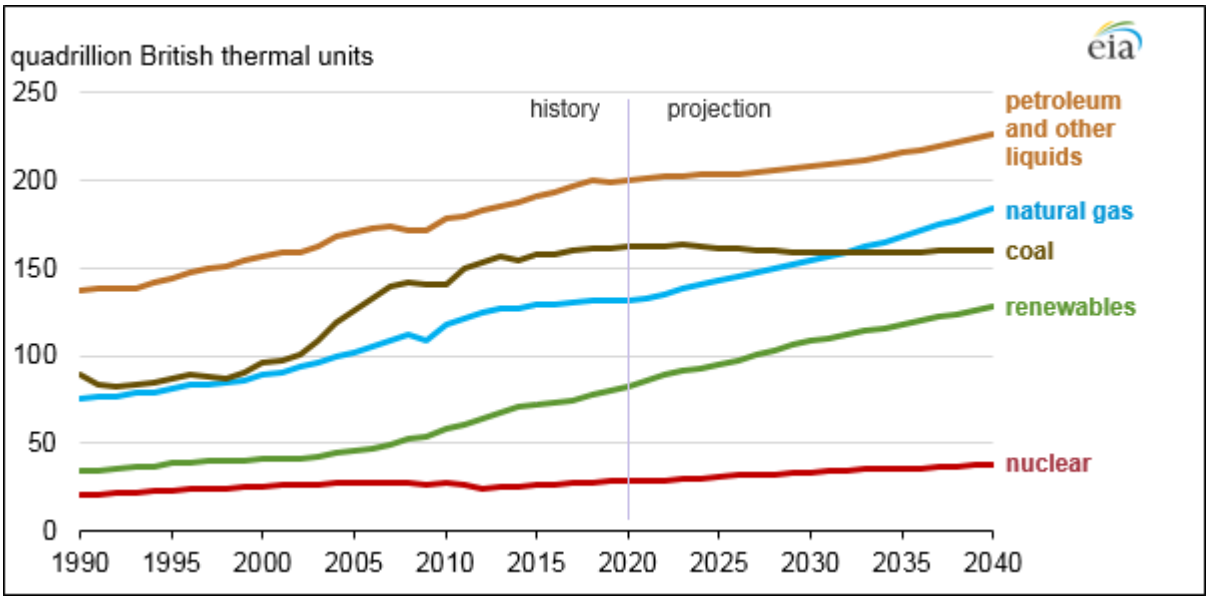

Figure 1.1. Global energy consumption by energy source, modified from (2)

According to US EIA, world energy consumption is expected to increase by approximately one fourth until 2040. (2) Rising demand to meet global energy consumption and the depletion of conventional petroleum resources require access to more petroleum resources.

Unconventional petroleum resources attracted attention in meeting increasing energy demands. Unconventional petroleum is expected to have a huge influence in energy supply. Joe Leimkuhler et al. states the growing demand of global economy to continuous supply of hydrocarbons even though the use of renewables increases. (3) (4)

Shale reservoirs, a form of unconventional petroleum, contribute to significant amount. They are expected to be necessarily greater than conventional reservoirs. (5) The challenge in production from shale reservoirs is the rock permeability, which, in shale reservoirs, are many

[1] 1 British Thermal Unit (BTU) is approximately 1.055 kJ.

times smaller than conventional sandstone or limestone reservoirs. The evolution of hydraulic fracturing, one of the most important stimulation techniques for tight reservoirs, led to advancements in natural gas production in the US. However, smaller permeability results in lower primary liquid recovery, i.e. 5 - 10% of STOIP for tight oil recoveries, although massively fractured long horizontal wells are produced. (6) (7) The enhanced liquid recovery techniques, i.e. huff-n-puff EOR, developed to increase recoveries in tight oil reservoirs gathered enough interest.

This study involves shale reservoirs (i.e. liquid-rich shale reservoirs). Understand the meaning of the terminology unconventional petroleum resources before discussing shale reservoirs in detail is important.

1.2 Unconventional Petroleum Resources

Petroleum resources can be divided into two broad classes, namely, conventional and unconventional resources, based on geology, technology and economy. (8) Phil Chan et al. describe conventional and unconventional resources as follows:

"*Conventional resources exist in discrete petroleum accumulations related to a localized geological structural feature and/or stratigraphic condition (typically with each accumulation bounded by a down-dip contact with an aquifer) that is significantly affected by hydrodynamic influences such as the buoyancy of petroleum in water. The petroleum is recovered through wellbores and typically requires minimal processing prior to sale.*

Unconventional resources exist in hydrocarbon accumulations that are pervasive throughout a large area and that are generally not significantly affected by hydrodynamic influences (also called "continuous-type deposits"). Such accumulations require specialized extraction technology, and the raw production may require significant processing prior to sale." (9)

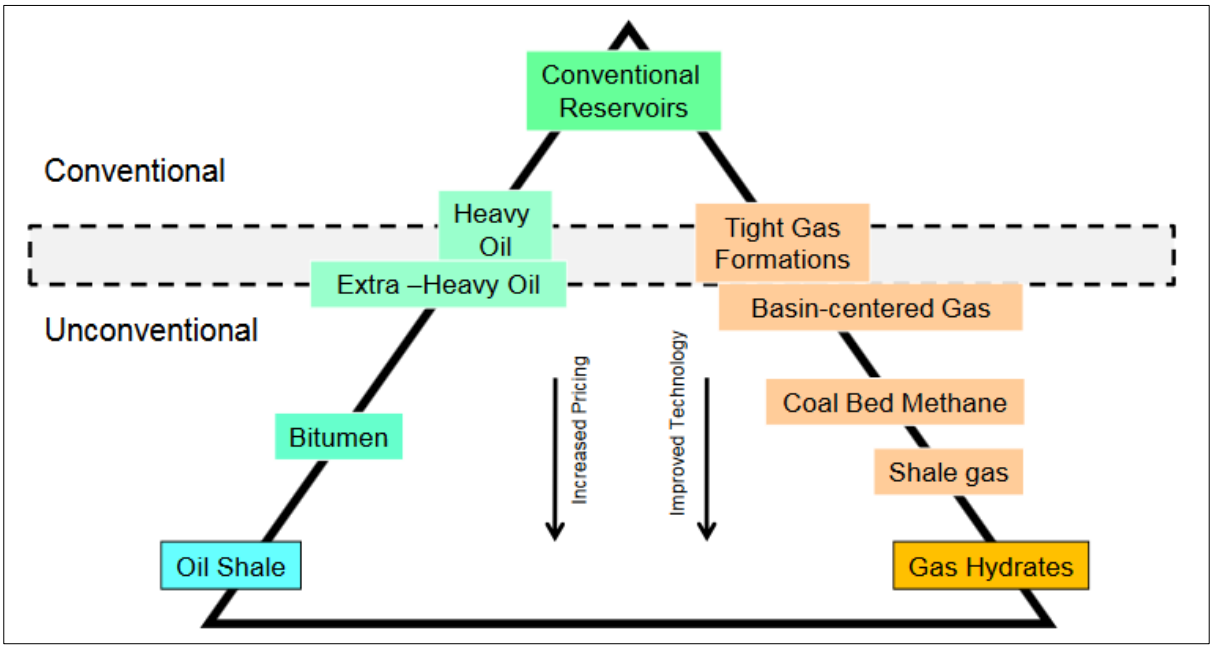

Figure 1.2. Petroleum resource triangle, data from (9)

Conventional petroleum resources are normally anticipated to be cheaper and easier to produce. On contrary, resources classified as unconventional require high technology and or investment than industry-standard levels to be extracted (i.e. require replacing the natural action of geological processes of the petroleum system with extra technology, capital and energy to produce). (10) (11) Figure 1.2 illustrates the resource triangle by Holditch. It becomes challenging to extract the petroleum resources as it goes from top to the bottom of the triangle. Despite the place of heavy oil and tight gas resources in the figure, there are still difficulties in implementing the assessment techniques that are used for conventional resources. (9)

Unconventional petroleum resources are normally characterised by two main indicators and two parameters. The indicators are as follows:

- *"Extensive, continuous distribution of petroleum with no indistinct trap boundaries,*
- *No stable natural industrial production and indistinct Darcy flow."* (8)

The parameters are as follows:

- *"Porosity less than* 10%,
- *Pore-throat diameter less than* 1 *mm (permeability less than* 0.001 *mD)."* (8)

The definition above does not provide information about the different types of unconventional resources. Unconventional resources are normally classified from distinct perspectives such as attributes and characteristics of unconventional resources which include reservoir rock type,

hydrocarbon origin, source-reservoir-cap assemblage, and occurrence state. Table 1.1 illustrates the different types of unconventional petroleum resources. The table also summarizes the classification scheme for different unconventional resources. (11)

Table 1.1. Unconventional petroleum resources classification table, data from (8)

Basis for Classification		Main Types
Reservoir type		Oil/gas tight sandstone, shale oil/gas, CBM, Cate fracture-cavity oil/gas, volcanic reservoir oil/gas, metamorphic reservoir oil/gas
Maturity, density, and viscosity		Oil shale, heavy oil, oil sandstone, shale oil, tight oil, shale gas, coal-derived gas, tight gas
Host and coupling relationship		Liquid/solid coupled (tight oil and gas, shale oil and gas, coal-derived gas), gas/water/solid integrated (natural gas hydrates), gas/water infused (water soluble gas), hydrodynamic barrier (hydrodynamic seal gas)
Oil/gas genesis	Maturity	Thermal-origin, biologic-origin, mixed-origin oil/gas
	Parent material source	Organic-origin, inorganic-origin, mixed-origin oil/gas
Source-reservoir-caprock assemblage	Source-reservoir relationship	Source-reservoir integrated, source-reservoir contacted, source-reservoir separated
	Source-reservoir assemblage	Self-source, self-reservoir oil/gas (CBM, shale oil/gas); nonself-source, self-reservoir oil/gas (tight sandstone oil/gas
	Oil/gas source	Self-source oil/gas (CBM, shale oil/gas), nonself-source oil/gas (tight sandstone oil/gas)
Occurrence state of coalbed methane		Adsorbed, free, mixed
Continuous property		Continuous petroleum accumulation, quasi-continuous petroleum accumulation

The status of unconventional petroleum resources is relative, not uniform, and with the technological and economical evolutions, it may be subject to change. In other words, unconventional resources may later become conventional. (11)

As no uniform and simple classification system is known to describe unconventional resources, different authors attempted to define unconventional resources in different and preferably simple ways. Cander, who is one of these authors, classifies unconventional and conventional petroleum based on the physical properties of rock and in-rock fluids. Certain definitions other than Cander's one are dependent on petroleum system and geological interpretations, and they usually exclude fluid properties. Cander suggested a solution by which the resources could be classified using the rock permeability and fluid viscosity (i.e. the mobility ratio (k/μ) defines unconventional resources). (12) He developed a chart of viscosity versus permeability shown in Figure 1.3.

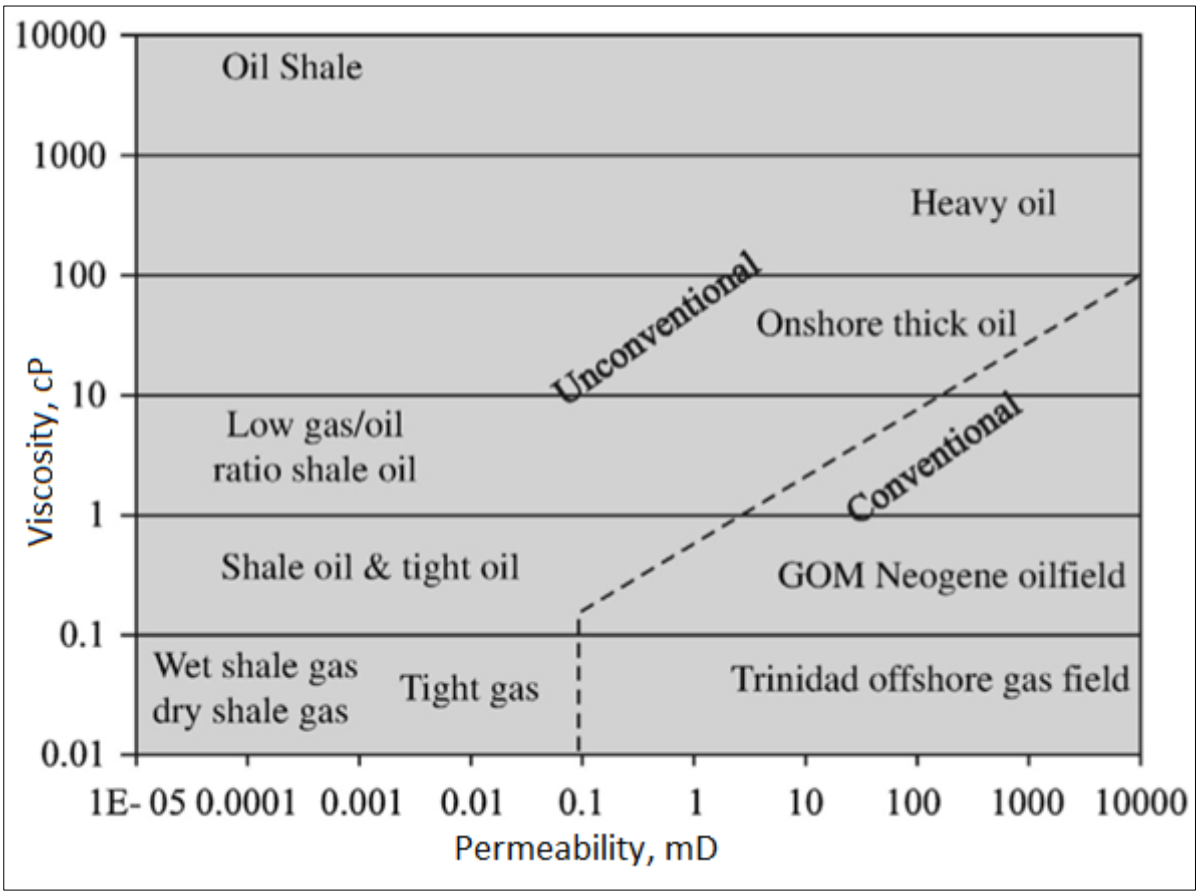

Figure 1.3. Viscosity-permeability characteristics of unconventional petroleum resources, data from (12)

The chart includes different types of unconventional petroleum including shale gas/oil, tight gas/oil, heavy oil. Conventional resources are grouped into the right bottom part, which is

characterised as having low fluid viscosity and high permeability. The unconventional petroleum resources occupy the rest of the chart.

The characteristic low fluid viscosity and high permeability allow conventional petroleum resources to be produced in industrial levels with no changes in rock permeability or fluid viscosity. This can be considered as the main production challenge for unconventional resources. Special techniques and technology are needed to change rock permeability or fluid viscosity to alter permeability-viscosity ratios (i.e. mobility) to provide industrial productivity for the extraction of unconventional petroleum. The problem requires significant investment and advancement in technology to be resolved. (8) (12)

C. H. Whitson also provides similar classification for conventional and unconventional using rock and fluid properties. Table 1.2 summarizes Whitson's classification of the most commonly known 3 types of conventional reservoirs: gas, oil and saturated (gas and oil) reservoirs. Whitson classifies conventional reservoirs as those having rock permeability greater than 0.1 mD and fluid viscosity less than 100 cP. These reservoirs are characterised by single porosity in rock side and high mobility. (13)

Table 1.2. Rock and fluid characteristics of conventional reservoirs

Reservoir Type	Rock	Fluid
Gas (Dry, Wet, Gas Condensate)	$k_h > 0.1$ mD	$\mu < 100$ cP
Oil		
Gas and Oil		

Whitson also provides the characteristics of some commonly known, typical unconventional reservoirs, which are heavy oil, tight reservoirs and coal bed methane summarized in Table 1.3. According to Whitson, petroleum resources can be unconventional either in the rock side or fluid side. (13)

Table 1.3. Rock and fluid characteristics of unconventional reservoirs

Reservoir Type	Rock	Fluid
Heavy Oil (Low P_{ri})	Single porosity k > 1000 mD	μ_o > 1000 – 10000 cP
Tight/Ultra-Tight (4500 < P_{Ri} (high) < 15000 psi)	k ~ 10^{-5} – 10^{-3} mD	μ_o < 1 cP
Coal bed methane	Coal	Adsorbed methane

1.3 Liquid-Rich Shale Reservoirs

1.3.1 Definition of LRS Reservoirs

Shale reservoirs can be considered a type of tight reservoirs for their characteristic low permeability. Tight reservoirs can be either source rocks or reservoir integrated organic rich resources. The terminology source-reservoir-integrated resources applies to all forms of tight reservoirs (i.e. sandstone, limestone oil and gas). (8) The classification used by Canadian Society for Unconventional Resources (CSUR) for tight reservoirs are shown in Table 1.4. The definition, which has been modified from US Energy, groups these reservoirs based on the rock permeability. The first three reservoir types in the table are characterized as tight (i.e. extremely tight, very tight and tight), and they are unconventional resources, while the latter three (i.e. low, moderate, high) are defined as conventional. (14)

Table 1.4. Reservoirs types based on the permeability cut offs, data from (14)

Permeability, mD	Reservoir Type	Rock Type
$0.0001 - 0.001$	Extremely tight	Shale
$0.001 - 0.01$	Very tight	Shale, tight sandstone
$0.01 - 0.1$	Tight	Limestone, tight sandstone
$0.1 - 1$	Low	Limestone, sandstone
$1 - 10$	Moderate	Sandstone
$10 - 100$	High	Sandstone

Note that the definition above for tight resources are based on permeability cut-off, therefore, shale reservoirs are classified as a specific form of tight reservoirs. However, Aguilera et al. define the resources as tight if hydrocarbons are generated in the source rock and migrated into the tight rock. Shale reservoirs are those if hydrocarbons are generated and stored within the shale and are considered a subset of tight formations. (15) (16)

Whitson characterizes tight reservoirs as having permeability normally in the range of 10^{-5} to $10^{-3} mD$, while fluid viscosity being less than $1\ cP$ (i.e. Table 1.3); they are considered unconventional in the rock side. Such reservoirs are characterized by typically high initial reservoir pressures ($P_{ri} > 4500\ psi$). From permeability point of view, Whitson's definition of tight resources corresponds to extremely tight reservoirs, shale reservoirs, in CSUR classification. On the other hand, Whitson et al. do not distinguish between shale and other ultra-tight rock types as they "*find no evidence that key PVT and fluid issues differ substantially*

because of the rock itself". The term "liquid-rich shale" (LRS) is used for any reservoir system which satisfies following two conditions:

- Permeability changing in the range of 10^{-5} *to* $0.001\ mD$,
- More than approximately 25% of revenues come from the oil or condensate sales. (17)

1.3.2 Geology of Shale Reservoirs

According to the Energy Resources Conservation Board (ERCB) of Alberta, Canada, the terminology "shale" stands for a lithostratigraphic unit that has organic content less than 50% by weight. ERCB states that for a unit to be defined as a shale, two conditions need to be followed (18):

- The percentage weight fraction of sedimentary clasts with grain sizes greater than 62.5 micrometres should be less than 10%,
- The percentage weight fraction of sedimentary clasts with grain sizes less than 4 micrometres should be more than 10%.

Some literatures simplify the definition of shales as rocks composed of fine-grained clastic sedimentary fragments of sizes less than 0.0625 mm. (16)

Blatt et al. state that shales are made of mud, which is composed of several clay minerals and tiny silt-sized particles or fragments of other minerals such as quartz and calcite. (19) Clays are characterized by complex mineralogy. (20) Table 1.5 summarizes the common minerals forming the clays.

Table 1.5. Common minerals found in clays, data from (16)

Minerals	Composition (%weight)
Quartz	21.5%
Feldspar	4.5%
Clay minerals	66.9%
Iron oxides	<0.5%
Carbonates	3.6%
Other minerals	<2%
Organic carbon	1%

Studies show that shale reservoirs are illite-rich, and frequently contain chlorite. Mica is also common mineral found in shales. According to Glorioso et al., *"non-clay-rich fine detrital*

fractions can be, in some cases, formed by predominantly quartz-rich silts containing other components such as feldspars, plagioclases and diagenetic products like silica, added to dense minerals like pyrite and siderite. In other instances, in the non-clay-rich fractions, fine-grained carbonates, calcites and dolomites and predominant." (21)

Shales due to their fine texture are associated with low energy environments. (22) Fine grained sediments that make up unconventional shale reservoirs commonly have either marine or lacustrine origins (i.e. sea or lake floors). (21) The fine-grained sedimentary debris, which can be moderate-to-deep marine or lacustrine, are mixed with organic matter and deposited in anaerobic environments, and they are buried deeply over the periods of millions of years by the overburden. When the sediments are buried deep enough, the maturity process will start. The pressure and heat will control maturity of organic matter and will produce kerogen and bitumen. (21) Over time, if the conditions are favourable (i.e. the shale formation heated up enough), certain amount of kerogen will have been converted to hydrocarbons. The temperature will control the generation of oil or gas. Hydrocarbon generation rises the pressure, and the pressure will expel part of petroleum from the shale formation and migrate it into the other formation forming conventional hydrocarbon reservoirs. (22) Number of regions and vast lands can be found around the world dominated by silt-rich clay formations. They hold potential of hydrocarbon generation. These shale formations are known as source rocks since hydrocarbons are generated in and expelled from these formations to more porous and permeable reservoir rocks. (21) They play a significant role as a source rock for conventional reservoirs. Shale formations are also sources for commercial in-place petroleum; certain amount, or seldom, the whole volume of hydrocarbons generated in shale can be trapped in the shale formation and form shale gas or light tight oil reservoirs. Shales can be source, reservoir and seal rocks simultaneously. (21) (22)

Both tight and shale reservoirs are characterized by their larger extensions which forms continuous accumulations (23). According to Smocker, continuous petroleum accumulations are "*those oil or gas accumulations that have large spatial dimensions and indistinctly defined boundaries, and which exist more or less independently of the water column.*" (24)

1.3.3 Shale Formations

Shales contain the world's most plentiful rock type and volumes in sedimentary basins. Like their abundance, shales are largest petroleum sources for oil and gas fields. (25) Figure 1.4 represents the map of global basins from one of the studies in which shale oil and shale gas formations have been assessed by US EIA. The study focused on 95 basins in 41 different countries. Note that the study only analysed the basins with geologic data that is considered enough for the resource assessment. (15)

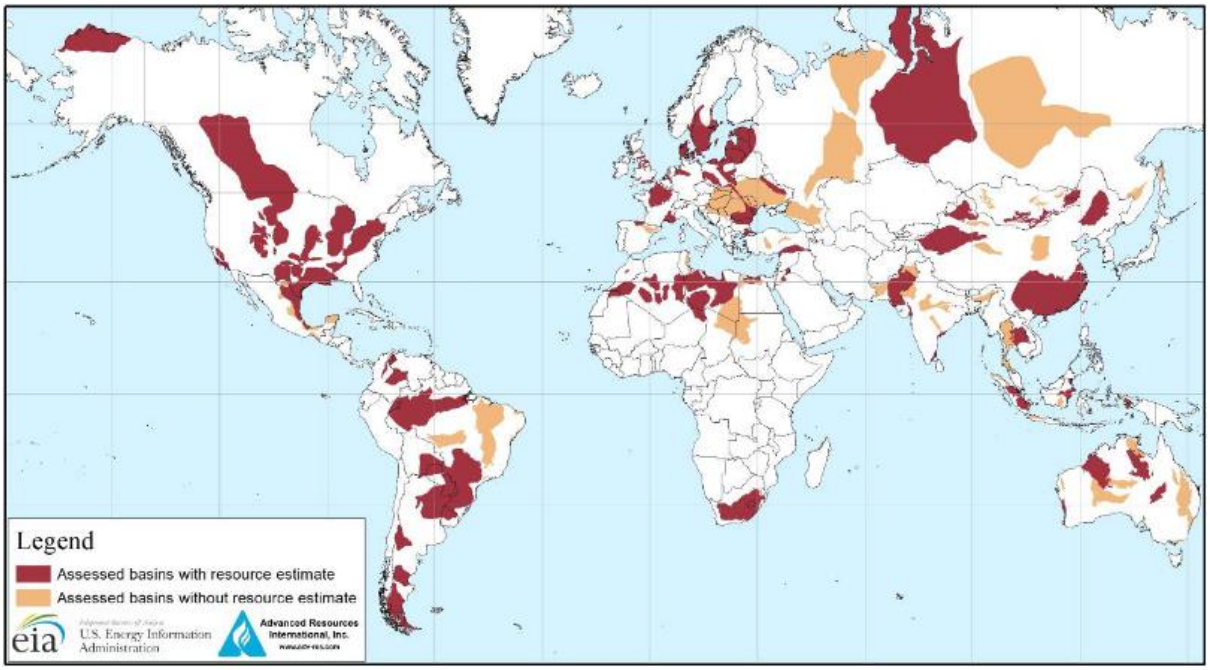

Figure 1.4. Basin map illustrating evaluated shale oil/gas formations, data from (15)

Table 1.6 represents the analysis results from US EIA report 2013. The study in 2013 revealed the significant amount of technically recoverable shale reserves with shale gas resources of 7299 trillion cubic feet and shale/tight oil resources of 345 billion barrels.

Table 1.6. Global technically recoverable resources (2013) EIA estimates, data from (15)

Number of countries	41
Number of basins	95
Number of formations	137
Technically recoverable resources, including US:	
Shale gas (trillion cubic feet)	7299
Shale/tight oil (billion barrels)	345

The other study, world shale resource assessments by US EIA (2015), revealed global unproved technically recoverable wet shale gas resources of 7576.6 trillion cubic feet and tight oil resources of 418.9 billion barrels. (26) The overall increase in global shale resources from 2013 to 2015 is associated with detailed investigations. (26) The conditions favourable for

unconventional gas extraction, are favourable for increasing levels of natural gas liquids, which are extracted from liquids-rich shale gas and light tight oil. "*In a price environment combining high oil prices and very low prices for natural gas, there is a strong economic incentive to target plays with higher liquids content.*" (14)

Shale reservoirs can be classified as shale gas and liquid-rich shale reservoirs (i.e. LRS oil reservoirs and LRS gas condensate reservoirs).

1.3.3.1 Shale Gas

Shale gas or tight gas is essentially natural gas produced from shale reservoirs and is also referred to as unconventional natural gas. (27) Shale gas production firstly started in the US, New York, in 1821 from shallow, low-pressure fractures. The development of horizontal drilling later in 1930s and the first fracked well in 1947 accelerated the production from shale and tight resources. (28) Shale gas revolution in the US have attracted attention of different countries. Availability and production from shale gas resources provided different countries such as China and the US with energy security. The global interest in shale gas resources provided significant investments to these resources which led to exponential growth worldwide. (29) Table 1.7 summarizes ten countries with the highest estimates of shale gas resources. China holds the first place in the list with 1115 trillion cubic feet of technically recoverable shale gas resources followed by Argentina, Algeria and the US.

Table 1.7. Technically recoverable shale gas resources of top 10 countries, data from (15)

Rank	Country	Shale gas (trillion cubic feet)
1	China	1115
2	Argentina	802
3	Algeria	707
4	U.S.	665
5	Canada	573
6	Mexico	545
7	Australia	437
8	South Africa	390
9	Russia	285
10	Brazil	245
	World Total	**7299**

The US holds significant place in shale gas production. EIA provides the map for the US shale gas plays. (30) It is shown in Figure 1.5 and includes 48 lower states shale plays.

Large-scale shale gas production in US started in 2000 with the Barnett shale gas becoming commercially available. Barnett shale is located in north-central Texas. The production from Barnett shale begun during 1980s and 1990s with different techniques of hydraulic fracturing. Hydraulic fracturing led to commercial production of shale gas. The success achieved in the Barnett shale encouraged companies to drill wells in the Barnet, and it was until 2005 that approximately 0.5 trillion cubic feet of gas was producing during a year. Following this, different new shale formations came under production, which included "*the Fayetteville Shale in northern Arkansas, the Haynesville in eastern Texas and north Louisiana, the Woodford in Oklahoma, the Eagle Ford in southern Texas, and the Marcellus and Utica shales in northern Appalachia"*. (31) Figure 1.6 shows monthly dry shale gas production from various US shale formations in billion cubic feet per day from 2006 to 2020 March. Increase in shale gas extraction is observed throughout the period from 2006 to 2020, and Marcellus has the highest production rates in between number of US shale formations. (31)

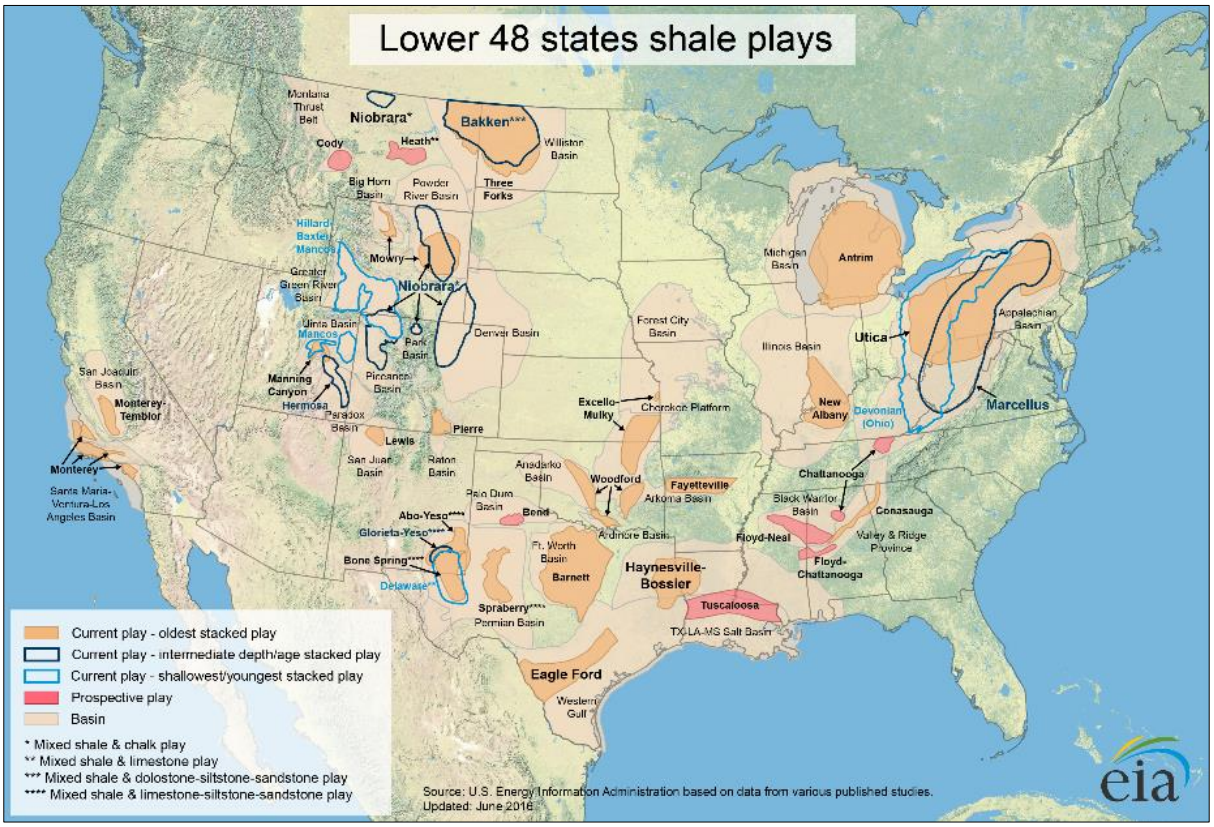

Figure 1.5. The United States shale gas plays as of 2016, data from (30)

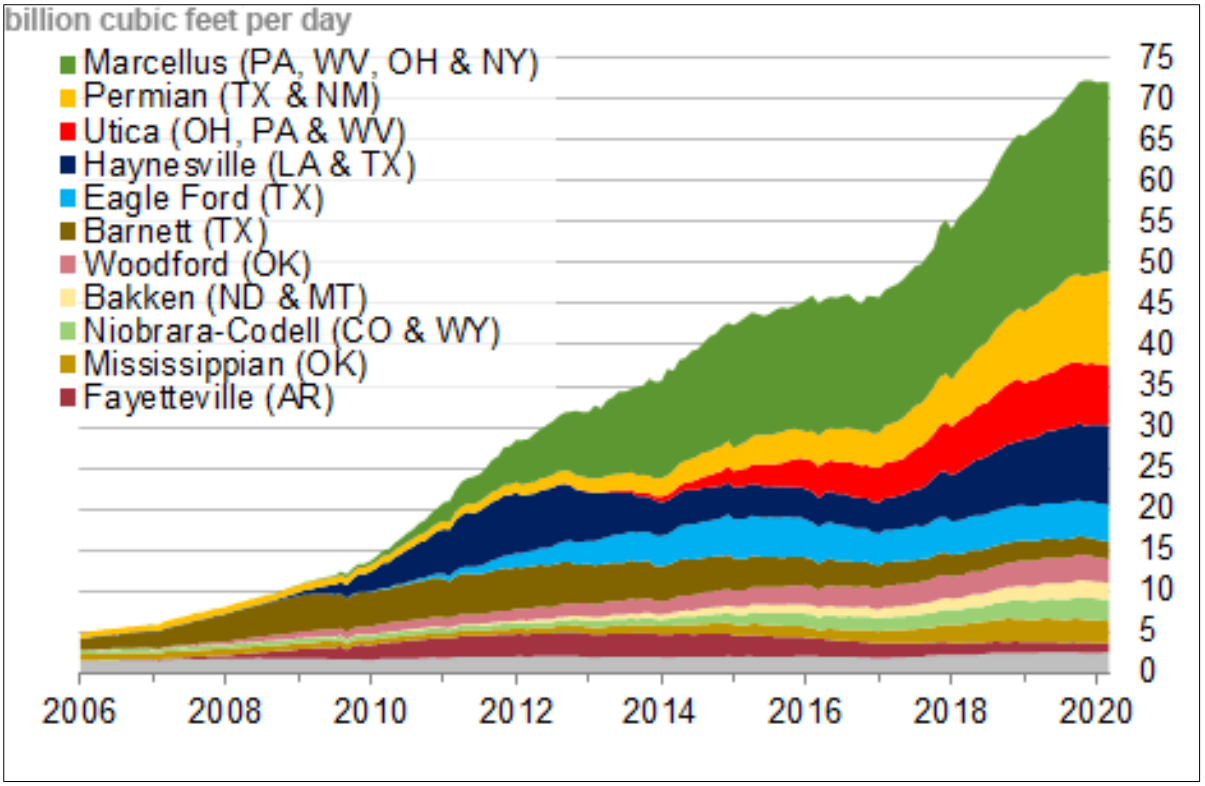

Figure 1.6. Monthly dry shale gas formations in billion cubic feet per day as of March 2020, data from (31)

The US EIA made an assessment for gas production in the US by type as well. The results are plotted in chart shown in Figure 1.7. Around 1.5 times increase in gas production is expected from shale and tight resources until 2050.

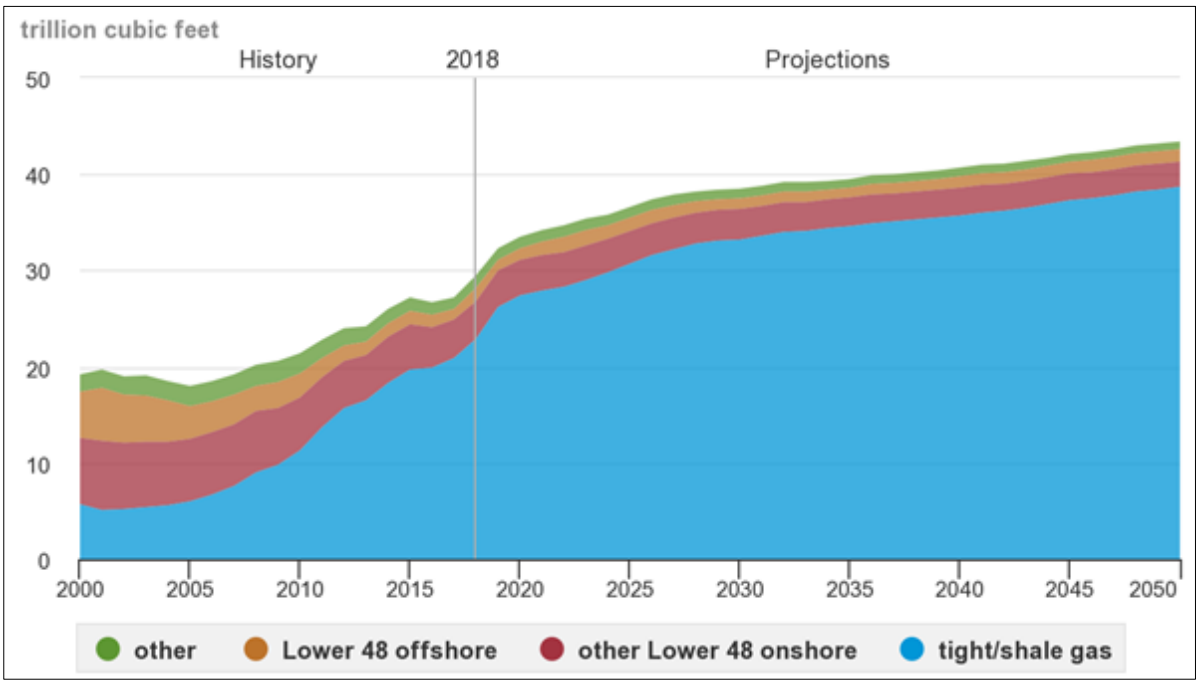

Figure 1.7. US dry natural gas production by type, 2000-2050, data from (31)

As is discussed in the previous sections, shale reservoirs, due to their fine-grained nature, have pores that are smaller than those of conventional reservoirs. This leads to gas being trapped and stored in shale reservoirs in several ways (16):

- *"Gas adsorbed and dissolved into kerogen material* (32)
- *Free gas trapped in nonorganic inter-particle (matrix) porosity*
- *Free gas trapped in microfracture porosity*
- *Free gas stored in hydraulic fractures created during the simulation of the shale reservoir*
- *Free gas trapped in a pore network developed within the organic matter or kerogen* (33) (34)" (16)

All these distinct storage types state the necessity for the shale gas reservoirs being characterised by at least quadruple porosity models (35) (36) (37) and by quintuple porosity models (38). This is not to be discussed in the study.

1.3.3.2 Liquid-Rich Shales

As is stated before, the terminology liquid rich shale does not only stand for shale resources, but also those that satisfy the permeability criteria. It covers LRS oil reservoirs and LRS gas condensate reservoirs, possibly wet gases, where more than a fourth of income comes from oil or condensate sales.

Tight formations that hold merely oil cannot be extracted economically nowadays. The presence of minimum 15–20% pore volume of natural gas is needed in reservoirs to drive the oil to borehole in tight reservoirs, or otherwise cannot be produced. (15)

Table 1.8 summarizes 10 countries with the highest estimates of shale oil resources. Russia holds the first place in the list with 75 billion barrels of technically recoverable shale oil resources followed by the US.

Table 1.8. Technically recoverable shale oil resources of top 10 countries, data from (15)

Rank	Country	Shale oil (billion barrels)
1	Russia	75
2	US	58
3	China	32
4	Argentina	27
5	Libya	16
6	Australia	18
7	Venezuela	13
8	Mexico	13
9	Pakistan	9
10	Canada	9
	World Total	**345**

US holds significant interest in shale resources. A study revealed that the US brought minimum 4000 new production wells in shale or tight oil reservoirs in 2012. The numbers are significantly comparable with the number of new conventional and unconventional producers completed in 2012 around the world except the US and Canada, which was less than 4000. (39)

The US have important tight oil formations including the Bakken Shale, the Eagle Ford Shale, Permian, the Niobrara Formation, and Barnett Shale. The production from tight resources in

the US sufficiently rises form 2010 and is associated with technological developments leading to higher drilling efficiency and lower drilling costs. (40) In 2015, the shale oil production exceeded 50% with tight oil production of 4.9 million barrels of oil per day and reached around 6.5 million bpd in 2018, which is 61% of US oil production. It is important to note that shale oil production is expected to rise around to 10 million bpd in the early 2030s with reducing drilling costs and efficiencies. (41)

The Bakken in North Dakota and Eagle Ford in South Texas shaped the global energy predictions and expectations in recent years. The Eagle Ford, one of the quickly developing shale formations in the world, contains more than 7 billion barrels of proved light sweet crude oil reserves. It has three different regions characterised by different petroleum fluids. The fluids range from dry gas, which is accumulated in the southern region, to black oil in the northern section. It has been found that there are also intermediate regions with volatile oil, retrograde gas condensate and wet gas.

Bakken formation is *"the largest continuous oil accumulation ever accessed in the US"*. (42) According to USGS, it was estimated in 2013 that the formation contains 7.4 billion barrels of oil, 6.7 trillion standard cubic feet of natural gas and 0.53 billion barrels of natural gas liquids on average. Note that USGS states that 4.4 to 11.4 billion barrels of undiscovered, technically recoverable oil can be present in the Bakken formation. (43)

Thus, these two shale formations are expected to be the main contributors of tight oil supply through 2050 in the US. They accounted for about 19% and 17% of cumulative tight oil production in 2019 respectively. (41)

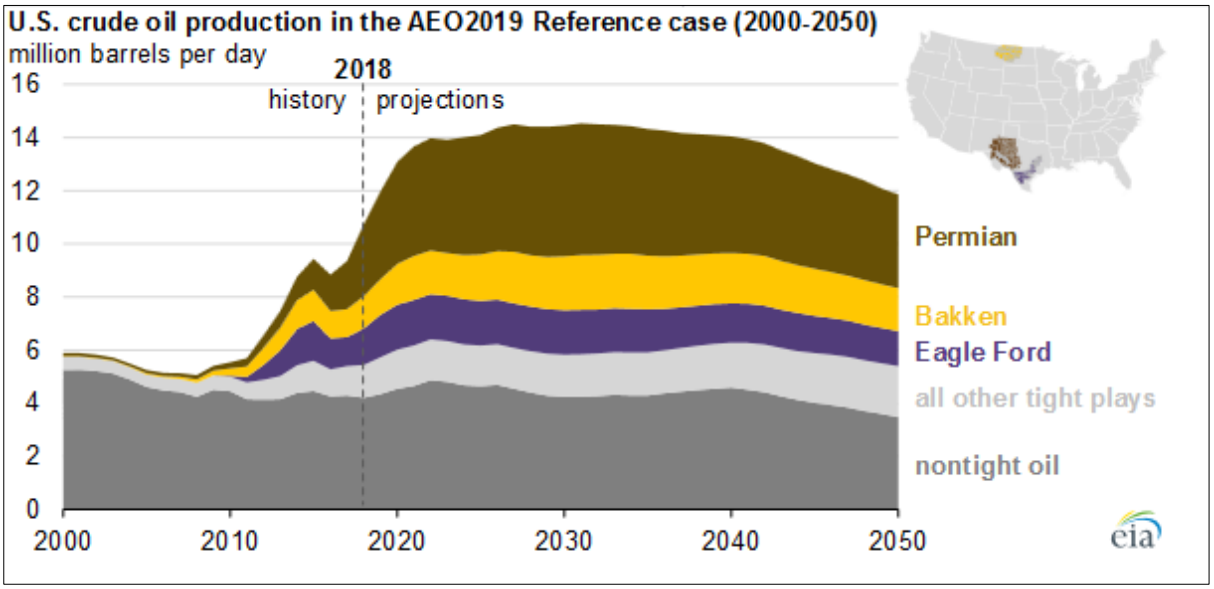

Figure 1.8. US crude oil production, data from (41)

CSUR forecasts a significant increase in tight oil production in the US (Figure 1.8), which is also predicted to extend to the other countries with tight oil resources. (14)

1.3.4 Liquid-Rich Shale Fluids

Tight liquid-rich shale (LRS) fluids hold increasing economic importance for energy market. They include:

- Volatile or near critical oil
- Retrograde gas condensates
- Wet gases (44)

The difference in these fluid types can best be explained by the phase diagrams of each fluid type with respect to initial reservoir conditions (i.e. Pressure and Temperature). Figure 1.9 shows the phase behaviour of three fluid types of liquid-rich systems. The composition of in-situ fluids, phase behaviour and initial reservoir pressure and temperature are considered main factors controlling the performance of the tight liquid-rich fluid systems. (44)

Volatile oils or near critical oils are characterised by critical temperature discernibly greater than reservoir temperature. This is an important indication of fluid being liquid in those conditions if initial reservoir pressure does not fall inside the two-phase region. Volatile oils derive the name from the amount of gas dissolved in them. The higher content of dissolved gas leads to volatile oils normally having high saturation pressure that can easily fall into the two-

phase region, where oil and gas phase are present. In this case, gas production will dominate during the production period. (44)

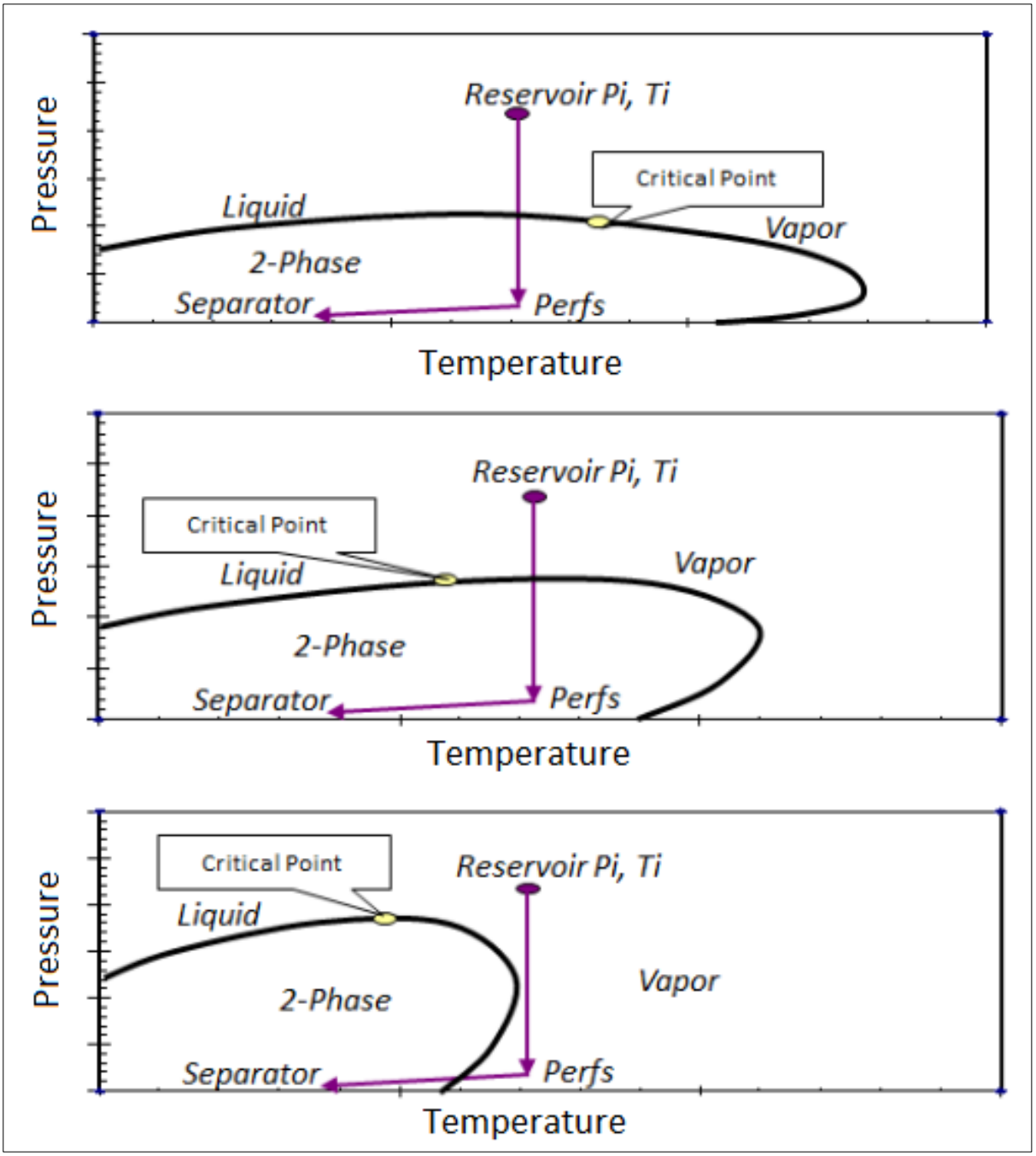

Figure 1.9. Fluid types in liquid-rich shales: phase behaviour for volatile oils at the top, retrograde gas in the middle and wet gases at the bottom, data from (44)

Retrograde gas condensates are similar to volatile oils in the context that their critical temperature is closer to reservoir temperature. Main difference is the reservoir temperature that is higher than critical temperature and less than circondentherm for gas condensates. They are

gas phase in the reservoir and are characterised by more producing gas-oil ratio in comparison with volatile oils. (44)

The most gas-dominated liquid-rich fluids are lean wet gases. Wet gases do not produce liquid in the reservoir conditions. The two-phase is achieved in the wellbore and at the surface with the fluid temperature decreasing to separator temperature. They normally contain the least amount of associated liquids having the advantage of high mobility and low viscosity. The issues regarding the relative permeability can be ignored for wet gas systems as the liquids are not present in the reservoir. (44)

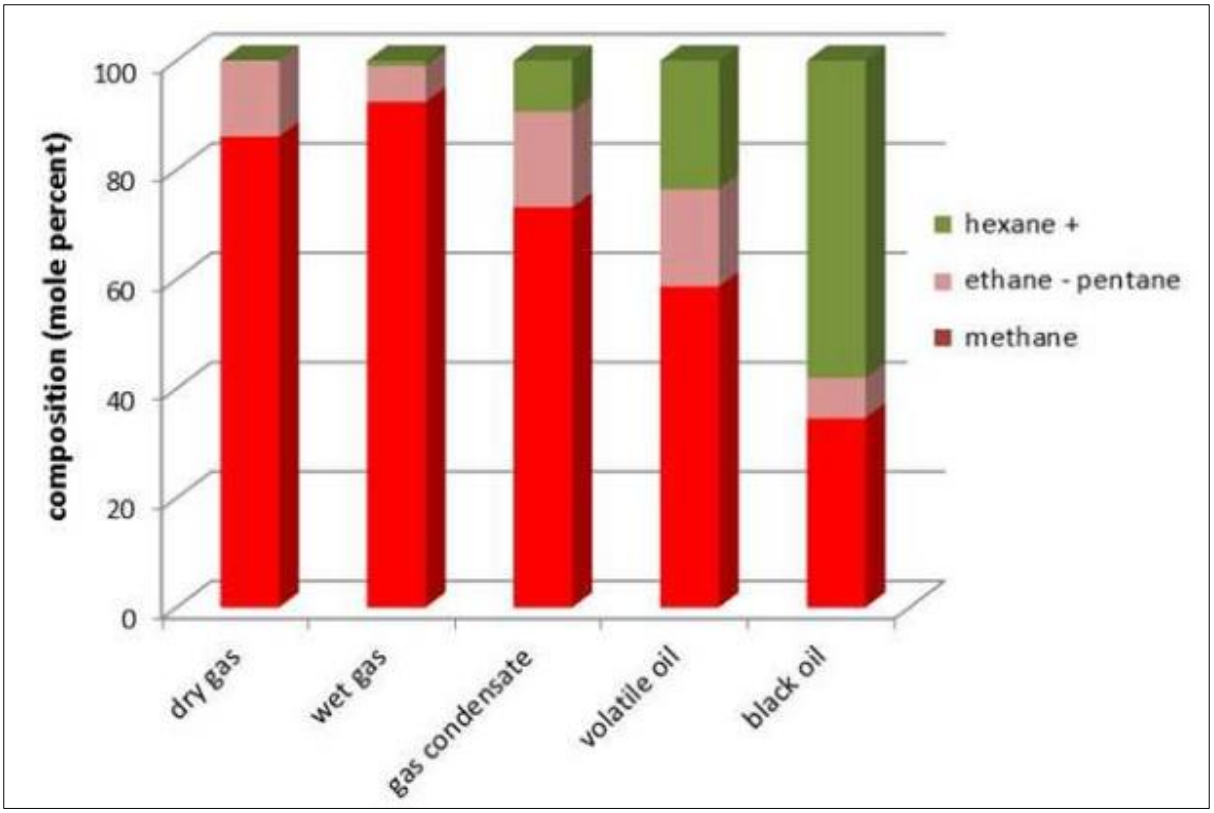

Figure 1.10. The common composition for reservoir fluid types, data from (44)

Figure 1.10 summarizes the composition of common reservoir fluid types. Wet gas contains the largest amount of oil among liquid-rich systems. The methane content is significant for gas condensates and volatile oils as well. Ethane-pentane and hexane plus contents rise slightly from wet gas to volatile oils. Volatile oils contain considerably high amount of hexane plus with ethane-pentane content similar to that of gas condensate.

1.3.5 Production Challenges in Shale Reservoirs

According to Holdtich, hydrocarbons cannot be extracted from shale reservoirs at economic rates. Shale reservoirs are not expected to achieve an acceptable ultimate recovery efficiency without enhancing the productivity with appropriate reservoir stimulation and multilateral horizontal wellbores. (45) The economic production from unconventional shale formations require:

- Horizontal drilling
- Stimulation treatments and
- Expensive recovery processes (i.e. huff-n-puff EOR for tight oil)

Horizontal drilling, multistage hydraulic fracturing and the implementation of developed proppants provided exploitation of the resources with low and ultra-low permeability at an acceptable revenue. Unconventional shale reservoirs have some factors unsolved that could otherwise lead to production cost reductions to maintain the place of shale petroleum in the global energy market. (45)

Production behaviour of shale reservoirs is controlled by different factors such as reservoir permeability, drainage area, fracture conductivity, reservoir porosity, initial water saturation etc. (46)

Reservoir permeability is considered the primary parameter controlling production forecasts in tight resources as it is an important parameter in field development decisions. As is discussed in the previous chapter, fine-grained, organic-rich (0.5 to 25%) characteristics of shales results in very low permeability. In comparison with conventional reservoirs, which normally have permeability $k > 0.1\ mD$, the shale reservoirs are almost impermeable with permeability $k < 0.001\ mD$. This ultra-low permeability does not allow sufficient fluid flow necessitating natural or artificial fracturing to produce the reservoir fluids. (47)

Mineralogy, microfracture network, and clay content control the shale permeability. Shales, as are fractured, hold two forms of permeability: fracture and matrix permeabilities. Fracture permeability is the ability of rock by which a fluid flows through the natural fractures and hydraulic fractures created in the shale, while matrix permeability is the ability of the rock by which a fluid flows within the intact portion of the shale. Although matrix permeability can be in the range of few nano-darcies, fracture permeability is typically in the range of some milli-

darcies. (47) Fractures are considered primary source of flow capacity in shale reservoirs. They are characterised by their capacity and conductivity, and changes in these properties can have a significant effect on the reservoir performance. (48) Fracture conductivity is a function of fracture geometry, proppant, multiphase flow, non-darcy inertial pressure drops, fluid-retained permeability end etc. (46) Fractures are important in shale petroleum production. The porosity and permeability of shale formations are functions of natural fractures. The natural fractures are less dense and can be less frequent in shale rocks. In the absence of the natural fractures, stimulation techniques (i.e. hydraulic fracturing) are applied to provide economic production from shale formations. (29) Various technologies were developed through the years to improve the production from shale reservoirs. Acid treatment is one of the oldest stimulation techniques that has been used for near wellbore permeability improvement in carbonate reservoirs. Hydraulic fracturing is another effective well-known stimulation technology utilized in ultra-low permeability shale reservoirs. (22) The economical production of shale reservoirs requires maximizing the contact area. The appropriate choice of completion and stimulation techniques can provide larger access to greater reservoir volumes of hydrocarbons.

The hydraulic fracturing together with horizontal well technology can provide economic productivity from shale reservoirs by creating multiple transverse fractures. (22) (47) Horizontal wells are important in achieving improved recoveries from the fields. They are specifically implemented to achieve (i) improved flow rates and accelerated production, (ii) increased recovery and drainage area per well, and (iii) enhancing the drainage in previously undrained areas. (49)

The application of horizontal drilling and hydraulic fracturing resulted in significant development of estimated natural gas reserves in the US recently with the production of natural gas from unconventional resources (i.e. tight gas formations, shale reservoirs, coal beds). It has also provided the drive for the development of tight oil resources in the US, such as the Bakken and Eagle Ford formations. (50)

After drilling the wells, hydraulic fracturing is carried out with huge volumes of water and propping agent(s), e.g. sand, and some specific chemicals. The fluid volume is injected into the rock at desired pressure to fracture the hydrocarbon formations. The purpose of proppants is to maintain the fractures open so that fluids, particularly oil and gas, can flow easily out of the formation through the fractures into the wellbore. The fluid used for fracturing and water

remaining in the fractured section need to be removed from the formation to surface as it can prevent the production. (50)

Tight reservoirs can be characterised by high pressure and temperature. They are more likely to challenge the hydraulic fracturing process. The study by Lau et al. on tight reservoirs in Chine shows that that too high surface pressure can be required for hydraulic fracturing for longer periods, which can usually be higher than $69\,MPa$. This can often bring some challenges due to limited availability of high-pressure equipment for hydraulic fracturing. A number of hydraulic fracturing techniques that lower formation breakdown pressure and the power requirements have been developed to overcome the problem. (51)

Openhole fracturing and multi-stage/zone fracturing can be typical examples of such technology. In addition to reducing the friction drop due the perforations, openhole completion can provide maximum contact between natural fractures and the wellbore. Increased contact can reduce the pumping pressure that is important to breakdown the formation and maximize the connectivity of the wellbore to the network of natural formations. The larger inflow area at the borehole also leads to reduced drawdown during production, as a result of which the probability of natural fracture collapses decreases. (51)

Multi-zone/stage fracturing techniques both in vertical and in horizontal wells are well known ways of the development of tight and shale reservoirs in North America. Multi-zone/stage fracturing treatments normally employ perf-and-plug methods using conventional through-tubing fracturing. Despite their effectiveness, these techniques demand multiple trips. The extent of their capabilities is limited. The conventional coiled tubing has constrained treatment rates together with its reach being limited in long horizontal shale wells. (51)

Enhanced liquid recovery from tight shale reservoirs has recently attracted important attention. (52) The distinct studies on the tight formations resulted in low primary recoveries between 5% and 10% after multi-stage hydraulic fracturing. (6) The results from the studies show that enhanced oil recovery technique, huff-n-puff EOR, can effectively increase recovery without drilling new wells. (52) There are different laboratory and numerical simulation studies evaluating the huff-n-puff EOR efficiency in tight formations. Lab studies represent improved recovery achieved by huff-n-puff, which is confirmed by simulation studies as well. Hoffman and Shoaib achieved additional recovery of 2.5%, Yu et al. obtained improved recovery of 4-5%. (6) (53) Piyush et al. showed that additional recoveries up to 9% can be achieved in Eagle

Ford if huff-n-puff is implemented. (54) Huff-n-Puff shows increasing attention recently and needs a detailed study.

1.4 PVT Terminology

Pressure Volume Temperature (PVT) analysis is a summary of experiments used for determination of fluid properties and behaviour, which involves fluid (i.e. oil and gas) sampling. Defining fluid properties is important in understanding the fluid flow, finding optimum recovery methods and possibly achieving cost-effective production.

PVT data obtained from the wells, including LRS wells, contain "*(1) primary separator gas composition, (2) producing test gas-oil ratio, or oil-gas ratio, (3) stock-tank oil gravity, and (4) reservoir temperature.*" (17) Fluid sampling is particularly important for providing samples reflecting in-place fluids and measuring PVT data that can be useful in tuning the EOS model and develop black-oil PVT tables. (17) The study particularly focuses on gas and oil relationships (i.e. GOR or OGR) of LRS wells.

Gas-oil ratio is necessary for defining the gas-oil richness of the system, which can later be useful in classifying the fluid type (i.e. volatile oil, gas condensate, wet gas etc.). It can also be useful in defining if the reservoir is undersaturated or saturated.

$$R_{go} = \frac{(V_g)_{sc}}{(V_o)_{sc}} = \frac{V_{\bar{g}}}{V_{\bar{o}}}$$

GOR can be defined as solution GOR and producing GOR.

The solution GOR, R_s, is the amount of gas in standard cubic feet that is dissolved in one stock tank barrel of oil when they are subject to the reservoir conditions (pressure and temperature) in unit of scf/STB. The producing GOR, R_p, is the instantaneous ratio of the total produced surface-gas volume divided by the total stock-tank-oil volume. (55) (56) At pressures above bubble point, the producing GOR will equal the solution GOR at dewpoint and remain constant. When conditions drop below bubble point, the situation will become complicated. Gas will start to come out of the solution, and the solution GOR will decrease. The producing GOR can be equal to or different from the solution GOR. The producing GOR can normally be 10 or 20 times greater than initial solution GOR as gas mobility rises and oil mobility decreases. (56)

The similar terminology used for gas condensates is oil gas ratio in unit of $STB/MMscf$. It is directly proportional to $1/R_{go}$:

$$r_{og} = \frac{(V_o)_{sc}}{(V_g)_{sc}} = \frac{V_{\bar{o}}}{V_{\bar{g}}} = \frac{1}{R_{go}}$$

The solution OGR, r_s, can be defined as the ratio of surface oil to surface gas produced from a single-phase reservoir gas. (56) The producing OGR, r_p, will be equal to solution OGR at dewpoint and remain constant above dewpoint. When pressure drop below dewpoint, the producing OGR will normally equal or remain just above the solution OGR. This is explained by the fact that flowing reservoir oil negligibly contributes to the surface oil production in many gas condensate reservoirs. (56)

According to Whitson et al., liquid-rich shale wells can be characterised by long periods of production through which production performance is similar to *"a well that drains an infinite reservoir without no-flow outer boundaries (between fractures and between wells)."* (17)

If the flowing bottomhole pressure is kept constant, the producing OGR is observed to be constant during infinite-acting production. It is during the infinite-acting period of liquid-rich shale wells that substantial volume of recovery can be obtained. (17)

2 Study Objective

The unconventional liquid-rich shale reservoirs have attracted significant attention in the recent years. Despite the growing interest, they have not been studied in detail, thus, not fully understood. The rock-fluid interaction is still not completely covered in ultra-low permeability reservoirs.

Low permeability liquid-rich shale reservoirs are characterised by several challenges and original behaviour in production, one of which is related to the producing gas-oil ratio. The producing gas-oil ratio in ultra-low permeability liquid-rich shale formations is a function of several parameters, which are directly or indirectly related to fluid, reservoir, production, and completion properties. Analytical solutions show that the producing gas-oil ratio (or oil-gas ratio) in liquid-rich shale wells represents a constant trend behaviour for a sufficient period of time during infinite acting, which may last for several years. Such a behaviour is distinctive characteristics of unconventional liquid-rich shale wells that are not observed in conventional wells. In comparison with the analytical approach, the numerical studies show significant oscillations in liquid-rich shale wells. The main purpose of the study is to analyse the OGR oscillations in highly undersaturated fluids that occur in numerical modelling of liquid-rich shale wells and evaluate the factors that contribute to the oscillations in numerical modelling.

3 Software Description

3.1 Sensor

SENSOR is an abbreviation standing for System for Efficient Numerical Simulation of Oil Recovery. Sensor is a 3-dimensional numerical modelling software that is used for the optimization of petroleum recovery processes. It is a simulation tool that includes compositional and black oil flow modelling in single porosity, dual porosity and dual permeability systems. The CPU run time of Sensor for both compositional and black oil fluid flow models is less than that required by other simulation software. This allows users to have faster and better decisions. It has been speeded up 10 times for compositional model. Coats Engineering states that Sensor is the simplest, most efficient and most accurate simulator for the cases up to 80 million cells in implicit and 320 million cells in impes on Windows 8. It is stable, reliable and user-friendly. Unlimited numbers of simultaneous jobs can be run on a single node-locked license. Sensor is two times more cost-effective than any other simulation software on both serial and parallel. Sensor is available for use in Windows 32- and 64-bit operating systems. (57) Sensor is used to run and analyse sensitivity cases in the study.

3.2 Microsoft Excel

Microsoft Excel, a very popular tool, is a spreadsheet software of Microsoft enabling a number of calculations from very easy to significantly complex ones to be carried out quickly and straightforwardly. The software provides several features including graphical tools, calculation tools, pivot tables, and macro programming language known as Visual Basic for Applications (VBA). (58) Microsoft Excel is used to analyse the simulation results and plot the data for interpretation purposes in the study.

4 Reservoir Model Description

One of the ideas in the original study SPE 155499 by Whitson et al. is to conduct numerical modelling of liquid-rich shale wells to evaluate the production performance of LRS wells producing against a constant flowing bottomhole pressure and define dimensionless infinite acting producing OGR for a planar fracture with a constant flowing bottomhole pressure, for oil and gas fluid systems with a wide range of initial gas-oil ratios and degrees of undersaturation.

This study implements the model from the SPE155499. The model description section provides the data needed to set up the base case model [A1] used in the study. Base case model is a black oil model solved fully implicitly. Note that the data necessary to set up the compositional model is also provided.

The model is geometrically gridded (i.e. rock grid dimension grows as it gets further away from the fracture). It includes fractures populated with significantly high permeability and appropriate porosity. High permeability values are intended to produce enough pressure drop in fractures. Figure 4.1 illustrates LRS well model sketch. The study only involves one side of the fracture (rate equals two times the rate from half-model multiplied by the number of fractures). (17)

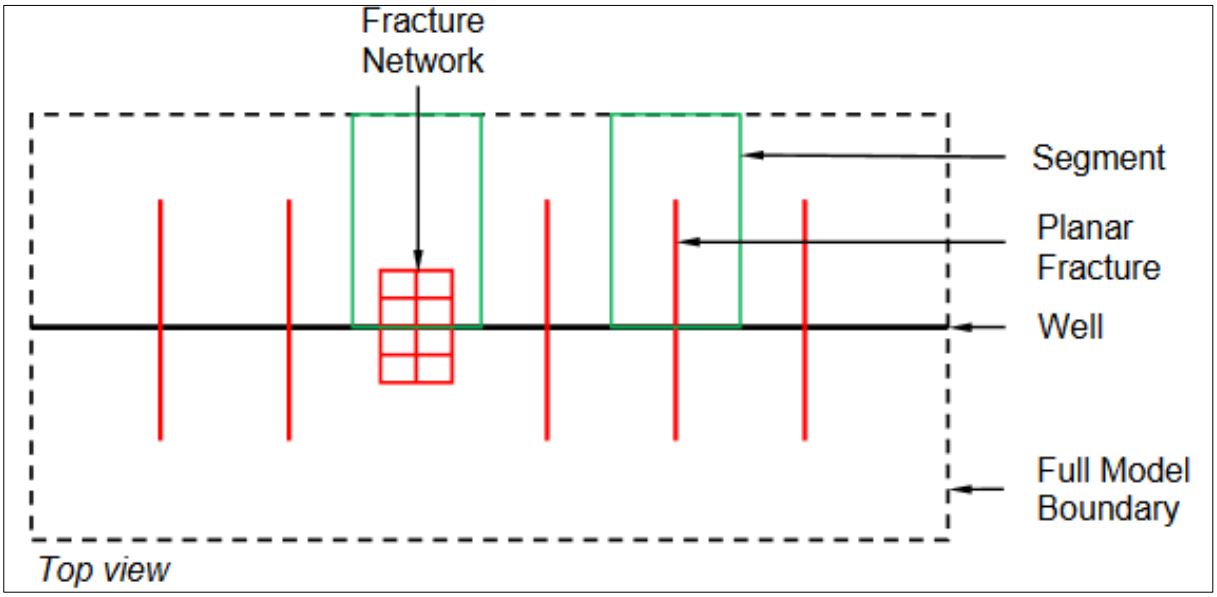

Figure 4.1. Sketches of LRS well models, data from (17)

This study only implements planar fracture. This is a simple 1D model neglecting the volume beyond the fracture tip. This leads to 1D flow in X direction. The reservoir and fracture dimensions are represented in Table 4.1.

Table 4.1. Reservoir and fracture dimensions used in the original (base case) model

Property	Value
Reservoir model length (X direction), ft	300
Reservoir model width (Y direction), ft	150
Reservoir model thickness, ft	250
Hydraulic fracture half-length, ft	150
Hydraulic fracture width, ft	0.0833
Number of grid cells, xyz	1001x1x1

The model has dimensions of 300x150x250 ft. 1D model has 1001 grid cells in X direction. Grid cells in X direction are variable in size; geometrically increasing away from the hydraulic fracture in both sides of the hydraulic fracture. This is represented in Figure 4.2. The unit is given in feet.

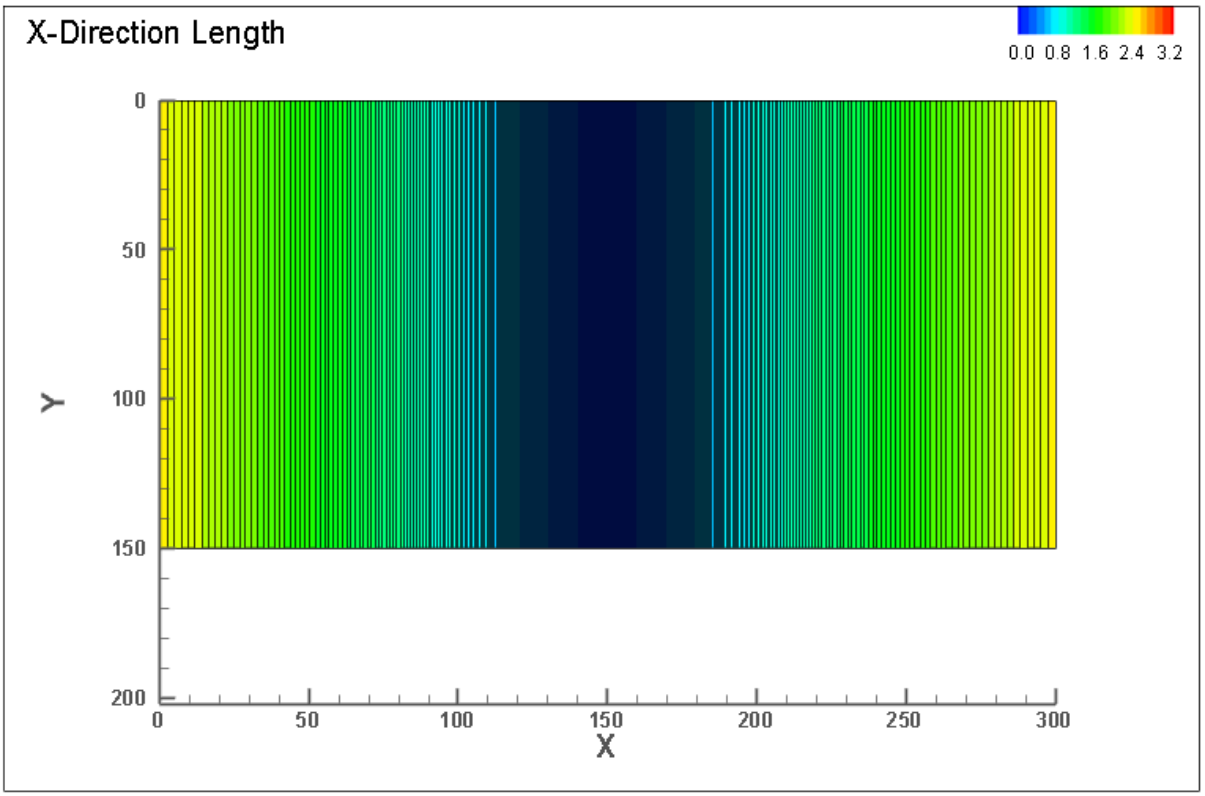

Figure 4.2. Model illustration in X and Y direction: Gridding in X direction

4.1 Rock and Fracture Properties

Reservoir properties applied in the study are assumed to be relevant for the LRS reservoirs. All reservoir and fracture properties are provided in Table 4.2. The depth to top of reservoir is 4500 ft.

Table 4.2. Reservoir matrix and fracture properties

Property	Value
Matrix porosity	0.05
Hydraulic fracture porosity	0.041
Matrix permeability, mD	0.0001
Hydraulic fracture permeability, mD	12005

The model is assumed to be isotropic, i.e. $k_x = k_y = k_z$. Table 4.3 summarizes the initial reservoir conditions and rock properties.

Table 4.3. Reservoir initial conditions and average compressibility at reference pressure (6000 psia)

Property	Value
Rock compressibility, $1/psia$	$4.0 * 10^{-6}$
Reservoir temperature, $°F$	250.0
Initial reservoir pressure, $psia$	4500
Gas Oil Contact, ft	4625

Desorption has been ignored due to uncertainty in liquid-rich systems; it is not clearly known if liquid-rich shales have greater or smaller sorption compared to dry gas formations and there are limitations on models for desorption of the components that are heavier than methane. (17)

4.2 Fluid Properties

Reservoir fluid is undersaturated ($P_{sat} = 4474\ psia$) in the initial reservoir conditions ($4500\ psia, 250$ °F).

4.2.1 Black Oil Table

The black-oil model implements BO table. Note that BO table is generated from a fluid composition and a convenient EOS data.

4.2.2 Oil (EOS) Properties

The compositional model implements the initial reservoir composition. It is provided in Appendix. Two mostly used equation of state are Peng-Robinson and Soave-Redlick Kwong EOS. They both provide the same accuracy for VLE predictions and satisfactory volumetric predictions for vapor and liquid phases if implemented together with volume translation. (56) The Soave-Redlick Kwong (SRK) EOS is implemented in the study. It is modified with volumetric shift for each component, which offers better predictions as it increases the accuracy of the model. The reservoir fluid characterization involves 31 components including a pseudo-component for C_{26+} fraction. The 2 cubic EOS coefficients, namely $OmegA$ and $OmegB$ are set to 0.427 and 0.087 respectively. Binary interaction coefficients are used to improve the phase equilibrium calculation accuracy and reliability. The EOS properties and binary interaction coefficients are provided in Appendix.

4.2.3 Water Properties

Water properties are shown in Table 4.5.

Table 4.4. Water properties

Property	Value
Formation Volume Factor, Rb/Stb (at 6 000 psia)	1.000
Density, $lb/ft3$ (at 14.7 psia, 60 °F)	62.40
Compressibility, $1/psia$	$3 * 10^{-6}$
Viscosity, cP	0.500

4.3 Relative Permeability Curves

The two sets of relative permeability curves are applied to set up the model (1) matrix relative permeability curves and (2) fracture relative permeability curves. Fracture relative permeability curves are straight lines, which have no residual fluid saturation values.

Sensor implements the keyword KRANALYTICAL to obtain the relative permeability curves analytically. These curves are directly used in the simulation, no interpolation in the relative permeability data is carried out. This can be necessary for achieving accurate results. The relative permeability curves are expressed by power-law relationship. (59) The data for the matrix and fracture analytical relative permeability curves are provided in Table 4.6.

Table 4.5. Relative permeability data for matrix and fracture

Properties	Values (matrix)	Values (fracture)
Relative Permeability to Water at S_{orw} ($k_{rw}(S_{orw})$)	1.0	1.0
Relative Permeability to Gas at S_{wc} ($k_{rg}(S_{wc})$)	1.0	1.0
Relative Permeability to Oil at S_{wc} ($k_{ro}(S_{wc})$)	1.0	1.0
Connate Water Saturation (S_{wc})	0.2	0.2
Residual Oil Saturation to Water (S_{orw})	0.2	0.2
Residual Oil Saturation to Gas (S_{org})	0.2	0.2
Critical Gas Saturation (S_{gc})	0.1	0.1
Power Law Water Exponent (n_w)	2.5	1.0
Power Law Oil Exponent Relative to Water (n_{ow})	2.5	1.0
Power Law Oil Exponent Relative to Gas (n_{og})	2.5	1.0
Power Law Gas Exponent (n_g)	2.5	1.0

Figures 4.3 and 4.4 represent the relative permeability curves used in the study.

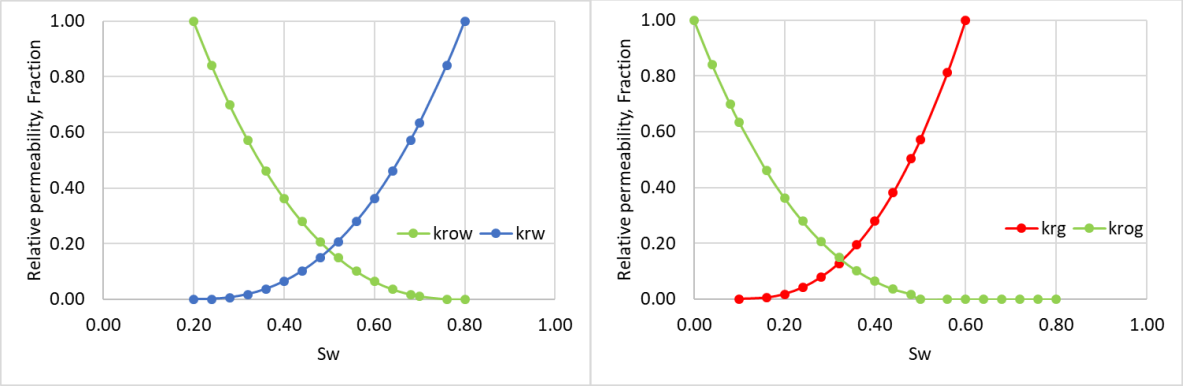

Figure 4.3. Oil-Water relative permeability curves (left) and gas-liquid relative permeability curves (right) for matrix

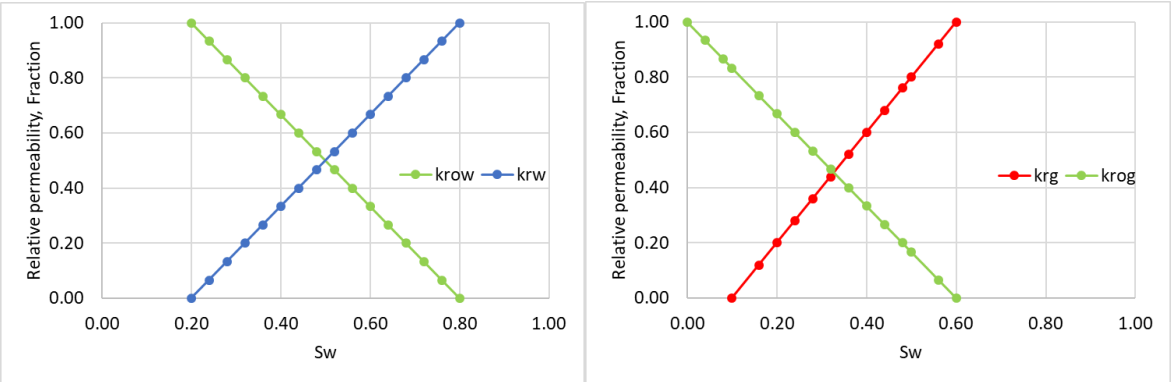

Figure 4.4. Oil-Water relative permeability curves (left) and gas-liquid relative permeability curves (right) for fractures

4.4 Production Data

In the original model with 1001 cells in X direction, the well is placed in the coordinates 501, 1, 1. This corresponds to hydraulic fracture. Well productivity index is pre-defined at 100 rb-cP/day-psia. Overall simulation period is set to 1000 days. The producer is a gas well with initial gas production rate of 10 $MMSCF/d$. The flowing bottomhole pressure has been set to 1000 psia.

4.4.1 Separator Conditions

The separator conditions are shown in Table 4.7.

Table 4.6. Separator conditions

Separator stage	Pressure, psia	Temperature, °F
1	440.0	104.0
2	14.7	60.0

All the inclusion files used to set up the model are provided in Appendix.

5 Case Study Analysis

Table 5.1 describes sensitivity analysis studies. Several studies are carried out in the work, which are categorised in 9 different sections and analysed in detail separately below.

Table 5.1. Descriptions of the case studies

Case ID	Description
A	Original cases from the study SPE155499
B	Case studies on hydraulic fracture width
C	Case studies on hydraulic fracture relative permeability endpoints
D	Case studies with no hydraulic fracture properties
E	Case studies on flowing bottomhole pressure
F	Case studies on grid cell number
G	Case studies on numerical solution at P_{ri}=8000 psia
H	Case studies on numerical solution at P_{ri}=10000 psia
I	Case studies on numerical modelling

Table 5.2 is the case-matrix table that provides detailed information for all cases.

Table 5.2. Case-matrix table

Case	Init. OGR	Nx	p_{Ri}	pwf	HF			Matrix	Model	Solution	PI	DELX	Min. Rock DELX
					yes/no	DELX	RELP	RELP					
ID	STB/MMscf		psia	psia		ft	Endpoints	EndPoints				Type	ft
[A1]	155	1001	4500	1000	yes	8.330E-02	original	original	BO	Implicit	100	Geometric	6.878E-04
[A2]	155	5999	4500	1000	yes	8.330E-02	original	original	BO	Implicit	100	Geometric	1.139E-04
[B1]	155	1001	4500	1000	yes	4.165E-02	original	original	BO	Implicit	100	Geometric	6.878E-04
[B2]	155	1001	4500	1000	yes	2.083E-02	original	original	BO	Implicit	100	Geometric	6.878E-04
[B3]	155	1001	4500	1000	yes	1.041E-02	original	original	BO	Implicit	100	Geometric	6.878E-04
[B4]	155	1001	4500	1000	yes	5.206E-03	original	original	BO	Implicit	100	Geometric	6.878E-04
[B5]	155	1001	4500	1000	yes	2.603E-03	original	original	BO	Implicit	100	Geometric	6.878E-04
[B6]	155	1001	4500	1000	yes	1.302E-03	original	original	BO	Implicit	100	Geometric	6.878E-04
[B7]	155	1001	4500	1000	yes	6.508E-04	original	original	BO	Implicit	100	Geometric	6.878E-04
[C1]	155	1001	4500	1000	yes	8.330E-02	0	original	BO	Implicit	100	Geometric	6.878E-04
[C2]	155	1001	4500	1000	yes	6.508E-04	0	original	BO	Implicit	100	Geometric	6.878E-04
[D1]	155	1001	4500	1000	no			original	BO	Implicit	100	Geometric	6.878E-04
[D2]	155	1001	4500	1000	no			original	BO	Implicit	100	Geometric	6.508E-04
[E1]	155	1001	4500	100	no			original	BO	Implicit	100	Geometric	6.508E-04
[E2]	155	1001	4500	300	no			original	BO	Implicit	100	Geometric	6.508E-04
[E3	155	1001	4500	500	no			original	BO	Implicit	100	Geometric	6.508E-04
[E4]	155	1001	4500	2200	no			original	BO	Implicit	100	Geometric	6.508E-04
[E5]	155	1001	4500	2600	no			original	BO	Implicit	100	Geometric	6.508E-04
[E6]	155	1001	4500	3000	no			original	BO	Implicit	100	Geometric	6.508E-04
[E7]	155	1001	4500	3500	no			original	BO	Implicit	100	Geometric	6.508E-04
[E8]	155	1001	4500	4000	no			original	BO	Implicit	100	Geometric	6.508E-04
[E9]	155	1001	4500	4400	no			original	BO	Implicit	100	Geometric	6.508E-04
[F1]	155	1001	8000	1000	no			original	BO	Implicit	100	Geometric	6.508E-04
[F2]	155	2999	8000	1000	no			original	BO	Implicit	100	Equal-size	1.000E-01
[F3]	155	5999	8000	1000	no			original	BO	Implicit	100	Equal-size	5.008E-02
[F4]	155	10001	8000	1000	no			original	BO	Implicit	100	Equal-size	5.008E-02
[F5]	155	20001	8000	1000	no			original	BO	Implicit	100	Equal-size	1.500E-02
[F6]	155	50001	8000	1000	no			original	BO	Implicit	100	Equal-size	6.000E-03
[F7]	155	100001	8000	1000	no			original	BO	Implicit	100	Equal-size	2.999E-03
[F8]	155	1001	4500	1000	no			original	BO	Implicit	100	Equal-size	2.997E-01
[G1]	155	5999	8000	1000	no			original	BO	Impes(CFL=1)	100	Equal-size	5.008E-02
[G2]	155	5999	8000	1000	no			original	BO	Impes(CFL=1)	Surface(0.1691)	Equal-size	5.008E-02
[G3]	155	5999	8000	1000	no			original	BO	Implicit	Surface(0.1691)	Equal-size	5.008E-02
[G4]	155	5999	8000	1000	no			original	BO	Imp.(ExpWell)	100	Equal-size	5.008E-02
[H1]	155	5999	10000	1000	no			original	BO	Impes(CFL=1)	Surface(0.1691)	Equal-size	5.008E-02
[H2]	155	5999	10000	1000	no			original	BO	Implicit	Surface(0.1691)	Equal-size	5.008E-02
[I1]	100	5999	10000	1000	yes			original	BO	Implicit	100	Geometric	1.139E-04
[I2]	100	5999	10000	1000	yes			original	COMP	Implicit	100	Geometric	1.139E-04

The main purpose of work is the analysis of the OGR oscillations. The oscillatory behaviour of the LRS well is assessed in two stages:

- Early OGR oscillation for the time period from the start of simulation to 100th day.
- Late OGR oscillation for the time period from the 100th day to 1000th day.

OGR oscillation for a given period is defined as a difference between maximum and minimum OGR values for the given time period.

5.1 Case Study A: Original Cases

Case study A includes the base case scenario for highly undersaturated system. The 2 case studies discussed are Case [A1] and Case [A2]. They are original models used in SPE155499. The base case model properties are discussed in model description section. The case properties are reviewed in Table 5.2.

Cases [A1] and [A2] are identical, the only difference is the gridding; case [A1] has 1001 grid cells and case [A2] has 5999 grid cells. Both models are geometrically gridded with the smallest rock cell width of 0.000688 ft and 0.000114 ft respectively. The difference in the smallest matrix cell size arises from the number of grid cells.

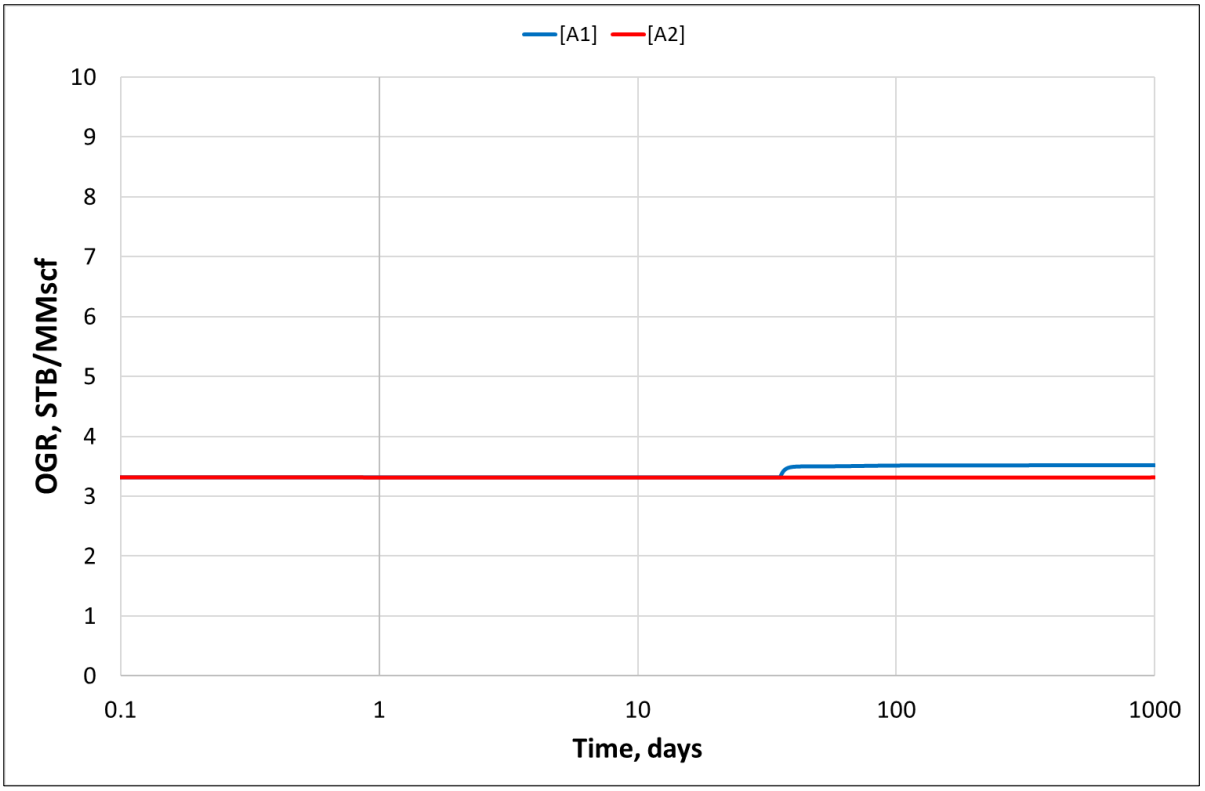

Figure 5.1. OGR trends for case study A

The log plot of oil-gas ratio for both cases are shown in Figure 5.1. Straight line behaviour with negligible oscillation is observed for both cases. The case [A1] results in higher early OGR oscillations compared to [A2]. Early OGR Oscillation for A1 is 47 STB/MMscf and 7 STB/MMscf for A2 as is clear from Table 5.3. Increase in the grid number shows considerable reduction in early OGR oscillations for the system with initial reservoir pressure of 4500 psia. The two cases experience no late OGR oscillation.

Table 5.3. OGR oscillation analysis for case study A

Case	Early OGR Oscillation	Late OGR Oscillation
ID	**STB/MMscf**	**STB/MMscf**
[A1]	47	0
[A2]	7	0

5.2 Case Study B: Hydraulic Fracture Width Analysis

Case B includes scenarios with different hydraulic fracture widths for highly undersaturated system. This study assesses the impact of fracture width on OGR oscillations. 7 case studies are discussed for which detailed information is given in Table 5.2.

Figure 5.2 illustrates OGR behaviour for the cases with different hydraulic fracture width. All cases experience straight line OGR behaviour. Flowing bottomhole pressure is kept constant at 1000 psia for all cases. Constant OGR behaviour is expected to be related to the constant flowing bottomhole pressure. Reducing the fracture grid size provides essentially faster drainage effect for the fracture, which also allows maintaining flowing bottomhole pressure and provides more constant OGR behaviour. The behaviour is confirmed in Figure 5.2.

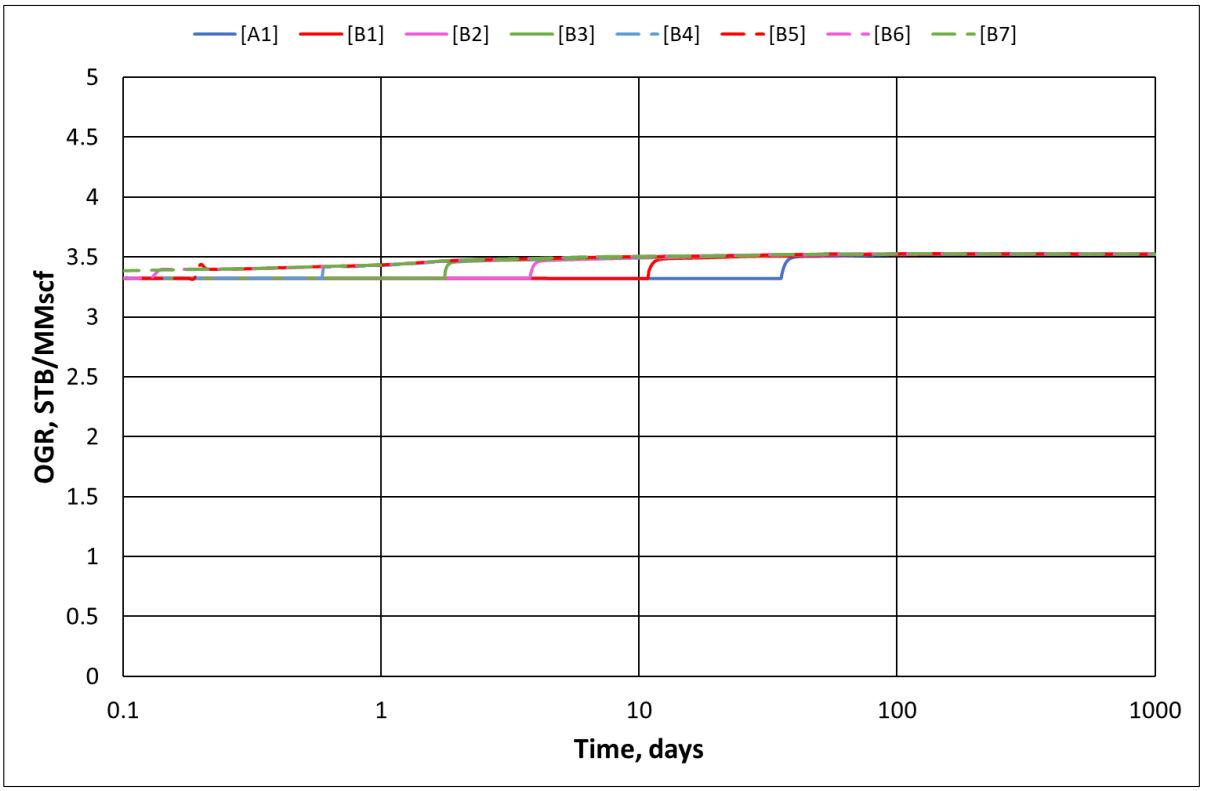

Figure 5.2. OGR trend for case study B

Reducing hydraulic fracture width reduces the oscillation, which is also captured in Table 5.4.

Table 5.4. OGR oscillation analysis for case study B

Case	Early OGR Oscillation	Late OGR Oscillation
ID	STB/MMscf	STB/MMscf
[B1]	35	0
[B2]	25	0
[B3]	19	0
[B4]	16	0
[B5]	14	0
[B6]	13	0
[B7]	12	0

Case [B7] has the smallest fracture size (0.00065 ft). It shows the smallest early OGR oscillation in comparison with the other cases. All cases experience no later OGR oscillation.

5.3 Case Study C: Fracture Relative Permeability Analysis

Case C studies the effect of hydraulic fracture relative permeability endpoints on the OGR oscillations for highly undersaturated systems. For the original fracture relative permeability endpoints, Table 4.6 can be referred to. For the study, all endpoint values are replaced by 0. Refer to Table 5.2 for detailed information. Two C cases are essentially original case [A1] and [B7] case with zero hydraulic fracture relative permeability endpoints.

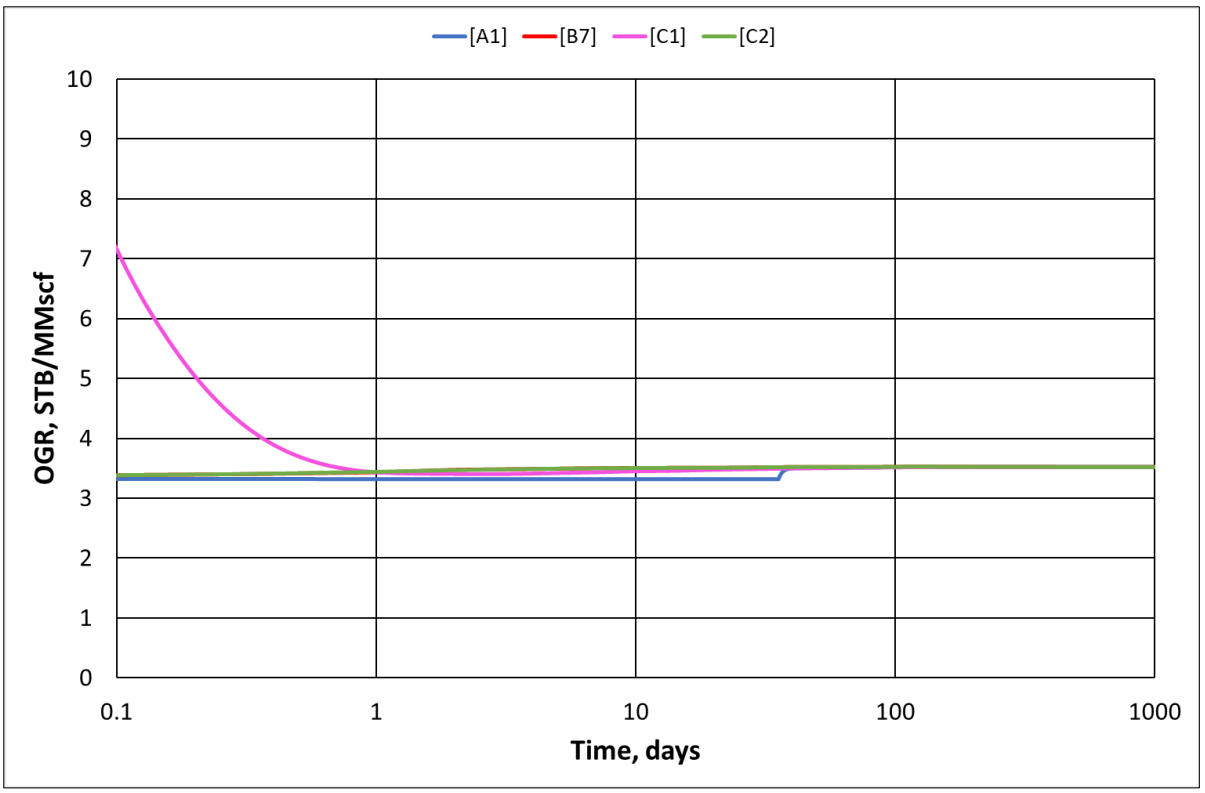

Figure 5.3. OGR trend for case study C

Case [C1] experiences high OGR at the early stages, which then drops to that of original case [A1]. Case [C2] follows the general OGR trend. Removing the relative permeability endpoints for hydraulic fracture results in increase in early OGR oscillations for both cases. No late OGR oscillations are observed for both cases.

Table 5.5. OGR oscillation analysis for case study C

Case	Early OGR Oscillation	Late OGR Oscillation
ID	STB/MMscf	STB/MMscf
[C1]	79	0
[C2]	15	0

5.4 Case Study D: No-Fracture Analysis

Case D analyses the scenarios with no fracture properties. Two cases, [A1] and [B7], with the greatest fracture cell width and the smallest fracture cell width respectively, are modified (i.e. fracture properties are removed) in case study D; they are treated as full rock model (i.e. with no fracture). Refer to Table 5.2 for detailed information.

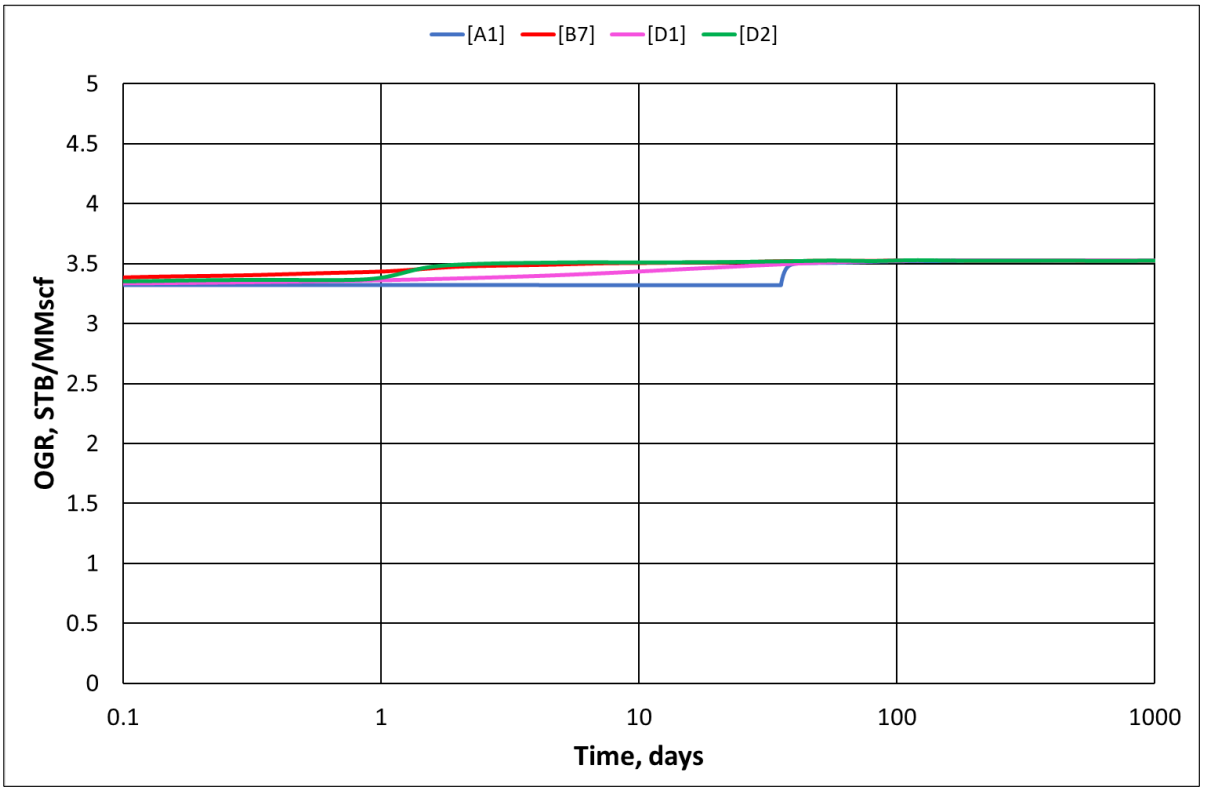

Figure 5.4. OGR trend for case study D

The OGR behaviour for Case D is shown in Figure 5.4. No significant oscillation is observed, the cases follow the straight line OGR trend. Oscillation analysis in Table 5.6 shows that no significant change in OGR oscillation is observed. Fracture properties show no clear impact on the oscillation behaviour; the presence or absence of fracture properties does not have a clear effect on OGR oscillation.

Table 5.6. OGR oscillation analysis for case study D

Case	Early OGR Oscillation	Late OGR Oscillation
ID	STB/MMscf	STB/MMscf
[D1]	25	0
[D2]	13	0

5.5 Case Study E: Flowing Bottomhole Pressure Analysis

Case E includes the studies carried out to analyse the effect of flowing bottomhole pressure on OGR oscillation for highly undersaturated system. 9 case studies are considered. Refer to Table 5.2 for detailed information.

Figure 5.5 shows different OGR trends for different flowing bottomhole pressure cases. All follow a straight line OGR behaviour, but all are characterised by different OGR values. Changing the flowing bottomhole pressure affects the production performance of the LRS well, which explains different OGR values for different cases. The saturation pressure for the system in all cases at gas oil contact is 4473 psia. Increasing flowing bottomhole pressure gradually from 100 psia to 4400 psia means getting closer to the saturation pressure above which the system is single phase. According to the definition of OGR, this explains why greater OGR is observed at higher flowing bottomhole pressure case [E9] (i.e. higher liquid fraction, lower gas fraction close to saturation pressure) although production rates are lower than the base case [A1]. For the production performance, Appendix can be referred to.

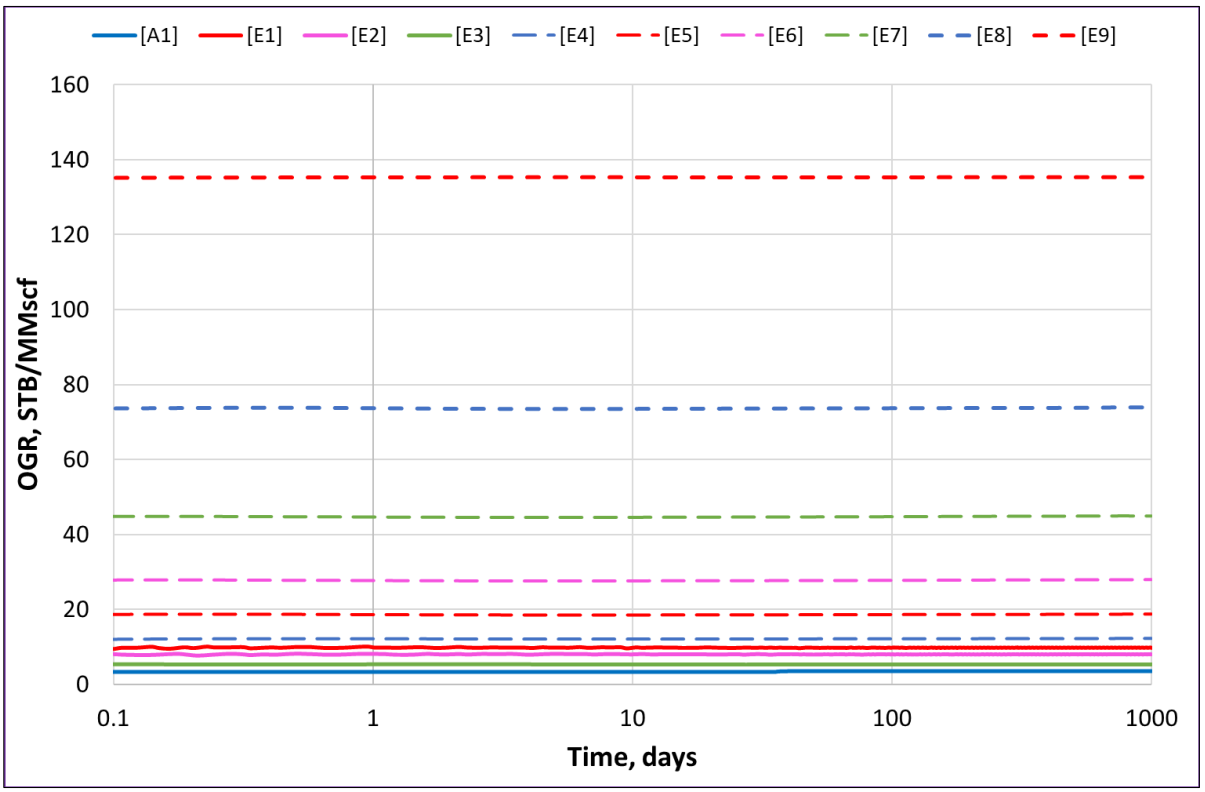

Figure 5.5. OGR trends for case study E

Table 5.7 shows that OGR oscillations for all cases are negligible with early OGR oscillations up to 19 STB/MMscf. No late OGR oscillations are observed.

Table 5.7. OGR oscillation analysis for case study E

Case	Early OGR Oscillation	Late OGR Oscillation
ID	STB/MMscf	STB/MMscf
[E1]	19	0
[E2]	14	0
[E3	14	0
[E4]	3	0
[E5]	2	0
[E6]	2	0
[E7]	2	0
[E8]	3	0
[E9]	1	0

5.6 Case Study F: Grid Cell Analysis

Case F summarizes the studies with different grid sizes, or more specifically, grid cell number. All cases are 1D equal-size models. Only the number of grid cells are changed in X direction. All cases have no fracture properties as case D shows that removing the fracture properties does not influence the oscillations at all. Equal-size gridding are implemented; geometric gridding is not applied.

The previous studies follow the initial reservoir pressure of 4500 psia. Also, Case A analyses the impact of grid cell number in OGR oscillation at 4500 psia. In this case study, initial reservoir pressure is raised to 8000 psia. The idea is to analyse the impact of high reservoir pressure on OGR oscillations and how it changes with grid cell number. Seven case studies are discussed. Refer to Table 5.2 for detailed information.

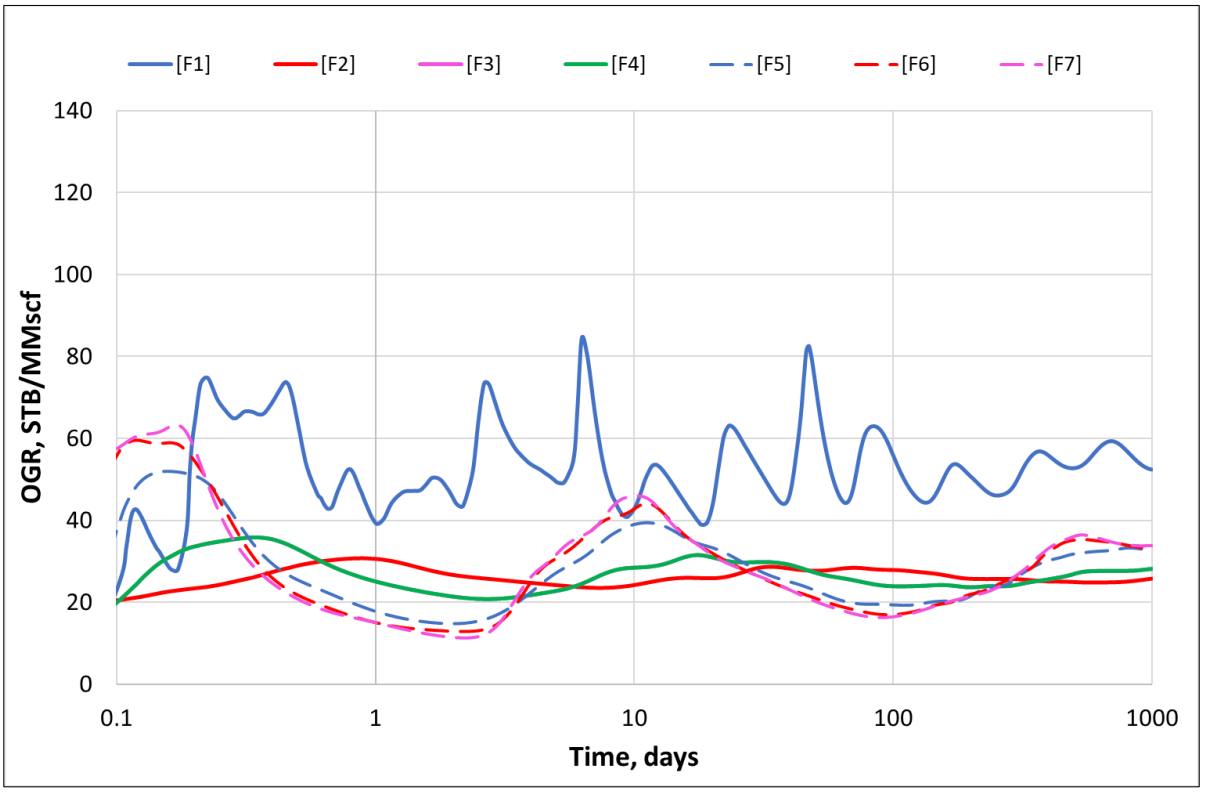

Figure 5.6. OGR trends for case study F

Figure 5.6 represents OGR trends for 7 cases. Significant OGR oscillations are observed at higher reservoir pressure conditions. Case [F1], which is equal-size gridded case with 1001 cells, shows the highest frequency for OGR oscillation. Increasing grid cell numbers from 1001 to 100001 converges solution. Later cases with greater number of grid cells (i.e. cases [F5], [F6], [F7] with 20001, 50001, and 100001 cells respectively) represent very similar results, and OGR trends with reduced oscillation frequency are also observed.

Despite the decrease in oscillation frequency with increasing grid cell number, OGR oscillation still cannot be avoided. Except case [F1] with 1001 grid cells, other cases result in almost closer early OGR oscillation values, specifically, cases [F5], [F6], and [F7]. They are shown in Table 5.8. Compared to the previous cases with lower initial reservoir pressure, late OGR oscillations are also observed at initial reservoir pressure of 8000 psia.

Table 5.8. OGR oscillation analysis for case study F

Case	Early OGR Oscillation	Late OGR Oscillation
ID	STB/MMscf	STB/MMscf
[F1]	179	15
[F2]	121	3
[F3]	113	4
[F4]	117	9
[F5]	117	14
[F6]	118	18
[F7]	117	20
[F8]	61	0

It is assumed that 2 factors are the main reasons of the early and late OGR oscillations at such high amplitudes. Firstly, as discussed above, it is the higher pressure that causes such a highly oscillatory GOR behaviour during IA flow.

The second reason behind the oscillations is thought to be the gridding. Equal size gridding (i.e. all the grids have the same size) causes deviation from the straight line OGR behaviour. A small study below compares OGR trends of geometrically gridded model and equal-size model. Both have 1001 grid cells and initial reservoir pressure of 4500 psia. Figure 5.8 represents both trends for OGR. Geometrically gridded model [A1] shows a straight line OGR behaviour, while case [F8] which is the model with equally sized grids. For case [F8], early OGR oscillations are observed considerably, which is around 61 STB/MMscf. Technically, the oscillation can rather be considered a deviation than oscillation. The late OGR oscillation is not observed.

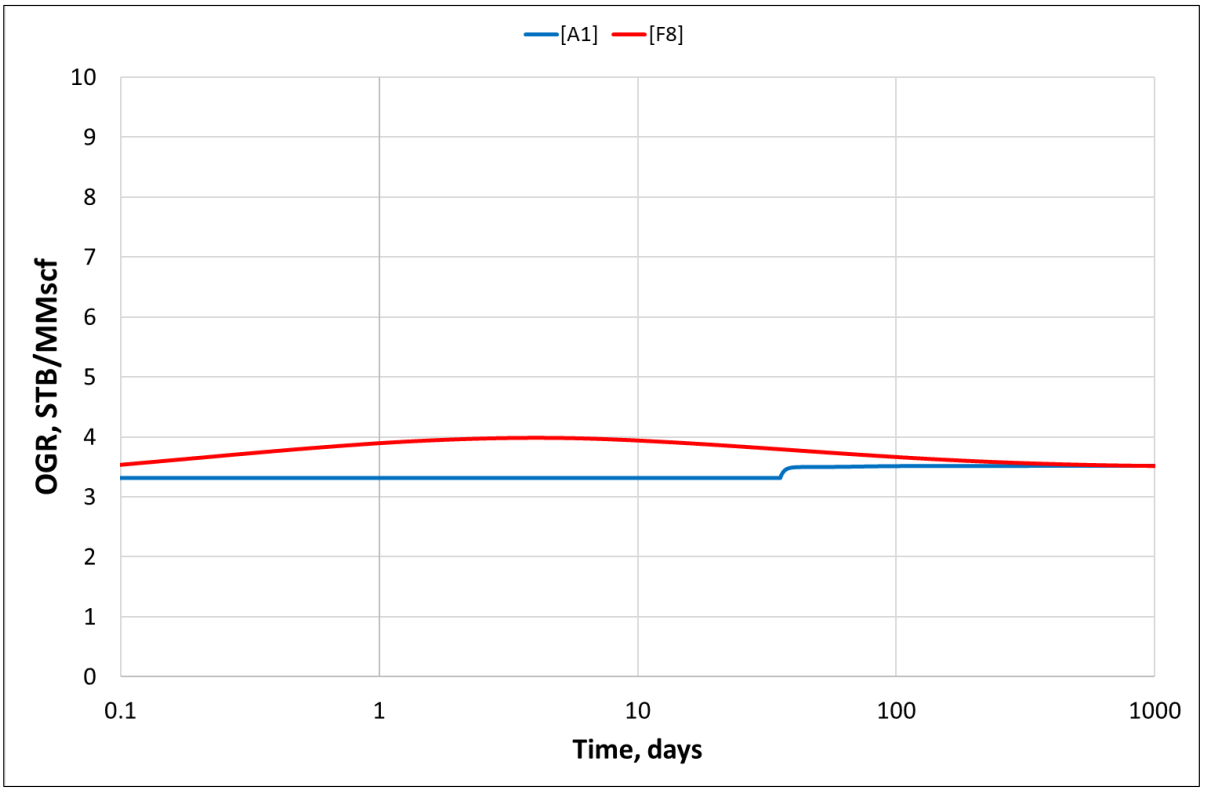

Figure 5.7. OGR trends for geometrically gridded model [A1] and equally gridded model [F8]

5.7 Case Study G: Numerical Solution Analysis

Case study G analyses the effect of numerical solution on the OGR oscillations. Following solutions are implemented in the study:

- Fully implicit solution with PI=100 rb cP/day psia
- Implicit solution with Surface label[2]
- Implicit solution with Explicit well treatment[3] and PI=100 rb cP/day psia
- Impes solution (CFL[4]=1) with PI=100 rb cP/day psia
- Impes solution (CFL=1) with Surface label

Case [F3] with fully implicit numerical solution is used as a base case to compare different numerical solutions. Refer to Table 5.2 for detailed information.

[2] Surface label, a keyword in sensor, allows well index to be calculated internally for planar surface wells. Surface label calculated PI is 0.1691 rb cP/day psia for the study.
[3] Explicit well treatment, a keyword in sensor, allows well terms treated explicitly with Implicit formulations in 1D model.
[4] The entry CFL is a logic used for calculating and implementing impes stable timestep size. (59)

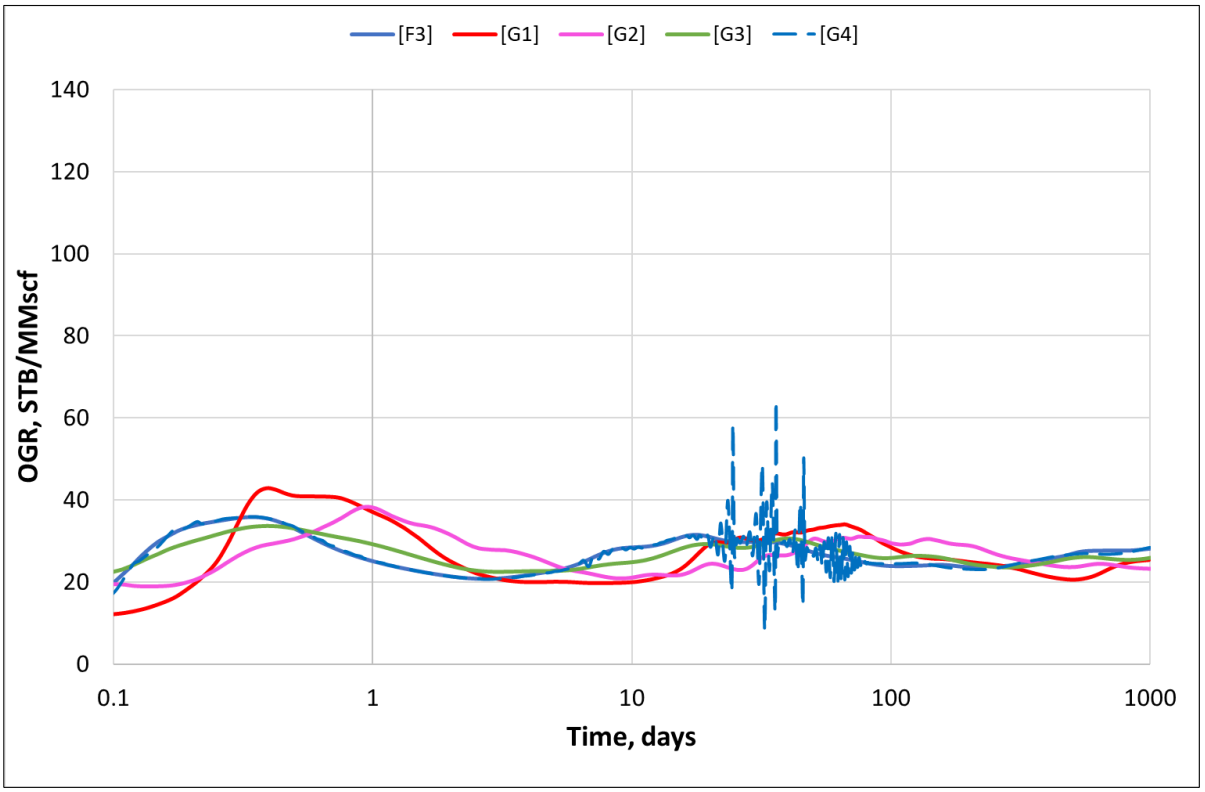

Figure 5.8. OGR trends for case study G

Figure 5.8 shows OGR trends for different numerical solutions. All solutions provide very close results. Only case [G4], Implicit solution with Explicit well treatment and PI=100 rb cP/day psia, shows significant frequent oscillations between days 10 and 100. All cases do not experience straight line behaviour.

Table 5.9. OGR oscillation analysis for case study G

Case	Early OGR Oscillation	Late OGR Oscillation
ID	STB/MMscf	STB/MMscf
[G1]	120	8
[G2]	103	7
[G3]	102	3
[G4]	116	5

Table 5.9 shows OGR oscillation analysis for case G. All cases are similar in terms of early OGR oscillation. Late OGR oscillations observed are very close and negligible.

5.8 Case Study H: High Reservoir Pressure Analysis

The case H analyses impes solution (CFL=1) and fully implicit solution at higher reservoir pressure (P_{ri}=10000 psia). The productivity indices are calculated internally with surface label. The idea is to analyse the impact of greater initial reservoir pressure on OGR oscillations and how OGR behaviour is affected by different solutions. Both cases are 1D equal-size gridded models. Refer to Table 5.2 for detailed information.

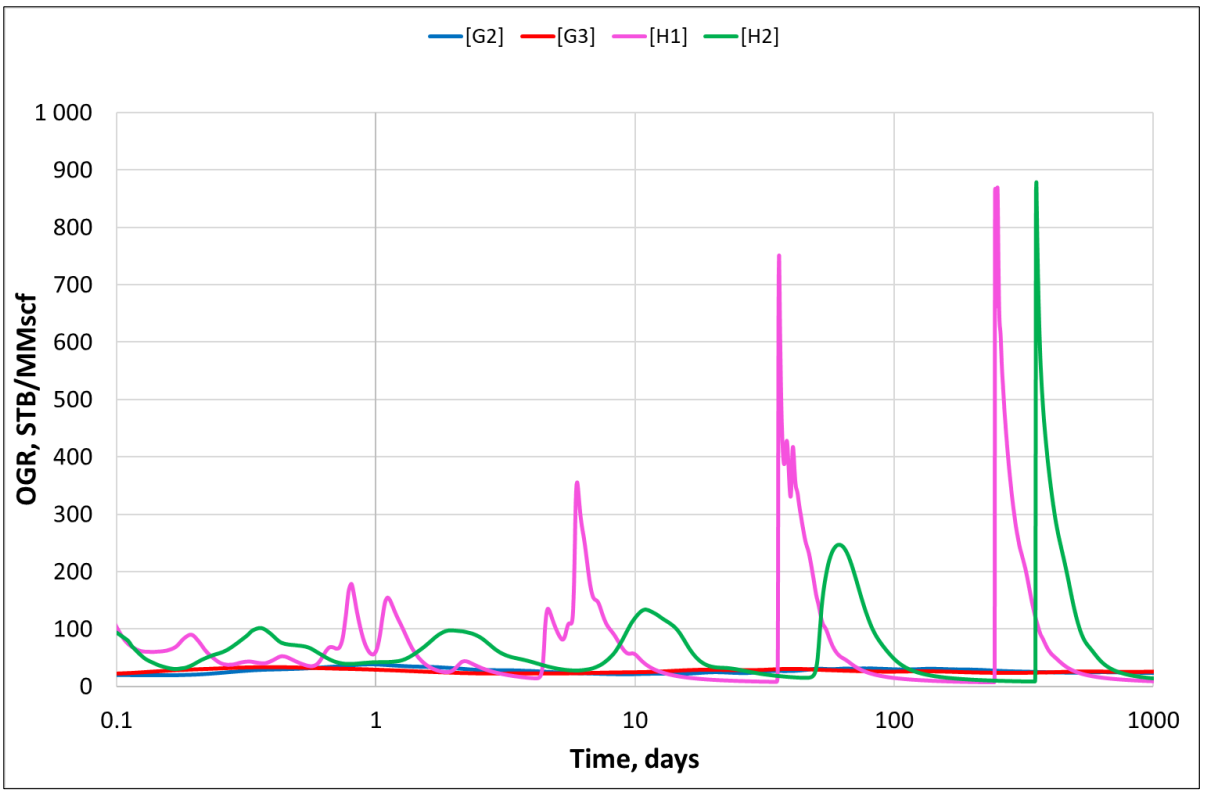

Figure 5.9 OGR trends for case study H

Figure 5.9 shows OGR trends for highly saturated LRS system. Changing the initial reservoir pressure from 8000 psia to 10000 psia significantly influences the OGR behaviour. Periodic surges of high producing OGR are observed for both cases. The surges are continuous throughout the whole simulation time. Table 5.10 shows late OGR oscillations outweigh the early OGR oscillations.

Table 5.10. OGR oscillation analysis for case study H

Case	Early OGR Oscillation	Late OGR Oscillation
ID	STB/MMscf	STB/MMscf
[H1]	743	862
[H2]	232	871

5.9 Case Study I: Numerical Modelling Analysis

The final study involves two cases with different modelling to analyse the impact of different modelling on OGR oscillations. Both cases are 1D geometrically gridded models, highly undersaturated system with initial reservoir pressure of 10000 psia and initial OGR of 100 STB/MMscf. The cases are solved implicitly with the productivity index of 100 rb cP/day psia. Case [I1] is black oil model, and case [I2] is compositional model. Refer to Table 5.2 for detailed information.

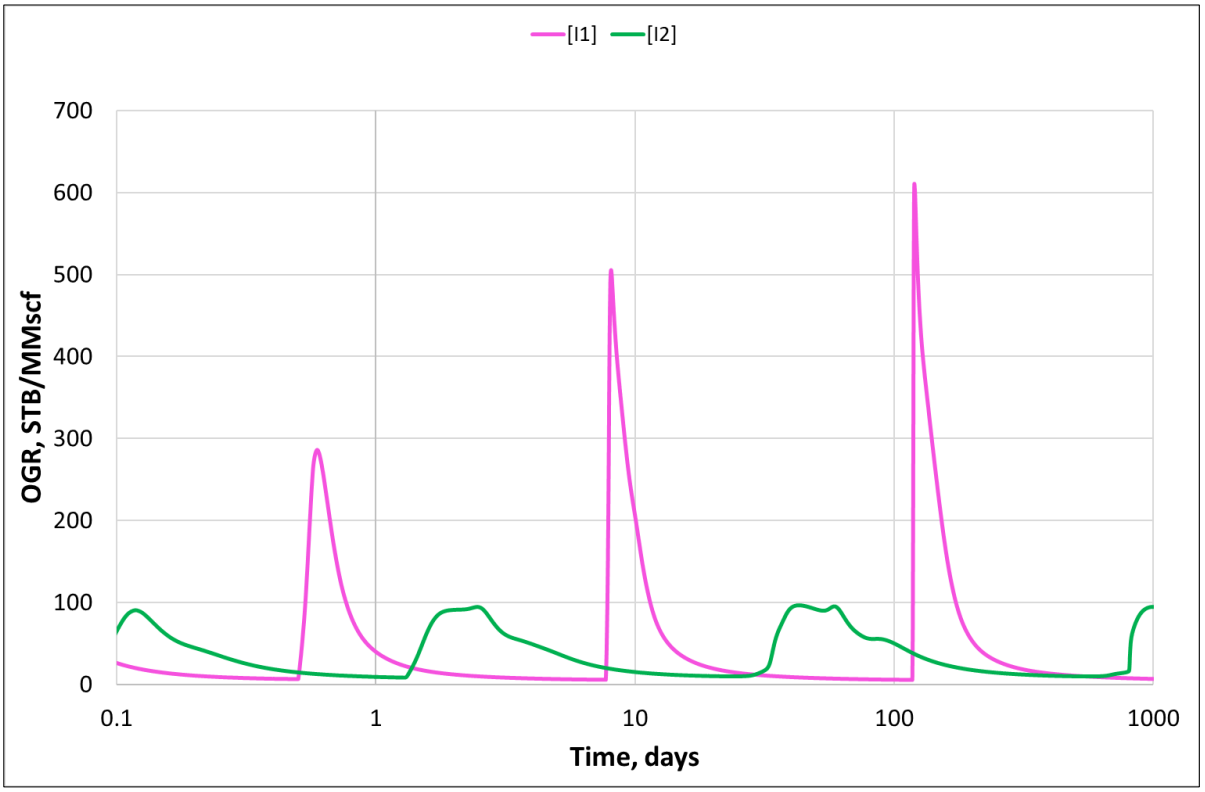

Figure 5.10. OGR trends for case study I

Figure 5.10 shows OGR trends for cases [I1] and [I2]. Case [I1] shows significant periodic OGR surges. Increase in surge amplitudes is observed towards the end of simulation period. Case [I2] with compositional modelling also shows periodic surges, however, they are significantly reduced. Table 5.11 confirms that compositional model shows significantly reduced early and late OGR oscillations (i.e. nearly reduced by a factor of 5 to 8 times).

Table 5.11. OGR oscillation analysis for case study I

Case	Early OGR Oscillation	Late OGR Oscillation
ID	STB/MMscf	STB/MMscf
[I1]	502	604
[I2]	93	84

The production performance for case study I shows that the two cases follow similar trend, although there is a slight mismatch between black oil model and compositional model results.

6 Conclusion

The project is carried out to study the impact of several factors on the OGR oscillations in liquid-rich shale wells.

- Studies show that hydraulic fracture width has discernible effect on the OGR oscillations. Reducing the hydraulic fracture width decreases the OGR oscillations. It is shown in the case study B that changing hydraulic fracture width from original 0.0833 ft to 0.01041 in case [B3] reduces early OGR oscillations considerably, but below that width it has negligible effect. No late OGR oscillations are observed for the cases. All the cases show identical behaviour in terms of production performance (i.e. cumulative production, and daily rates).
- Removing fracture relative permeability shows considerable increase in early OGR oscillations for case [C1] and negligible increase in [C2]. This study, due to time limit, could not be analysed in detail. It could be worth to look at this specific case to understand the impact of fracture relative permeability endpoints on OGR oscillations.
- Removing the fracture properties and treating the model as fully rock, shows no significant changes in early OGR oscillations. No late OGR oscillations are observed. Both cases in study D have the same production performance.
- Changing the flowing bottomhole pressure does not change the OGR behaviour; straight line trend is observed for all cases. However, OGR values vary for the cases, and this is thought to be related to the production behaviour. At lower flowing bottomhole pressures, phase separation is more likely to occur, and greater volumes of gas release. According to the definition of OGR, it stands for lower OGR values. This explains the higher OGR values for higher flowing bottomhole pressures. Higher flowing bottomhole pressure also results in lower oil production.
- The effect of grid cells at lower reservoir pressures are analysed in case A. Case F analyses the similar impact for higher undersaturated systems (8000 psia). Increasing the grid cell numbers converge the solution. This explains the similar production behaviour of the cases with greater number of grid cells. All the cases show highly oscillatory OGR behaviour. Changing the gird cell number does not influence the oscillation amplitude for early and late cases. However, the frequency of oscillation is reduced by increasing the number of cells.

- A small study done for the analysis of the effect of geometric gridding and equally sized gridding in the study F shows that equal-size gridding can be a factor leading to OGR oscillations.
- The impact of different numerical solutions is also analysed. All cases show almost similar results. Only implicit solution with surface label show negligibly good result in terms of OGR oscillation amplitudes. Production performance of all cases match each other.
- It has been found that the degree of undersaturation has a clear effect on OGR oscillations. The level of OGR oscillations rises at higher reservoir pressures. The results show that different numerical solution may not converge fully to each other at higher undersaturation cases (i.e. 10000 psia).
- The OGR oscillations are also related to numerical modelling. Two studies with different numerical models (i.e. black oil model and compositional model) show similar repeated surges. Significant periodic surges of OGR in black oil modelling are observed. In comparison, the compositional modelling results in reduced amplitude of surges. Compositional modelling is more likely to be implemented for liquid-rich shale well modelling for highly undersaturated system to achieve constant OGR behaviour.

All the cases, except those that change the production behaviour (case E) and solution convergence (case F), show that the presence of OGR oscillations does not influence the production behaviour, in fact the same or similar results are achieved for the cases in each category. Eliminating the OGR oscillations does not alter the production behaviour. That brings the question that if it is important to completely get rid of OGR oscillations in numerical studies or accept it to some extent. The study shows that OGR oscillations are significant in highly undersaturated systems that can even have an impact on liquid production performance.

7 References

1. IEA. 2020. Data-Statistics - IEA. [online] Available at: https://www.iea.org/data-and-statistics?country=WORLD&fuel=Energy%20consumption&indicator=Total%20final%20consumption%20(TFC)%20by%20source. [Accessed 3 May 2020].
2. EIA projects 28% increase in world energy use by 2040 - Today in Energy - U.S. Energy Information Administration (EIA). 2020. [online] Available at: https://www.eia.gov/todayinenergy/detail.php?id=32912. [Accessed 4 May 2020].
3. Leimkuhler, J. and Leveille, G., 2012. Unconventional resources. The Way Ahead, 8(01), pp.27-28.
4. Song, C. and Yang, D., 2013, November. Performance evaluation of CO2 huff-n-puff processes in tight oil formations. In SPE Unconventional Resources Conference Canada. Society of Petroleum Engineers.
5. Chakraborty, N. and Karpyn, Z.T., 2015, September. Gas permeability evolution with soaking time in ultra-tight shales. In SPE Annual Technical Conference and Exhibition. Society of Petroleum Engineers.
6. Shoaib, S. and Hoffman, B.T., 2009, January. CO2 flooding the Elm Coulee field. In SPE Rocky Mountain Petroleum Technology Conference. Society of Petroleum Engineers.
7. Christensen, J.R., Stenby, E.H. and Skauge, A., 1998, January. Review of WAG field experience. In International petroleum conference and exhibition of Mexico. Society of Petroleum Engineers.
8. Zou, C., 2017. Unconventional petroleum geology. Elsevier.
9. SPE, AAPG, WPC, SPEE & SEG. 2011. Guidelines for Application of the Petroleum Resources Management System. 2011. Society of Petroleum Engineers.
10. Unconventional Petroleum Resources. Geoscience Australia. 2020. [online] Available at: https://www.ga.gov.au/scientific-topics/energy/resources/petroleum-resources/unconventional-resources. [Accessed 12 May 2020].
11. OECD. Publishing and International Energy Agency, 2013. World energy outlook 2013. International Energy Agency.
12. Cander, H., 2012. PS what are unconventional resources? A simple definition using viscosity and permeability. In AAPG Annual Convention and Exhibition. Tulsa, US: American Association of Petroleum Geologists and Society for Sedimentary Geology.

13. C. H. Whitson, 2018. TPG4150 Reservoir Recovery Techniques Lecture Notes, NTNU
14. Canadian Society for Unconventional Resources (CSUR). Understanding Tight Oil. Calgary. [online] Available at: www.mpgpetroleum.com/home/docs/Understanding_TightOil_FINAL.pdf. [Accessed 12 May 2020].
15. Oil, T.R.S., 2013. Shale Gas Resources: An Assessment of 137 Shale Formations in 41 Countries Outside the United States. Washington: Independent Statistics & Analysis and US Department of Energy.
16. Aguilera, R., 2013. Flow Units: From Conventional to Tight Gas to Shale Gas to Tight Oil to Shale Oil Reservoirs. Society of Petroleum Engineers.
17. Whitson, C.H. and Sunjerga, S., 2012, January. PVT in liquid-rich shale reservoirs. In SPE Annual Technical Conference and Exhibition. Society of Petroleum Engineers.
18. Oil and Gas Conservation Rules. Alberta Regulation 151/1971. [online] Available at: www.qp.alberta.ca/documents/Regs/1971_151.pdf. [Accessed 14 May 2020].
19. Harvey Blatt, Robert J. Tracy, Robert Tracy, 1995. Petrology: Igneous, Sedimentary, and Metamorphic, 2nd ed. W. H. Freeman.
20. Shaw, D.B. and Weaver, C.E., 1965. The mineralogical composition of shales. Journal of Sedimentary Research, 35(1), pp.213-222.
21. Glorioso, J.C. and Rattia, A., 2012, March. Unconventional reservoirs: basic petrophysical concepts for shale gas. In SPE/EAGE European Unconventional Resources Conference & Exhibition-From Potential to Production (pp. cp-285). European Association of Geoscientists & Engineers.
22. IEA. 2013. Golden Rules for a Golden Age of Gas, IEA, Paris. [online] Available at: www.iea.org/reports/golden-rules-for-a-golden-age-of-gas. [Accessed 12 May 2020].
23. Law, B.E., 2002. Basin-centered gas systems. AAPG bulletin, 86(11), pp.1891-1919.
24. Smocker, J.W., 2005. US Geological Survey Assessment Concepts for Continuous Petroleum Accumulations 1995.
25. Usman Ahmed, D. Nathan Meehan, Stephen A. Holditch, 2016. Unconventional oil and gas Resources Exploitation and Development, CRC Press.
26. U.S. Energy Information Administration (EIA). 2020. [online] Available at: https://www.eia.gov/analysis/studies/worldshalegas/. [Accessed 18 May 2020].

27. Natural gas explained - U.S. Energy Information Administration (EIA). 2020. [online] Available at: https://www.eia.gov/energyexplained/natural-gas/. [Accessed 20 May 2020].
28. Stevens, P., 2012. The shale gas revolution: Developments and changes (pp. 2-3). London: Chatham House.
29. Sohrab Zendehboudi, Alireza Bahadori, 2016. Shale Oil and Gas Handbook: Theory, Technologies, and Challenges. Elsevier Science.
30. Maps: Oil and Gas Exploration, Resources, and Production - Energy Information Administration. 2020. [online] Available at: www.eia.gov/maps/maps.htm. [Accessed 21 May 2020].
31. Where our natural gas comes from - U.S. Energy Information Administration (EIA). 2020. [online] Available at: www.eia.gov/energyexplained/natural-gas/where-our-natural-gas-comes-from.php. [Accessed 21 May 2020].
32. Javadpour, F., Fisher, D. and Unsworth, M., 2007. Nanoscale gas flow in shale gas sediments. Journal of Canadian Petroleum Technology, 46(10).
33. Ruppel, S.C. and Loucks, R.G., 2008. Black mudrocks: lessons and questions from the Mississippian Barnett Shale in the southern Midcontinent. The Sedimentary Record, 6(2), pp.4-8.
34. Wang, F.P. and Reed, R.M., 2009, January. Pore networks and fluid flow in gas shales. In SPE annual technical conference and exhibition. Society of Petroleum Engineers.
35. Aguilera, R., 2010. Flow Units: From Conventional to Tight Gas to Shale Gas-Reservoirs. Paper SPE 132845 presented at the SPE Trinidad and Tobago Energy Resources Conference, Port of Spain, Trinidad, 27-30 June.
36. Andrade, J., Civan, F., Devegowda, D. and Sigal, R.F., 2011, June. Design and examination of requirements for a rigorous shale-gas reservoir simulator compared to current shale-gas simulators. In North American Unconventional Gas Conference and Exhibition, The Woodlands, Texas, USA. Society of Petroleum Engineers.
37. Swami, V., 2013. Development of a ‘Quad Porosity’ Numerical Flow Model for Shale Gas Reservoirs (Master's thesis, Engineering).
38. Aguilera, R. and Lopez, B., 2013, August. Evaluation of quintuple porosity in shale petroleum reservoirs. In SPE Eastern Regional Meeting. Society of Petroleum Engineers.

39. Maugeri, L., 2013. The shale oil boom: a US phenomenon. Harvard Kennedy School, Belfer Center for Science and International Affairs.
40. Tight oil expected to make up most of U.S. oil production increase through 2040 - Today in Energy - U.S. Energy Information Administration (EIA). 2020. [online] Available at: https://www.eia.gov/todayinenergy/detail.php?id=29932. [Accessed 22 May 2020].
41. US Energy Information Administration (EIA). 2019. Annual Energy Outlook. [online] Available at: www.eia.gov/outlooks/aeo/pdf/aeo2019.pdf. [Accessed 25 December 2019]
42. Khanal, A., Khoshghadam, M., Makinde, I. and Lee, W.J., 2015, October. Modeling production decline in liquid rich shale (LRS) gas condensate reservoirs. In SPE/CSUR Unconventional Resources Conference. Society of Petroleum Engineers.
43. How much oil and gas are actually in the Bakken Formation. 2020. [online] Available at: www.usgs.gov/faqs/how-much-oil-and-gas-are-actually-bakken-formation?qt-news_science_products=0#qt-news_science_products. [Accessed 22 May 2020].
44. Wan, J., Barnum, R.S., Digloria, D.C., Leahy-Dios, A., Missman, R. and Hemphill, J., 2013, March. Factors controlling recovery in liquids rich unconventional systems. In IPTC 2013: International Petroleum Technology Conference (pp. cp-350). European Association of Geoscientists & Engineers.
45. Holditch, S.A., 2006. Tight gas sands. Journal of Petroleum Technology, 58(06), pp.86-93.
46. Khan, W.A., Rehman, S.A., Akram, A.H. and Ahmad, A., 2011, January. Factors affecting production behavior in tight gas reservoirs. In SPE/DGS Saudi Arabia Section Technical Symposium and Exhibition. Society of Petroleum Engineers.
47. Mallick, M. and Achalpurkar, M.P., 2014, November. Factors controlling shale gas production: geological perspective. In Abu Dhabi International Petroleum Exhibition and Conference. Society of Petroleum Engineers.
48. Ali, T.A. and Sheng, J.J., 2015, October. Evaluation of the effect of stress-dependent permeability on production performance in shale gas reservoirs. In SPE eastern regional meeting. Society of Petroleum Engineers.
49. Joshi, S.D. and Ding, W., 1996, January. Horizontal well application: reservoir management. In International Conference on Horizontal Well Technology. Society of Petroleum Engineers.

50. Amber L. Tuft, 2015. Unconventional Oil and Shale Gas: Growth, Extraction, and Water Management Issues, New York: Nova Science Publishers, Incorporated
51. Lau, H.C. and Yu, M., 2013, March. Production technology challenges of tight and shale gas production in China. In IPTC 2013: International Petroleum Technology Conference (pp. cp-350). European Association of Geoscientists & Engineers.
52. Kanfar, M.S. and Clarkson, C.R., 2017, February. Factors affecting huff-n-puff efficiency in hydraulically-fractured tight reservoirs. In SPE Unconventional Resources Conference. Society of Petroleum Engineers.
53. Yu, W., Lashgari, H. and Sepehrnoori, K., 2014, April. Simulation study of CO2 huff-n-puff process in Bakken tight oil reservoirs. In SPE Western North American and rocky mountain joint meeting. Society of Petroleum Engineers.
54. Pankaj, P., Mukisa, H., Solovyeva, I. and Xue, H., 2018, August. Enhanced oil recovery in eagle ford: opportunities using huff-n-puff technique in unconventional reservoirs. In SPE Liquids-Rich Basins Conference-North America. Society of Petroleum Engineers.
55. Dake, L.P., 1983. Fundamentals of reservoir engineering. Elsevier.
56. Curtis H. Whitson, Michael R. Brulé. 2000 Phase behavior, Richardson, Tex: Henry L. Doherty Memorial Fund of AIME, Society of Petroleum Engineers.
57. About Sensor. 2020. [online] Available at: www.coatsengineering.com/sensor_reservoir_simulator.htm. [Accessed 26 May 2020].
58. Techopedia.com. 2020. What is Microsoft Excel? - Definition from Techopedia. [online] Available at: https://www.techopedia.com/definition/5430/microsoft-excel. [Accessed 26 May 2020].
59. CEI, S., 2011. System for Efficient Numerical Simulation of Oil Recovery, SENSOR Manual, Coats Engineering. Inc., April 1.

8 Nomenclature

8.1 Acronyms

$STOIP$ – Stock Tank Oil in Place

EOR – Enhanced oil recovery

$CSUR$ – Canadian Society for Unconventional Resources

LRS – Liquid-Rich Shale

$ERCB$ – Energy Resources Conservation Board

EIA – Energy Information Administration

$USGS$ – U.S. Geological Survey

bpd – Barrels per day

PVT – Pressure, Volume and Temperature

GOR – Gas-oil ratio

OGR – Oil-gas ratio

EOS – Equation of state

STB – Stock tank barrel ($MSTB$ =1000 STB)

scf – Standard cubic foot ($MMscf$ =10^6 scf)

$RELP$ – Relative Permeability

BO – Black oil

$COMP$ – Compositional

8.2 Symbols

P_{Ri} = Initial reservoir pressure, psia

P_{wf} = Flowing bottomhole pressure, psia

P_{sat} = Saturation Pressure

R_{go} = Gas-oil ratio

r_{og} = Oil-gas ratio

R_p = Producing gas-oil ratio

r_p = Producing oil-gas ratio

R_s = Solution gas-oil ratio

r_s = Solution oil-gas ratio

$V_{\bar{g}} = \left(V_g\right)_{sc}$ = Surface gas volume (i.e. gas volume at standard conditions)

$V_{\bar{o}} = (V_o)_{sc}$ = Stock-tank oil volume (i.e. oil volume at standard conditions)

μ = Viscosity

k = Permeability

k_h = Horizontal permeability

k_{ri} = Relative permeability for phase i, i can be oil (o), water (w) and gas (g)

k_{orw} = Relative Permeability to Oil Relative to Water

k_{org} = Relative Permeability to Oil Relative to Gas

k_{rg} = Relative Permeability to Gas

S_i = Saturation of phase i, i can be oil (o), water (w) and gas (g)

S_{gc} = Critical saturation of gas

S_{orw} = Residual Oil Saturation to Water

S_{org} = Residual Oil Saturation to Gas

S_{wc} = Connate Water Saturation

n_w = Power Law Water Exponent

n_{ow} = Power Law Oil Exponent Relative to Water

n_{og} = Power Law Oil Exponent Relative to Gas

n_g = Power Law Gas Exponent

Nx = Number of grids in x direction

$DELX$ = Grid cell dimension in x direction

PC = Criticial Pressure, psia

TC = Critical Temperature, °R

MW = Molecular weight

$PCHOR$ = Parachor

AC = Acentric factor

$SHIFT$ = Shift factor

$CRITZ = Z_c$ factors

9 Appendix

9.1 Production Performance

9.1.1 Case Study A

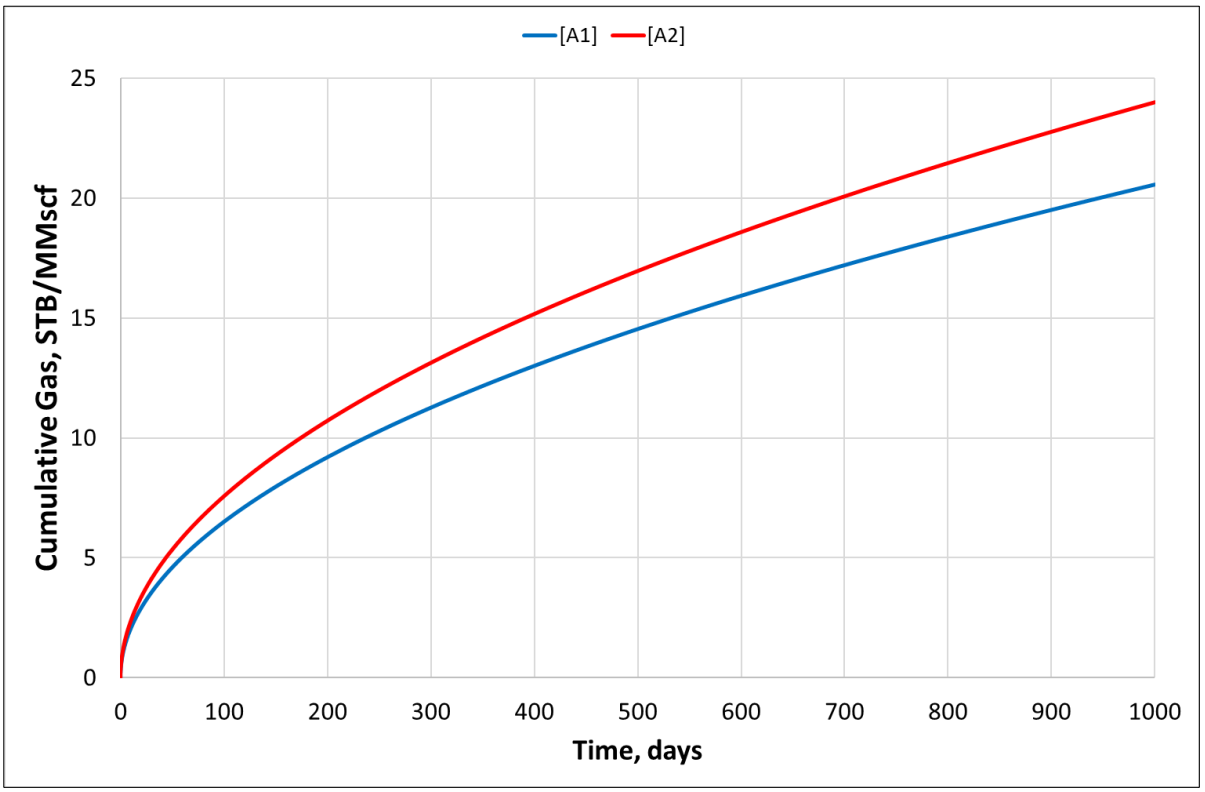

Figure 9.1. Cumulative gas production for case study A

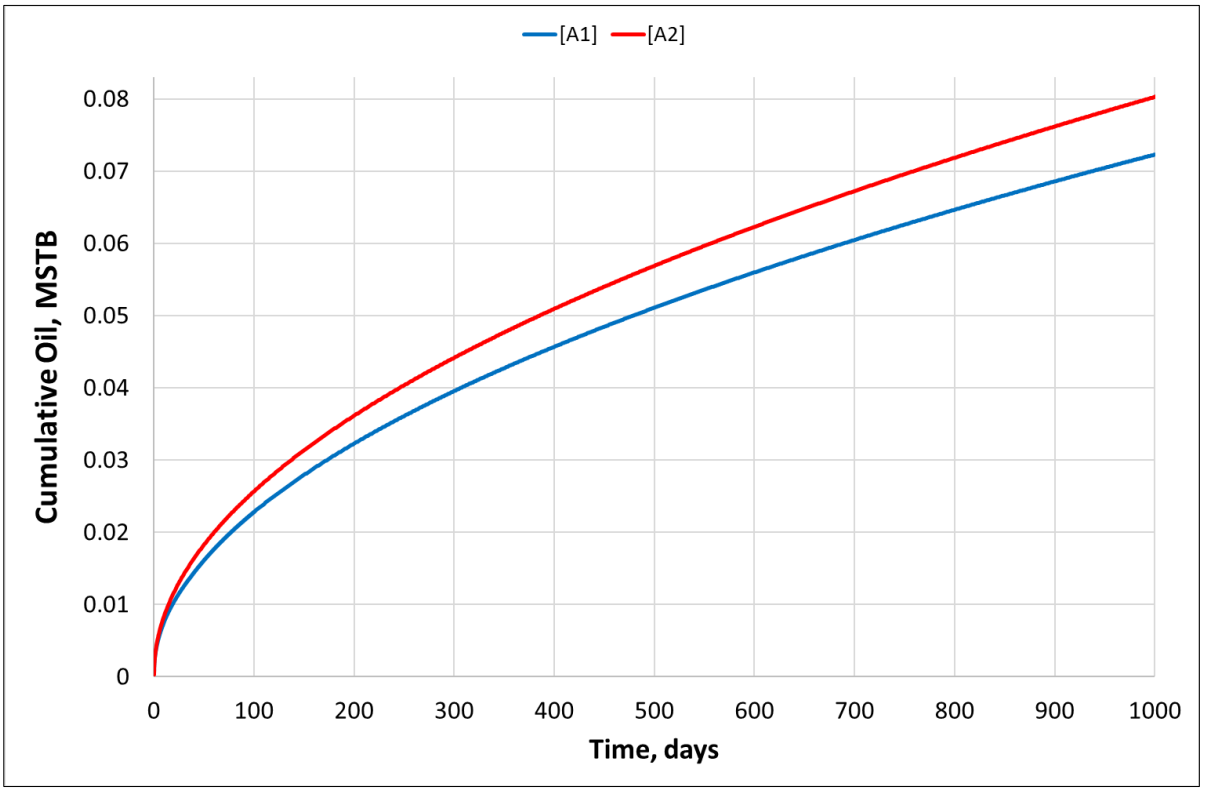

Figure 9.2. Cumulative oil production for case study A

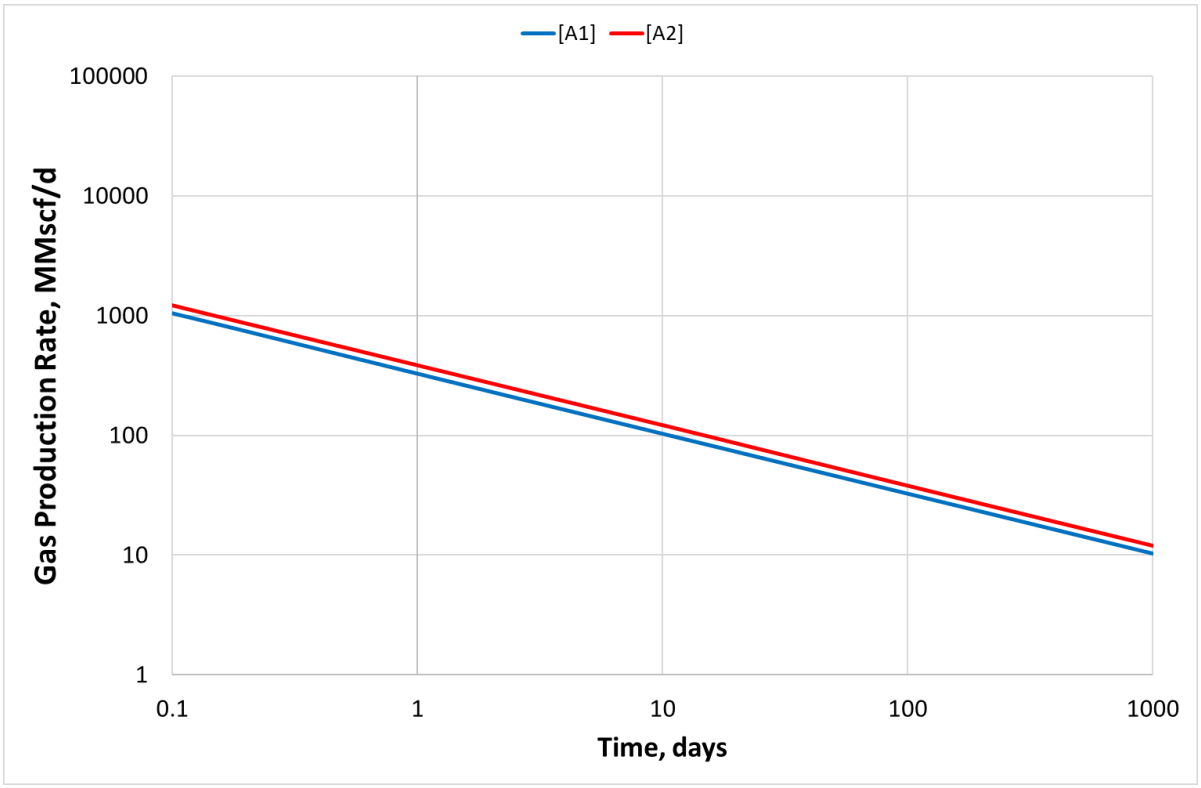

Figure 9.3. Log-log plot for gas production rates for case study A

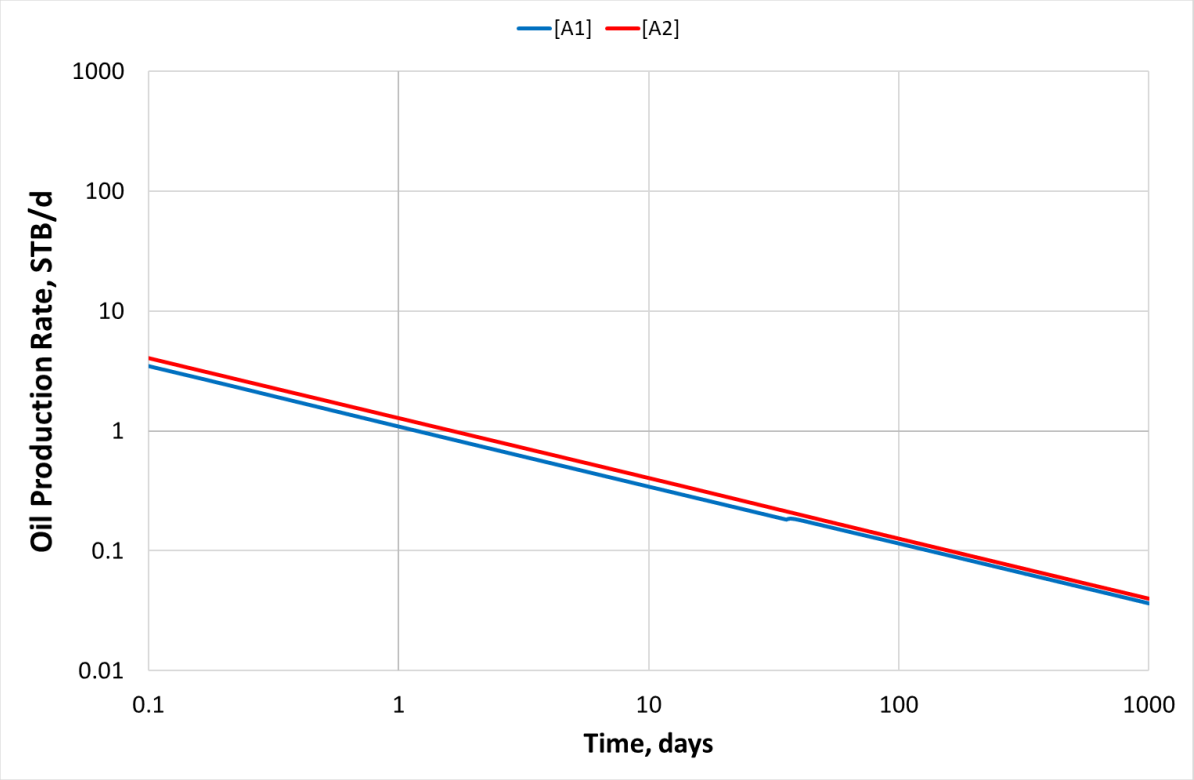

Figure 9.4. Log-log plot for oil production rates for case study A

9.1.2 Case Study B

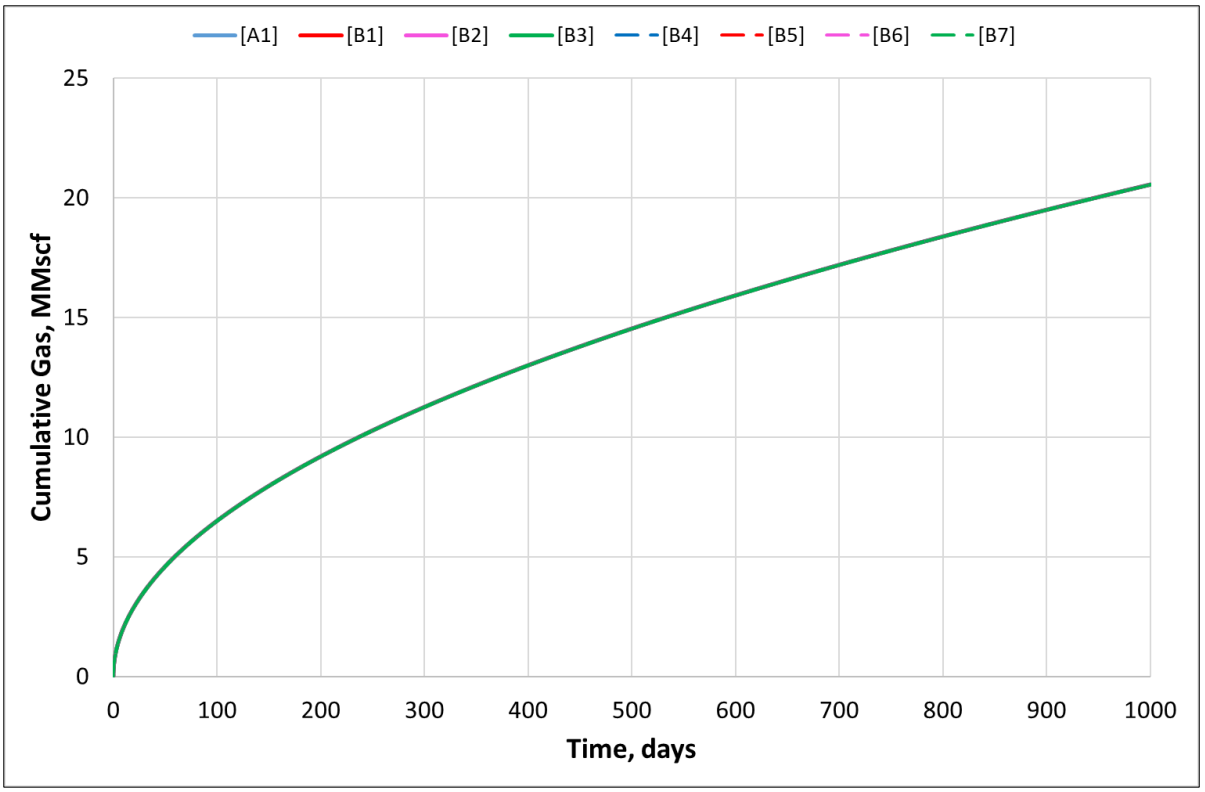

Figure 9.5. Cumulative gas production for case study B

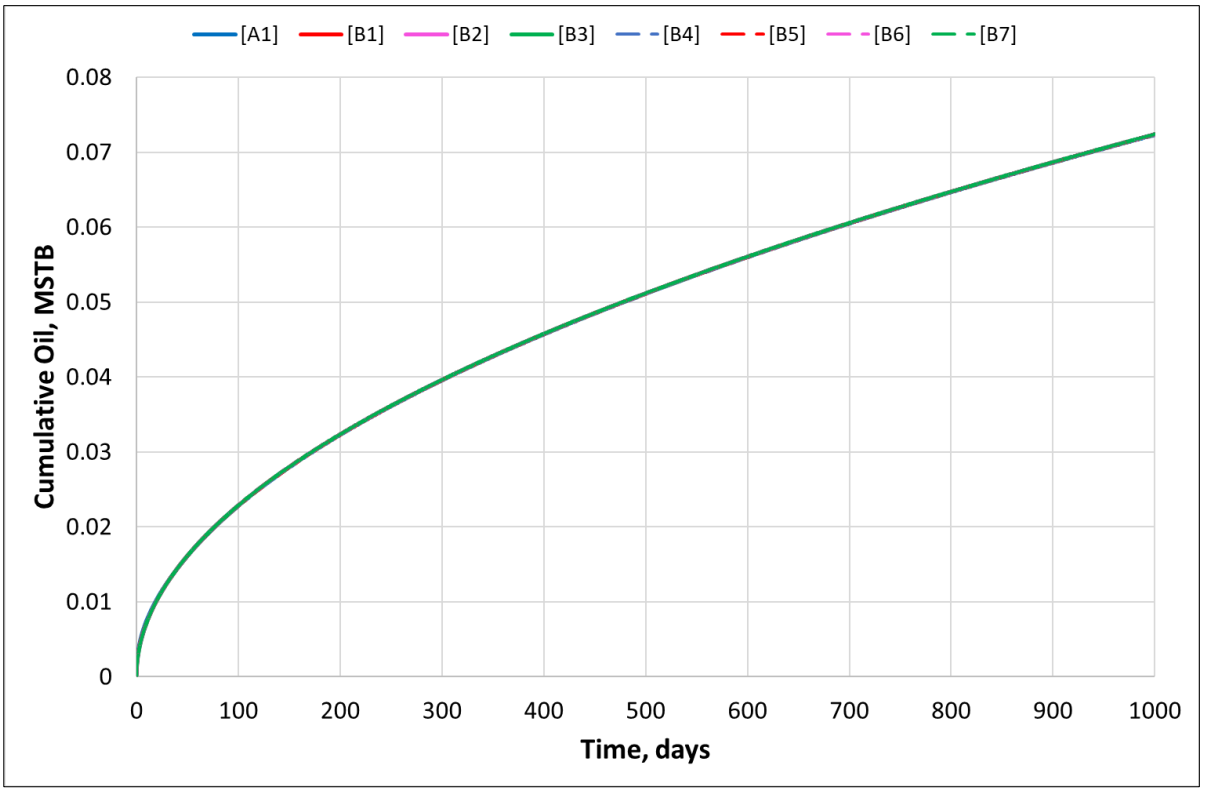

Figure 9.6. Cumulative oil production for case study B

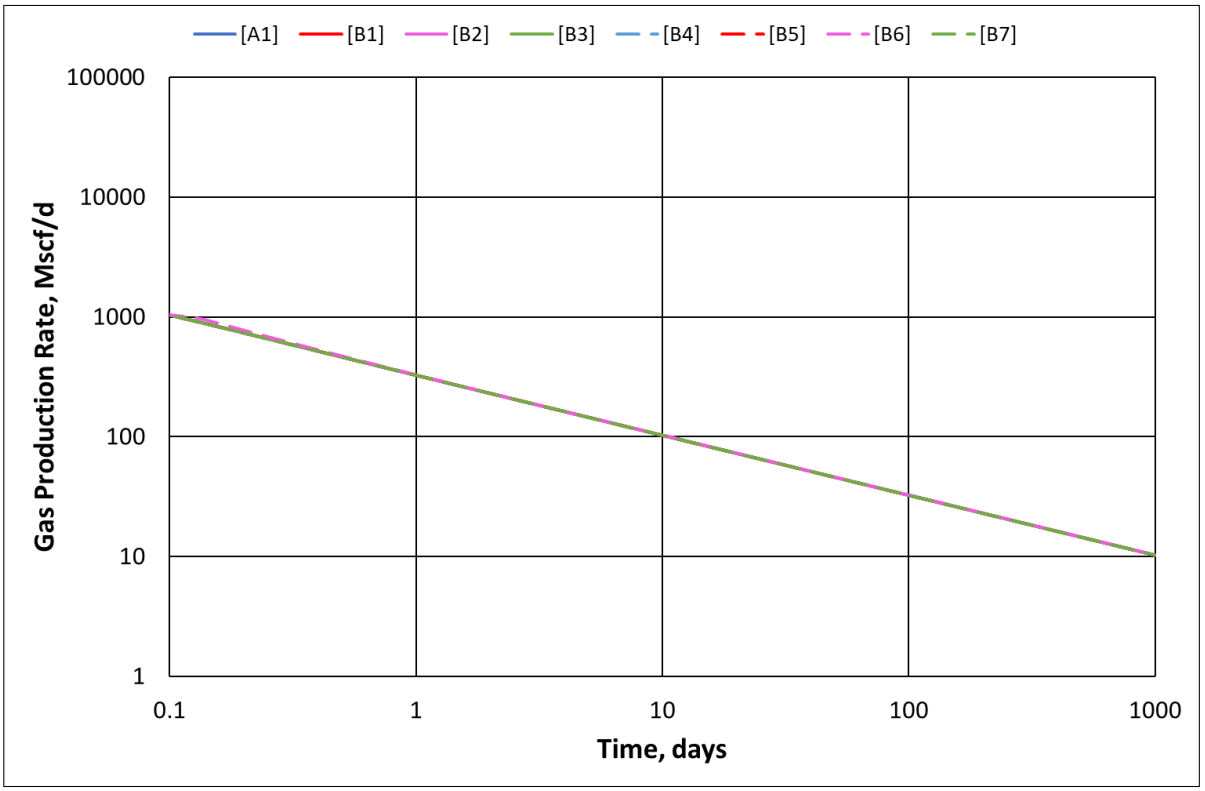

Figure 9.7. Log-log plot for gas production rates for case study B

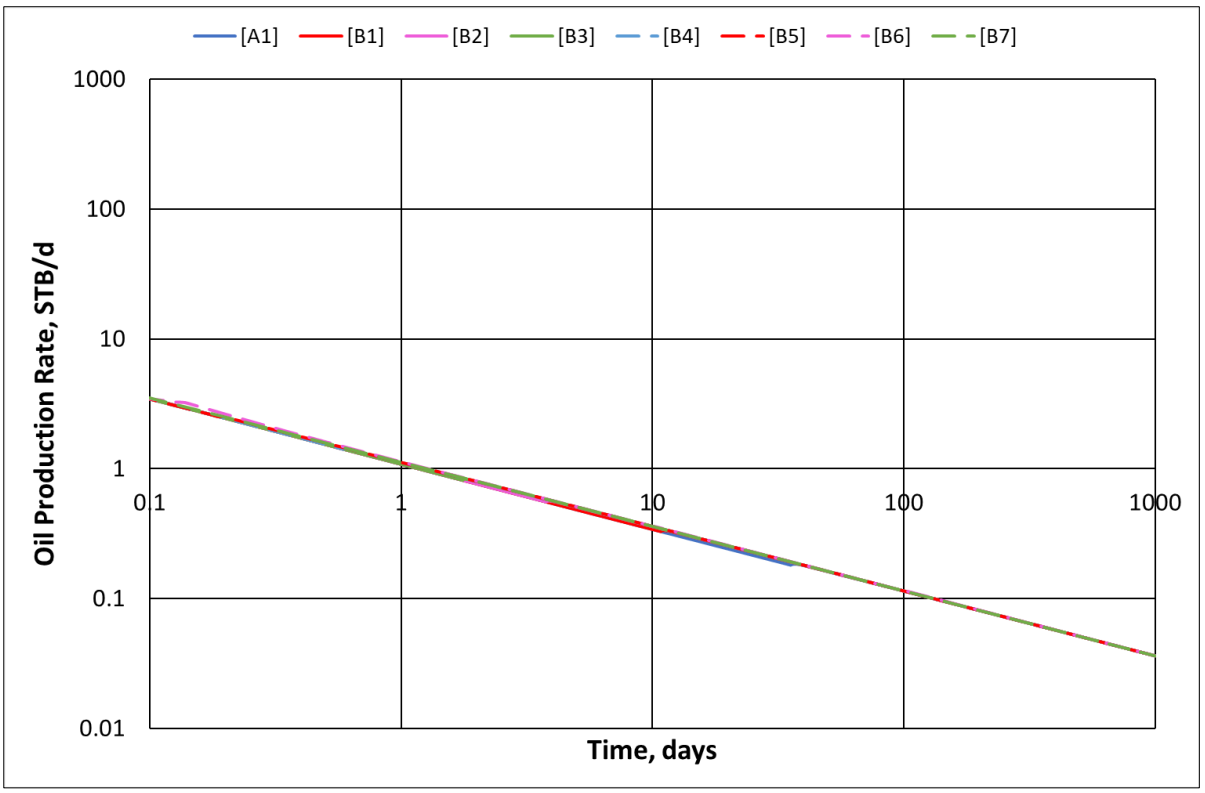

Figure 9.8. Log-log plot for oil production rates for case study B

9.1.3 Case Study C

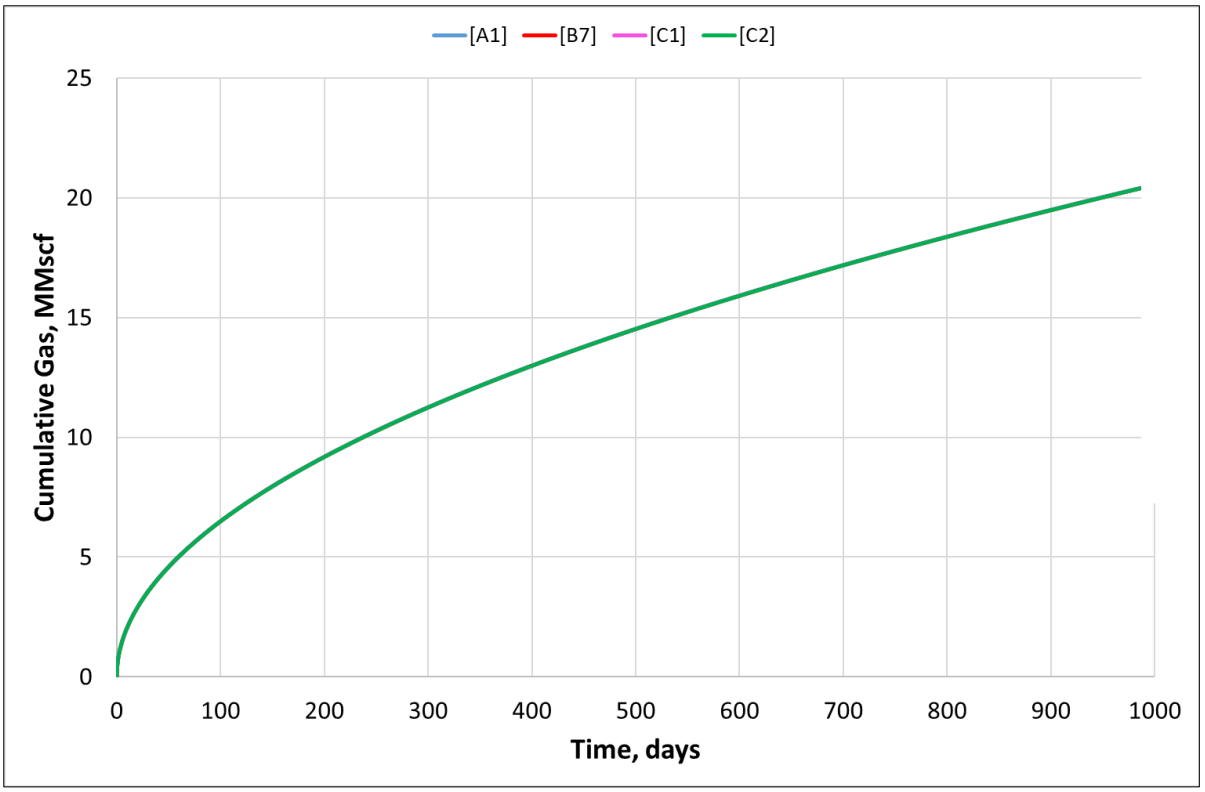

Figure 9.9. Cumulative gas production for case study C

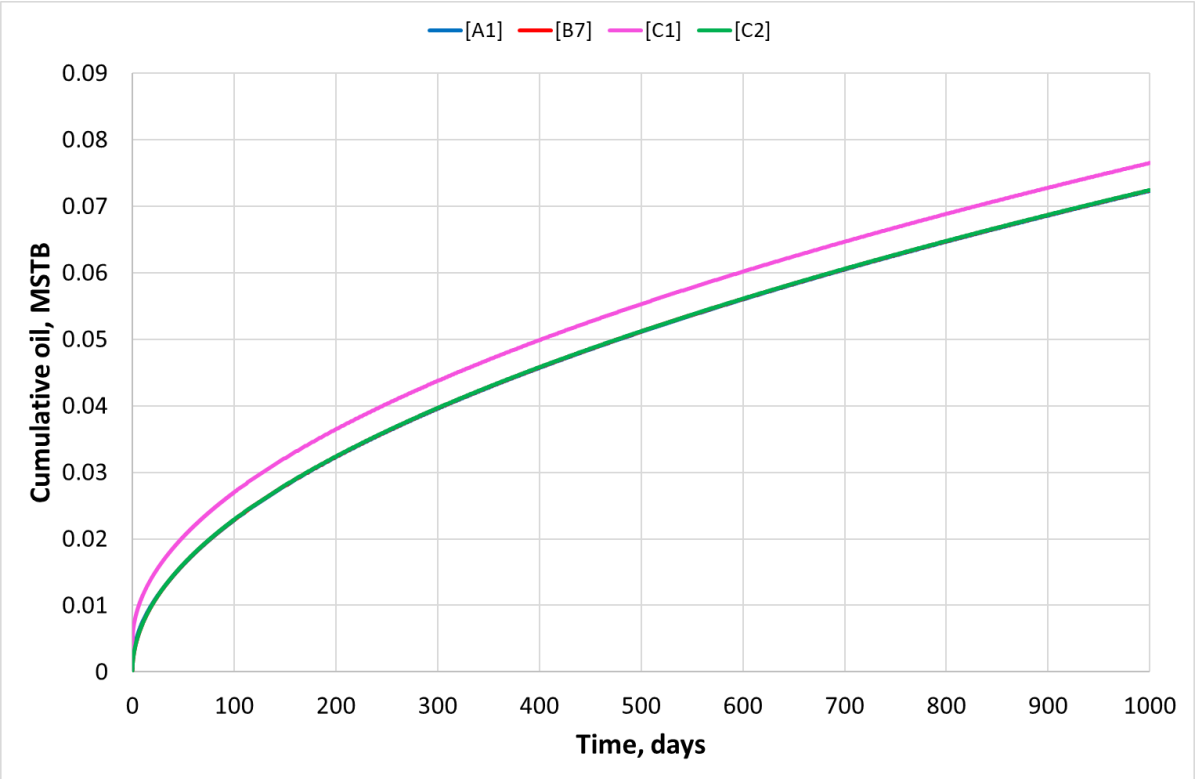

Figure 9.10. Cumulative oil production for case study C

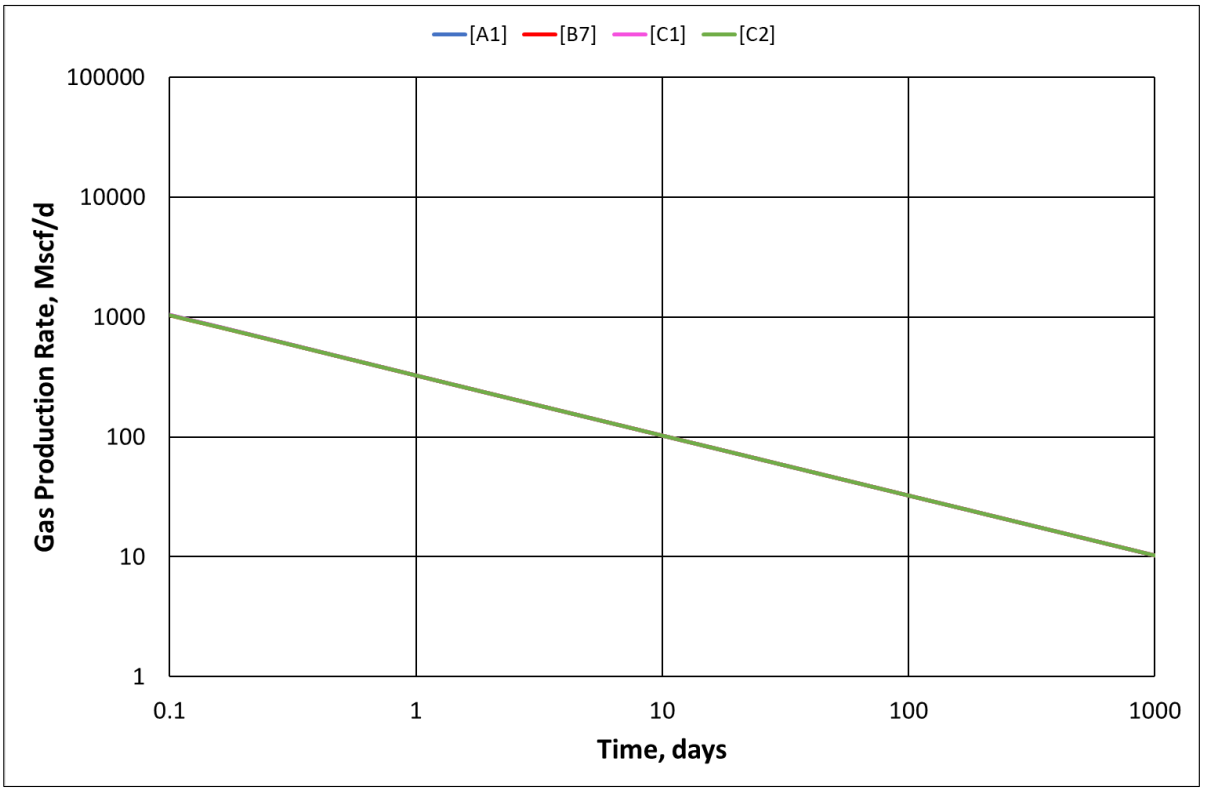

Figure 9.11. Log-log plot for gas production rates for case study C

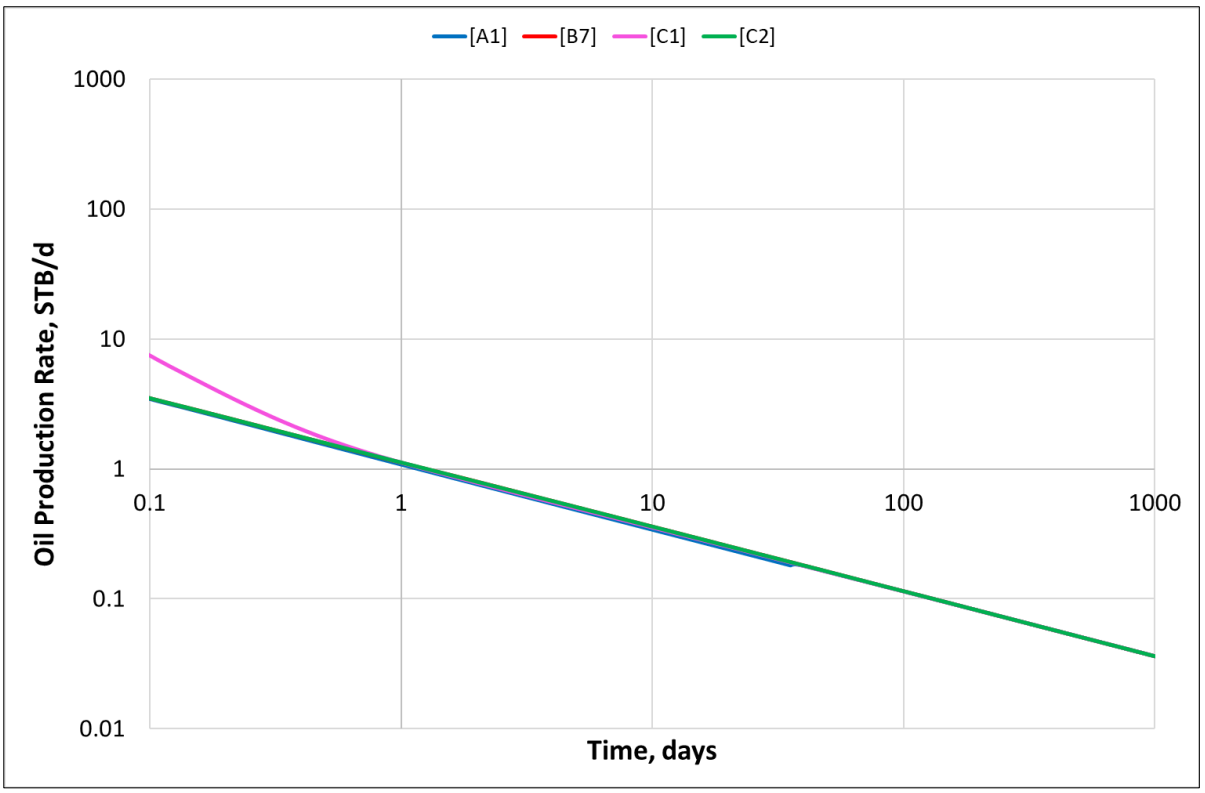

Figure 9.12. Log-log plot for oil production rates for case study C

9.1.4 Case Study D

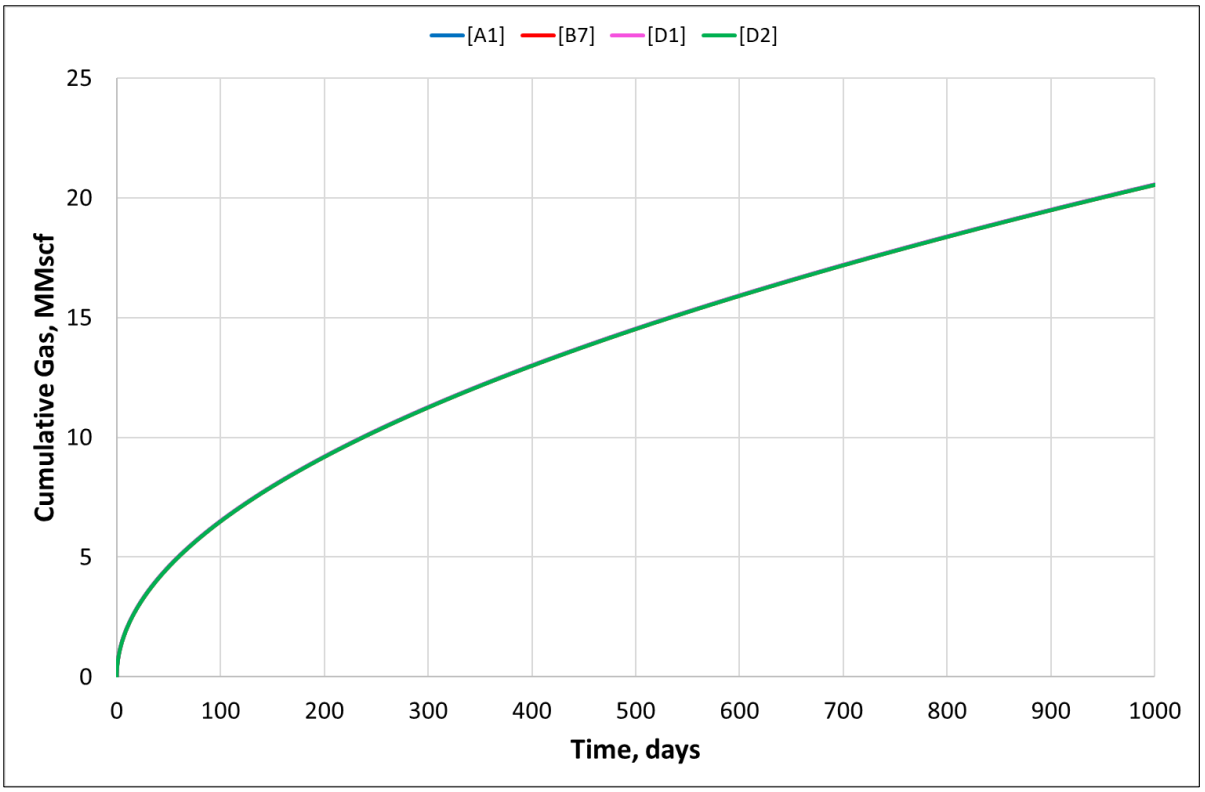

Figure 9.13. Cumulative gas production for case study D

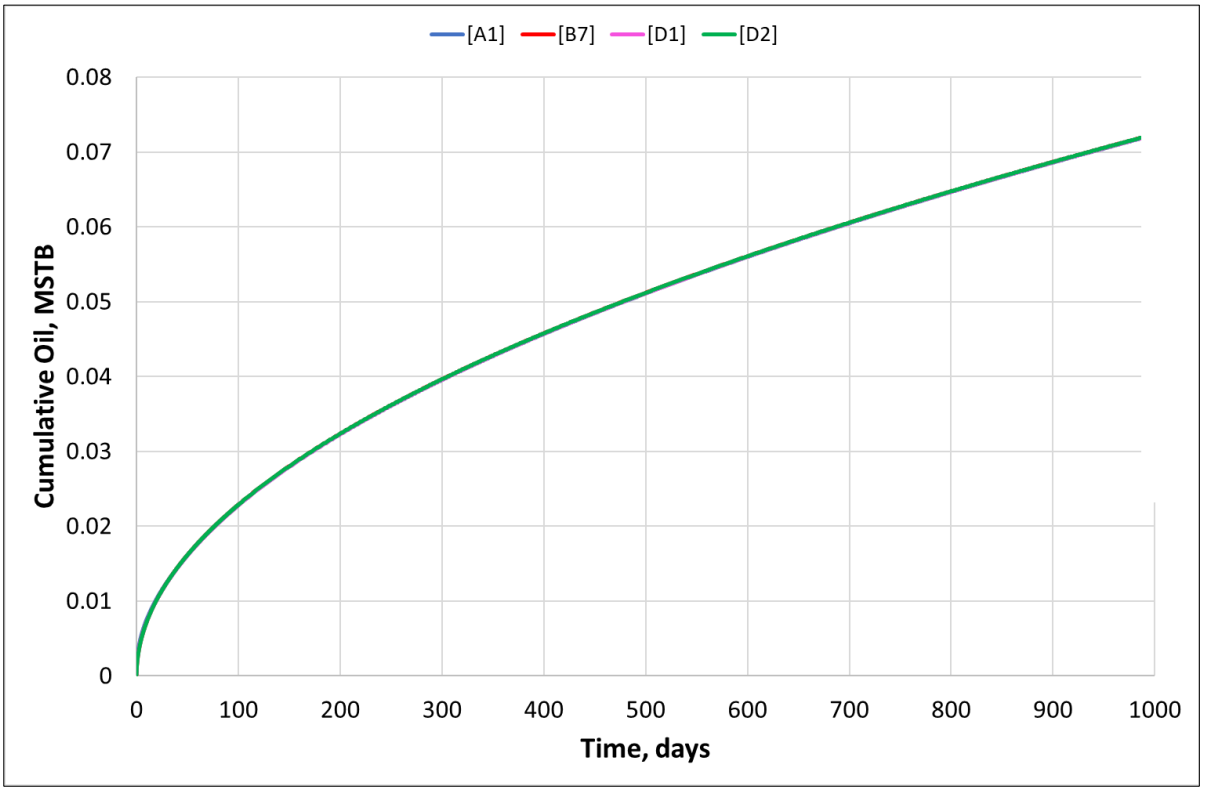

Figure 9.14. Cumulative oil production for case study D

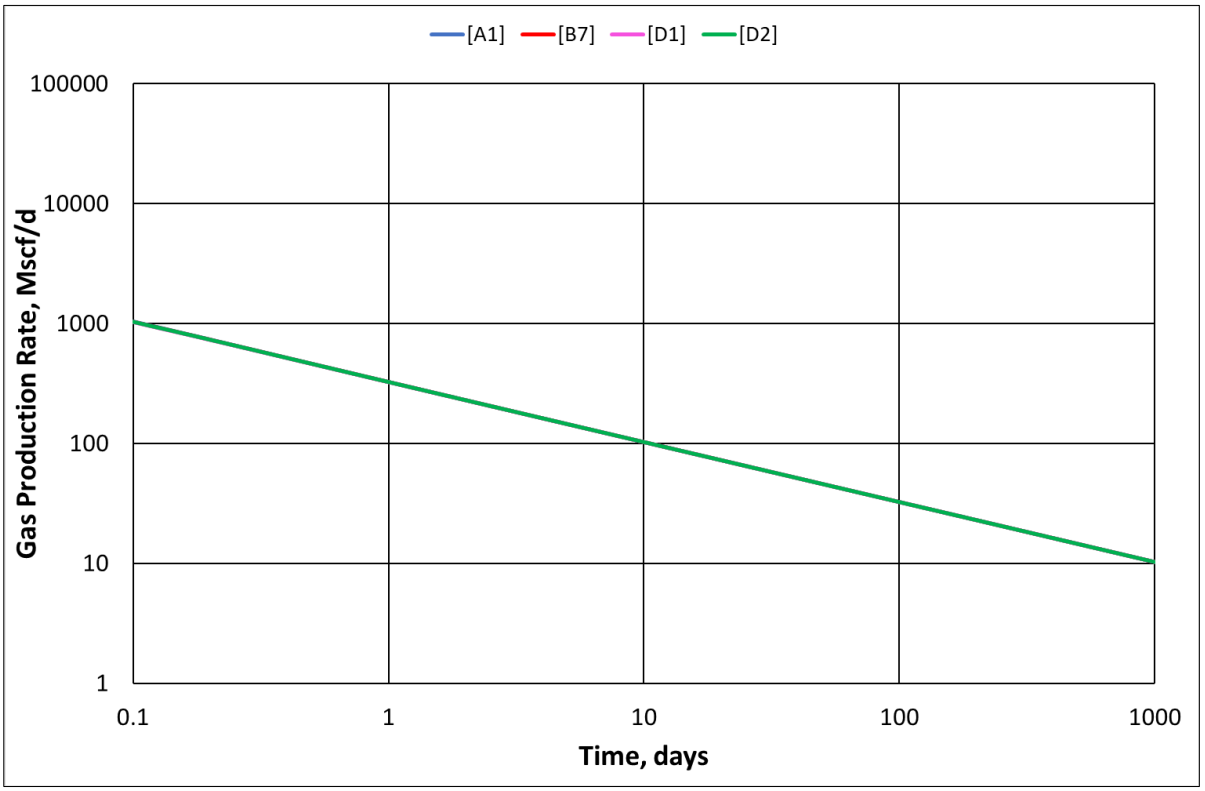

Figure 9.15. Log-log plot for gas production rates for case study D

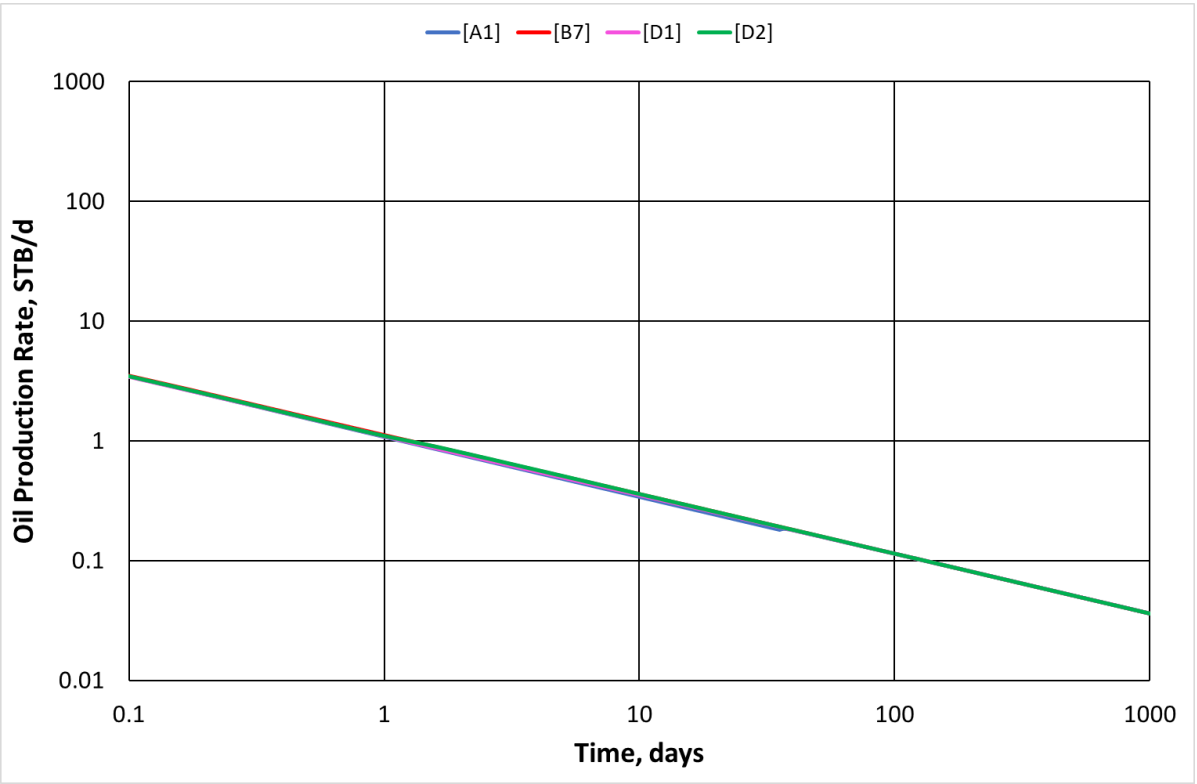

Figure 9.16. Log-log plot for oil production rates for case study D

9.1.5 Case Study E

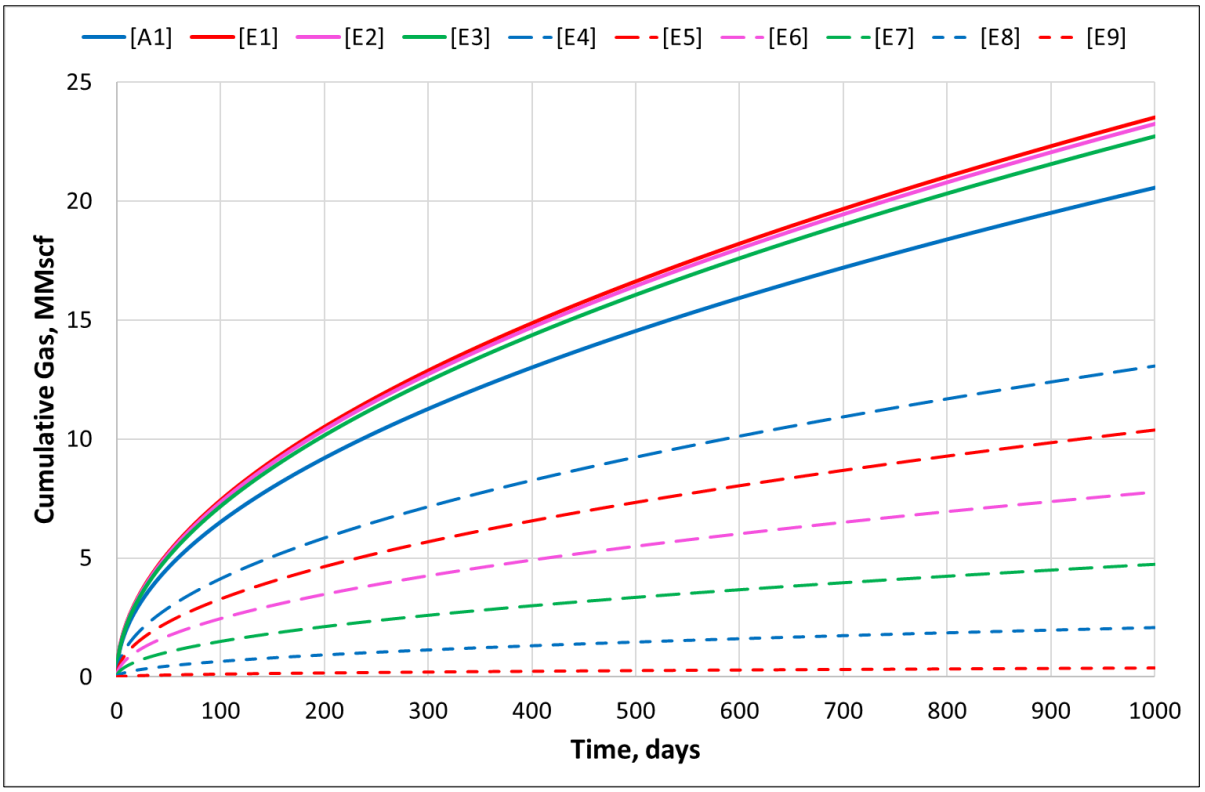

Figure 9.17. Cumulative gas production for case study E

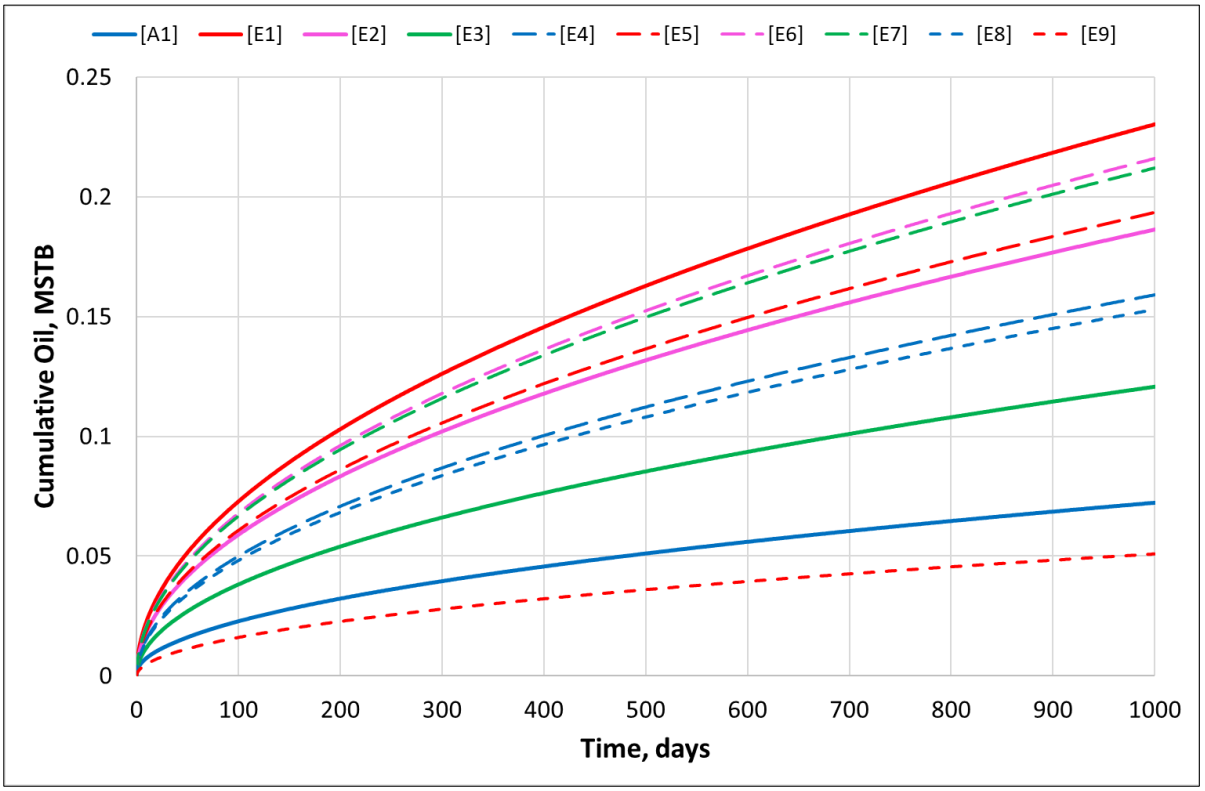

Figure 9.18. Cumulative oil production for case study E

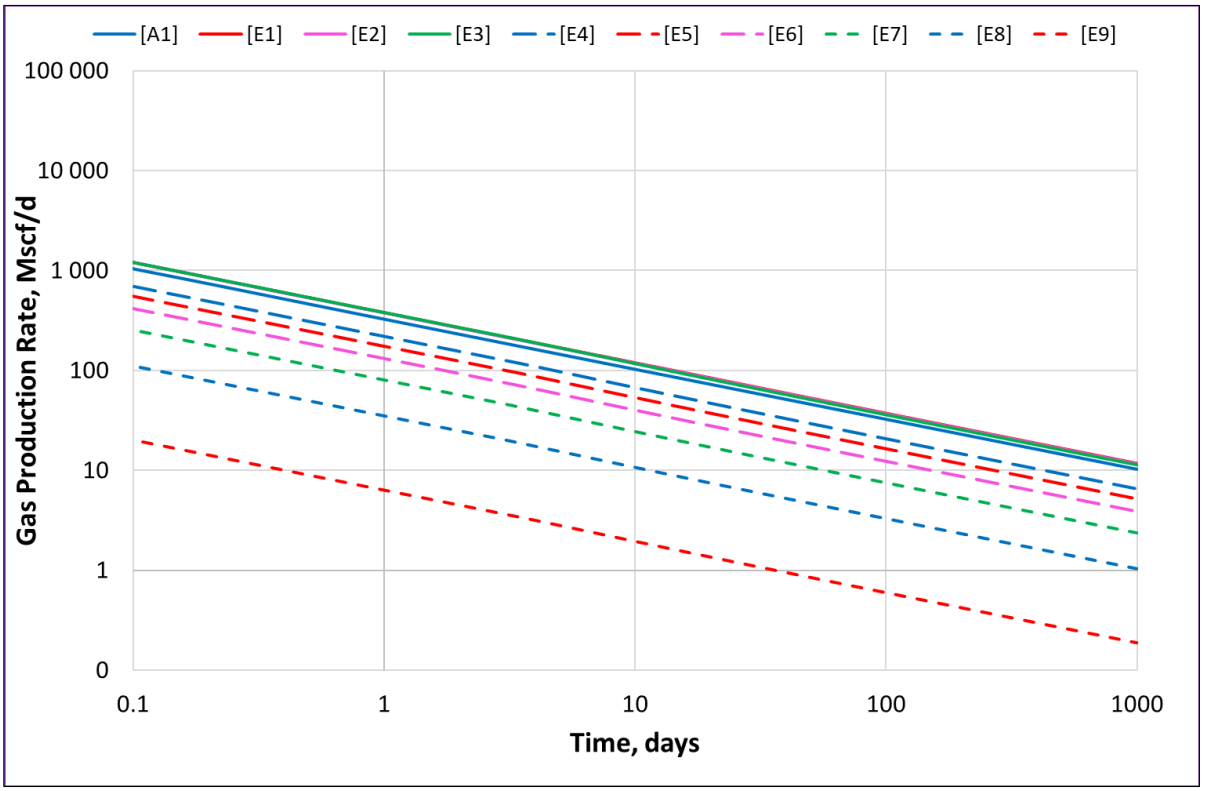

Figure 9.19. Log-log plot for gas production rates for case study E

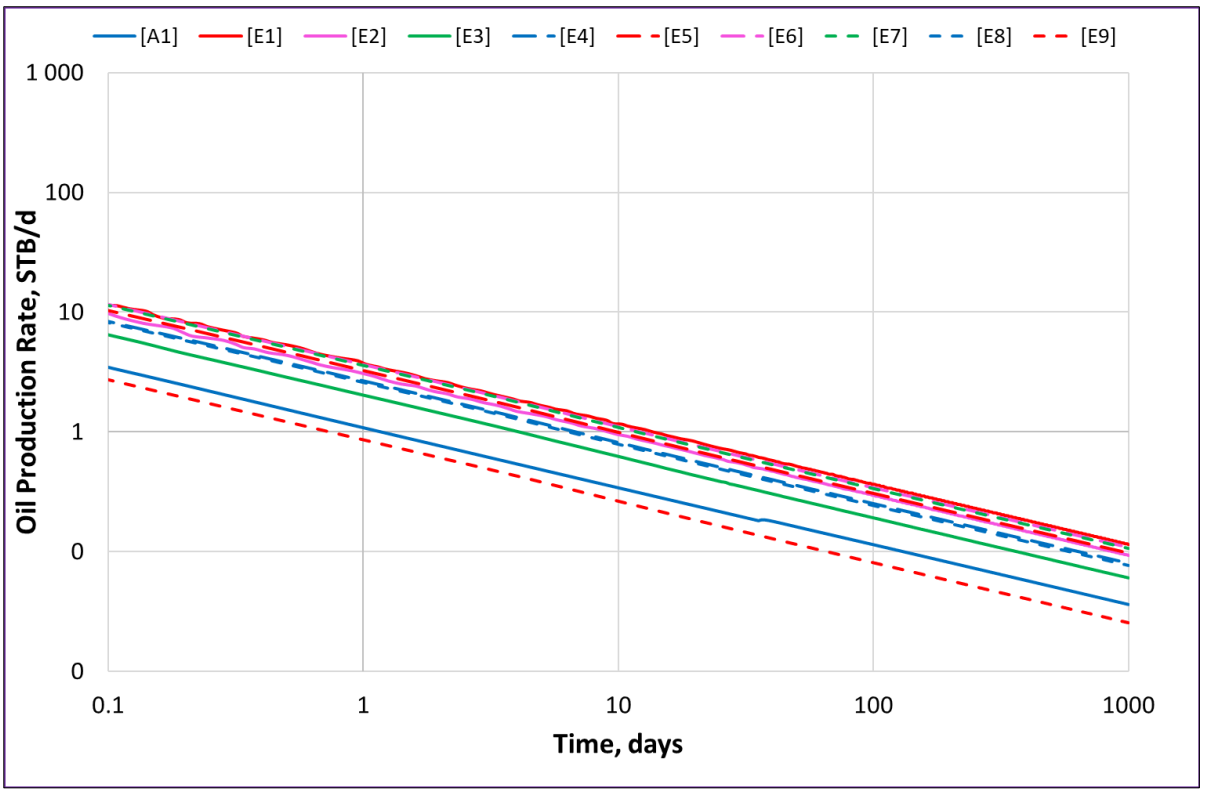

Figure 9.20. Log-log plot for oil production rates for case study E

9.1.6 Case Study F

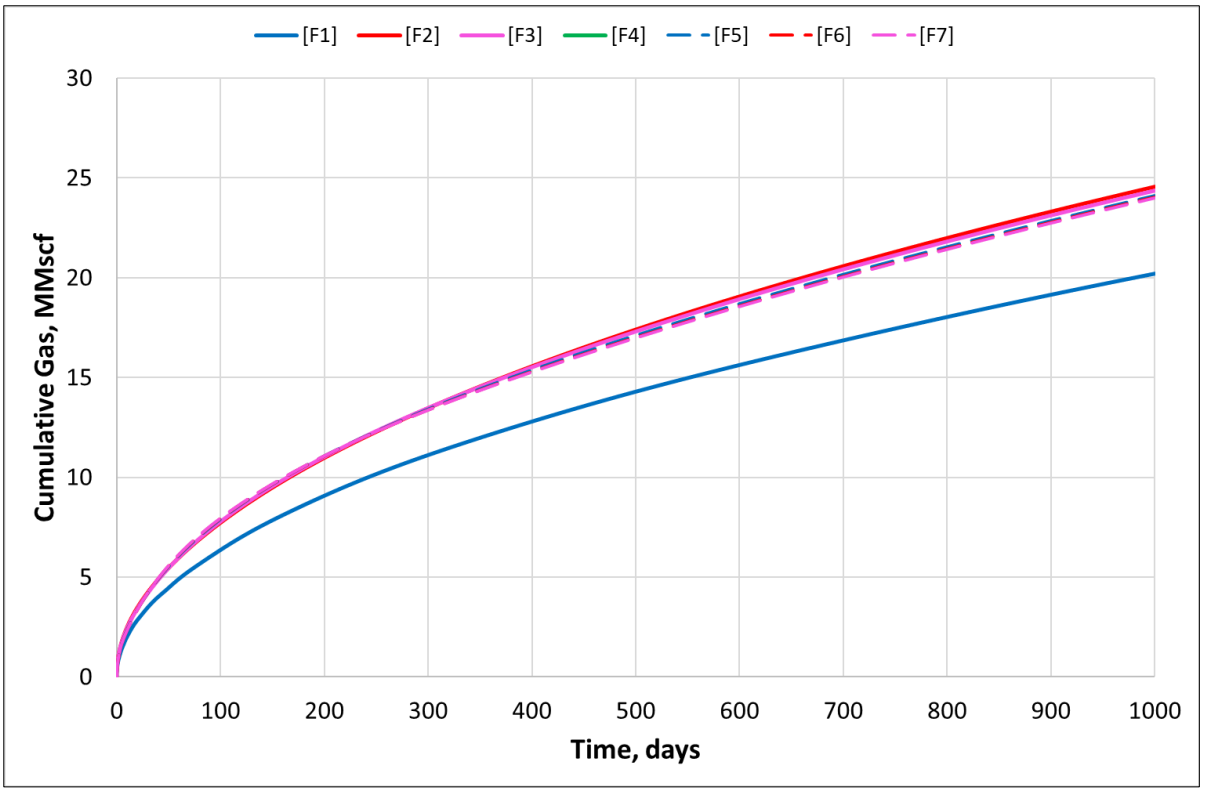

Figure 9.21. Cumulative gas production for case study F

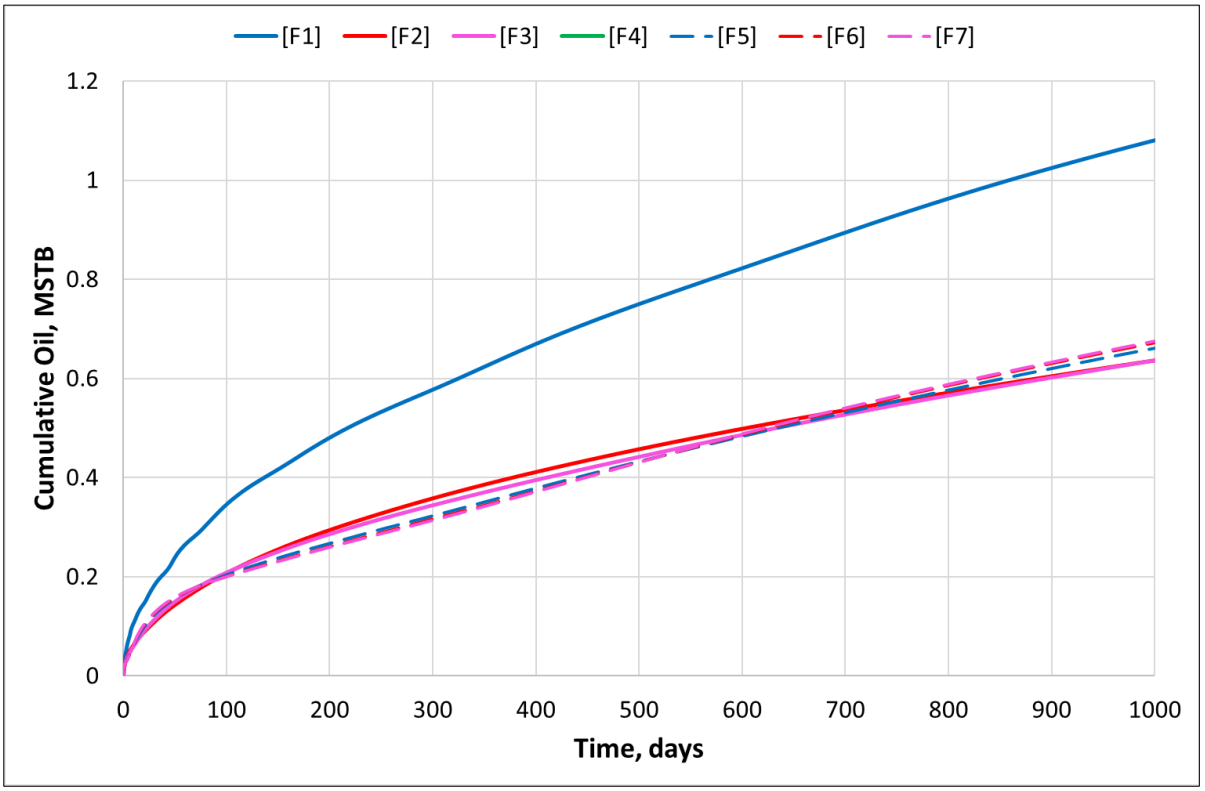

Figure 9.22. Cumulative oil production for case study F

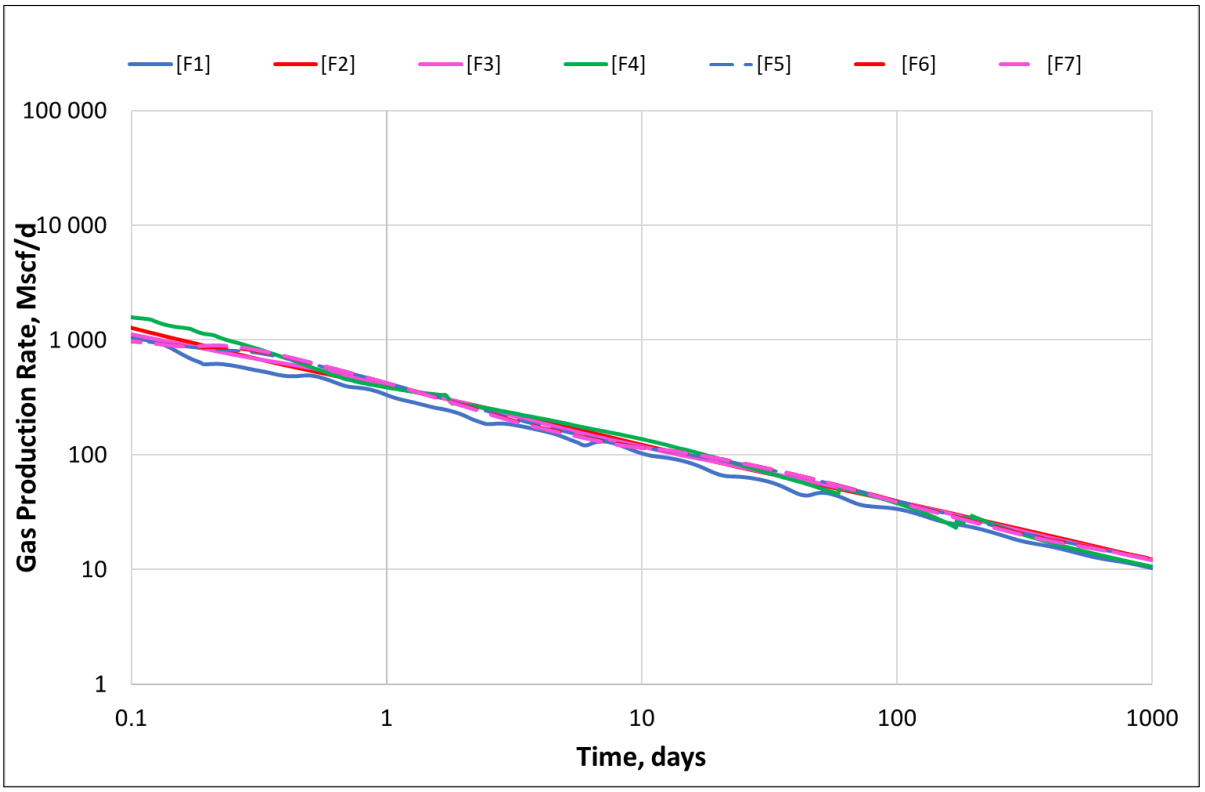

Figure 9.23. Log-log plot for gas production rates for case study F

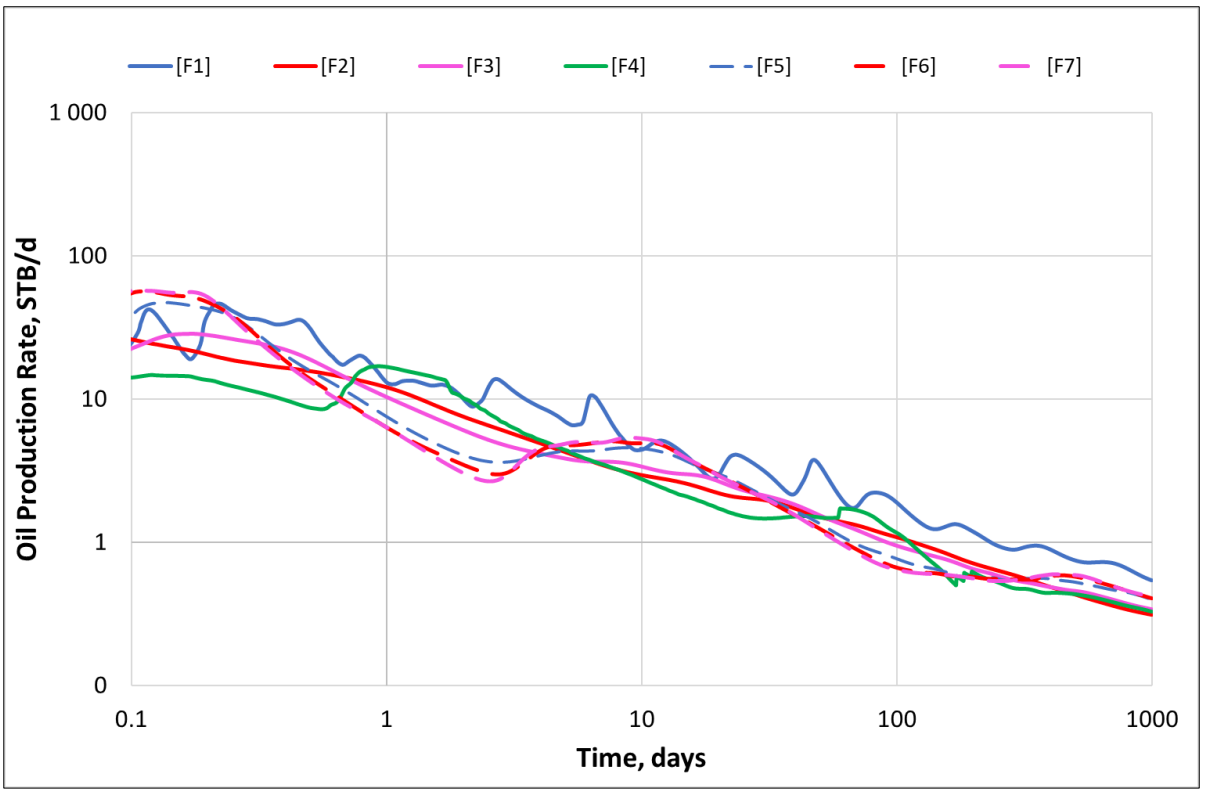

Figure 9.24. Log-log plot for oil production rates for case study F

9.1.7 Case Study G

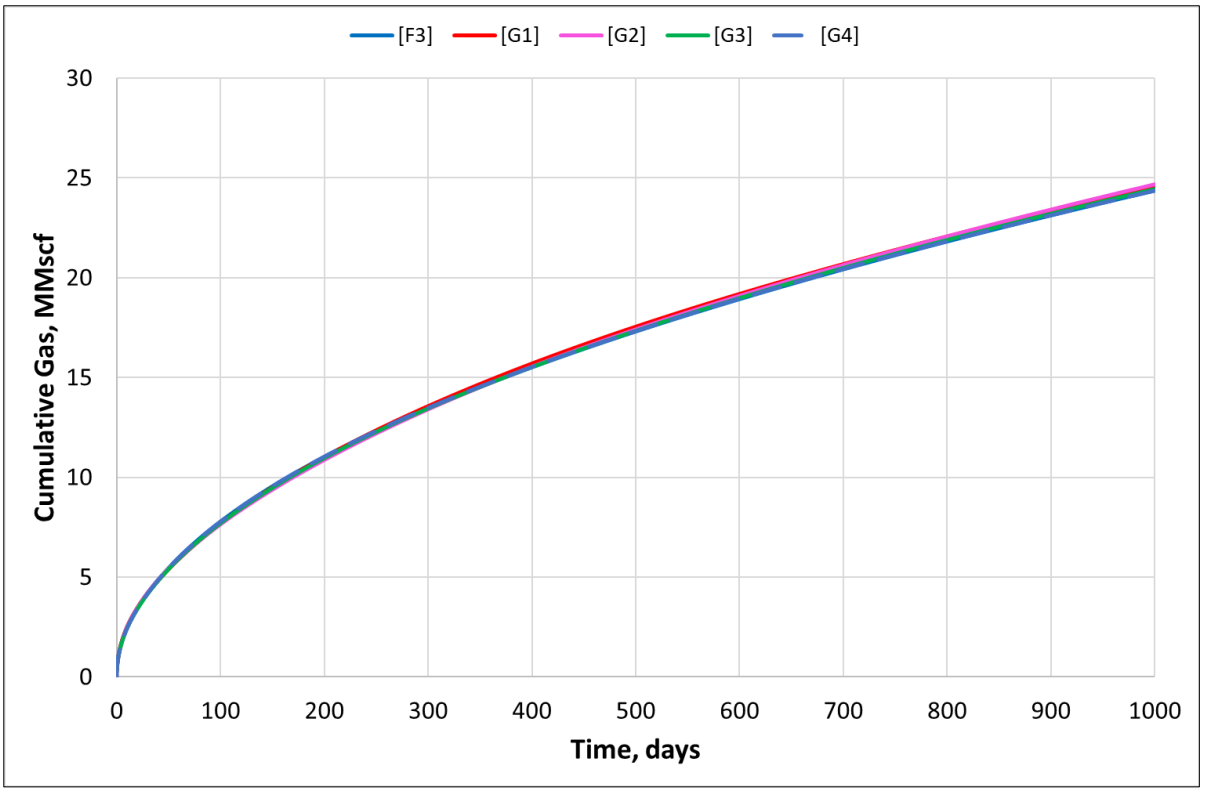

Figure 9.25. Cumulative gas production for case study G

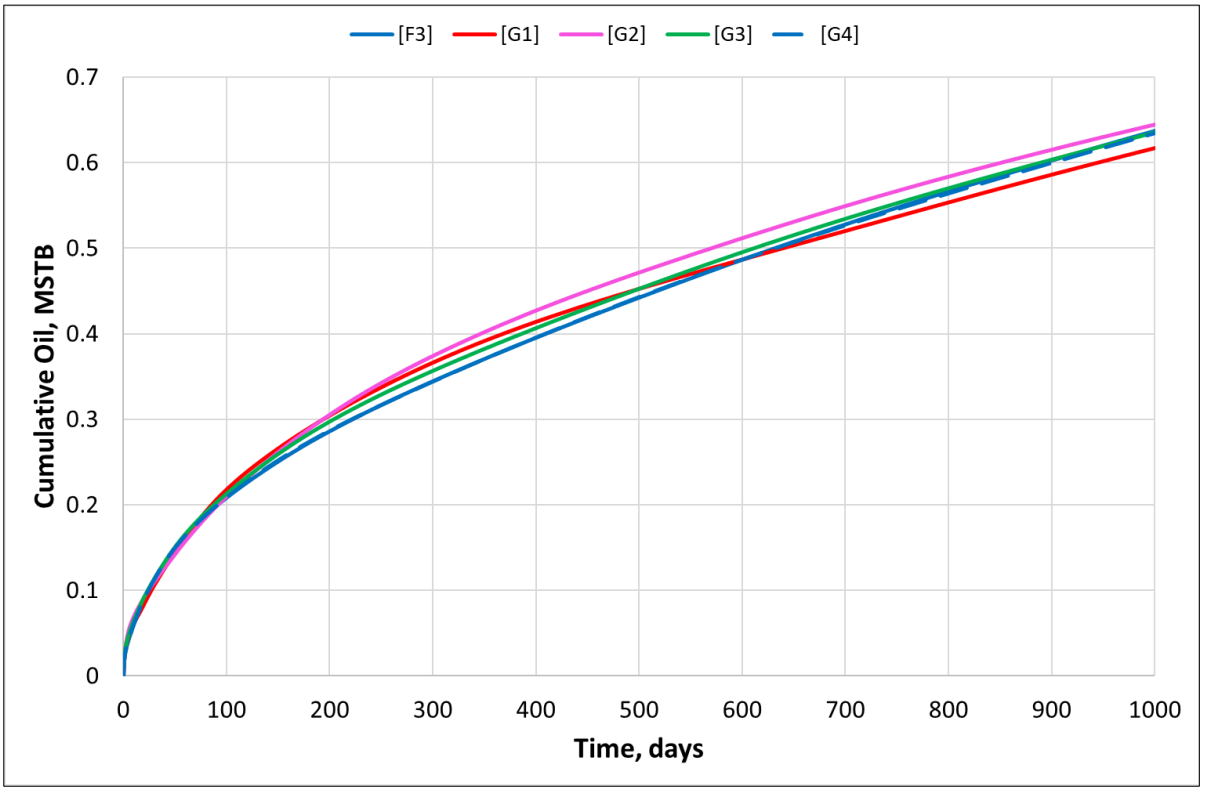

Figure 9.26. Cumulative oil production for case study G

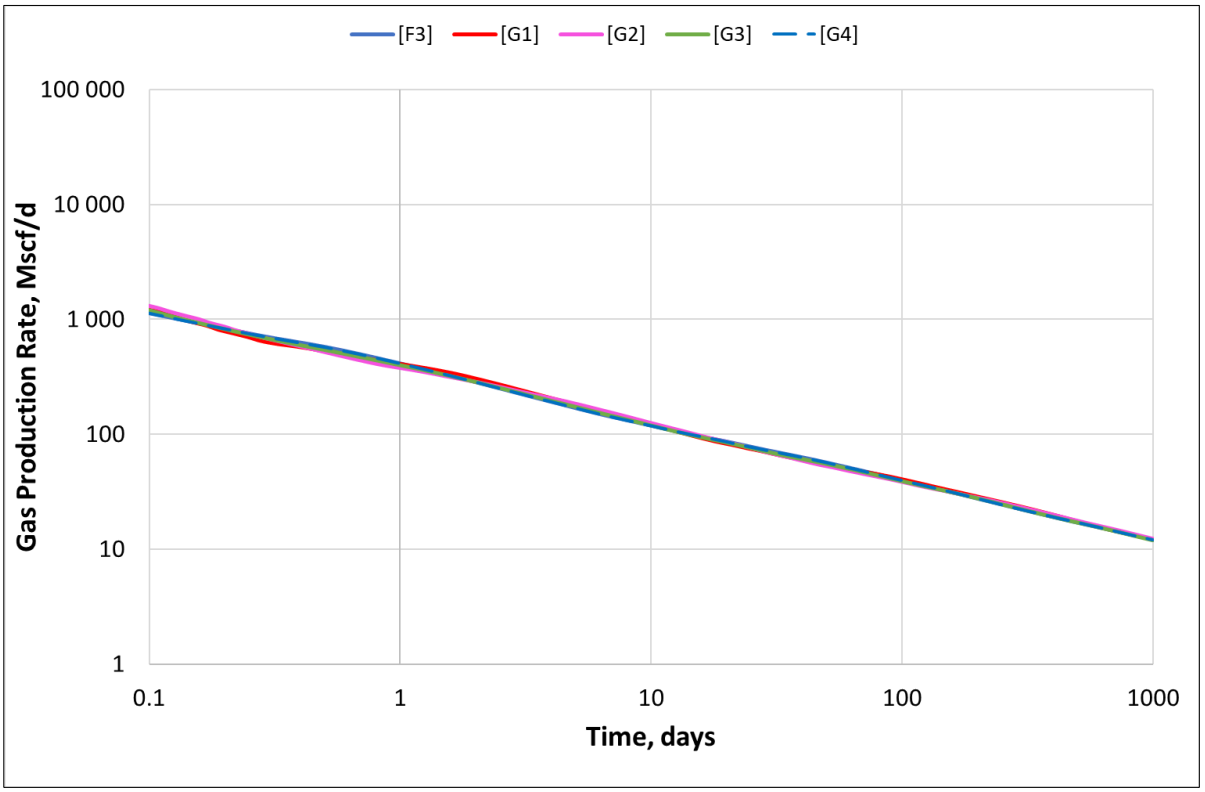

Figure 9.27. Log-log plot for gas production rates for case study G

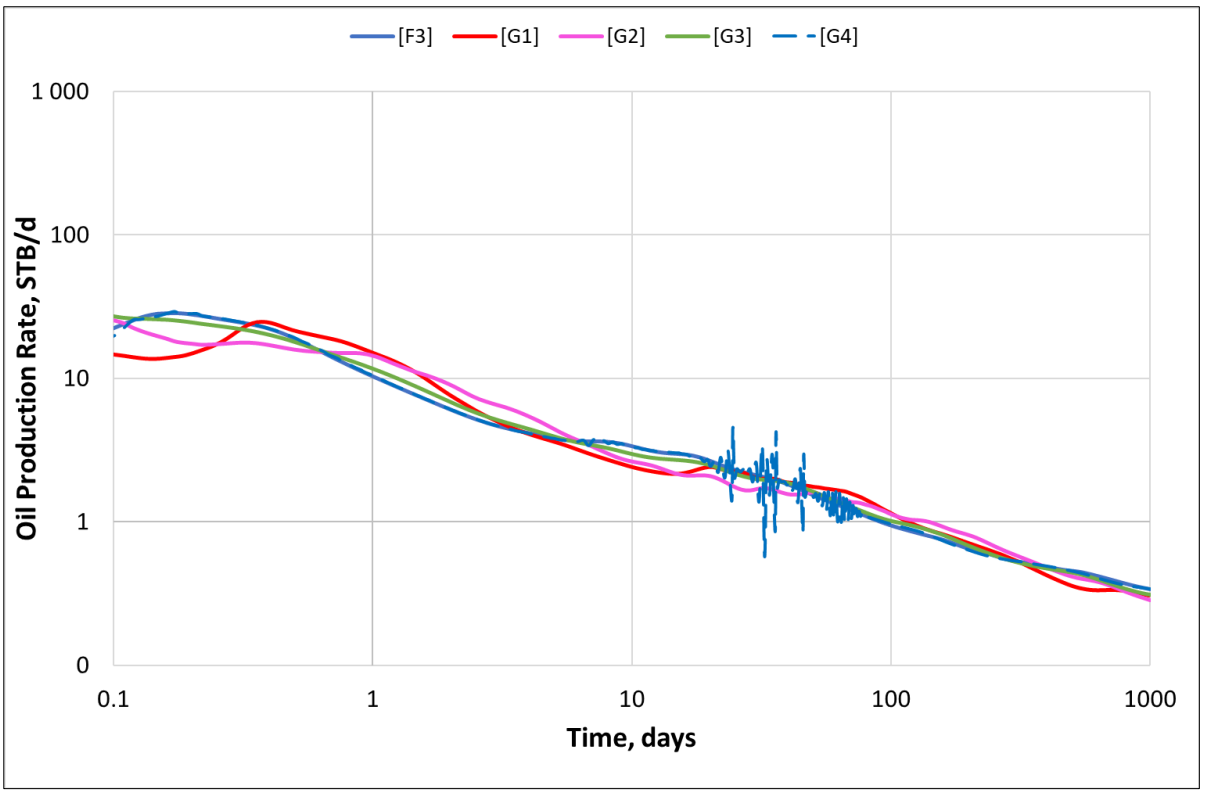

Figure 9.28. Log-log plot for oil production rates for case study G

9.1.8 Case Study H

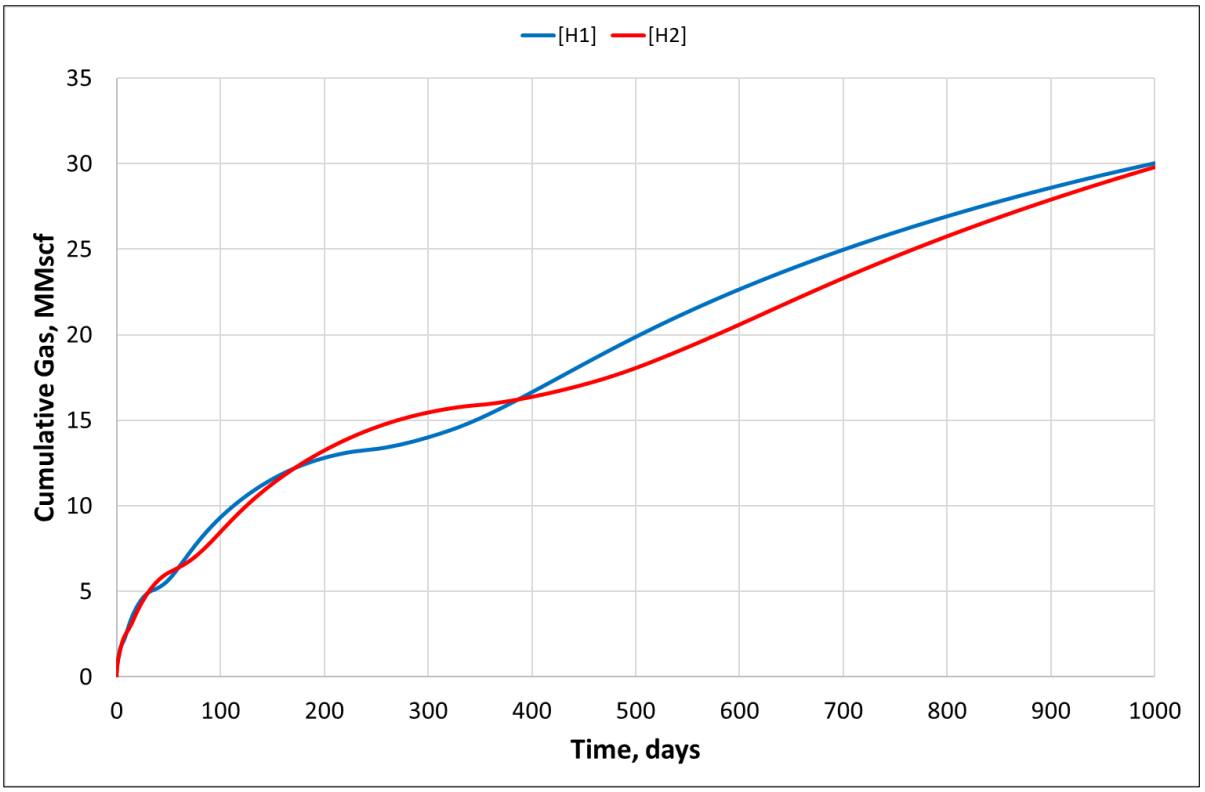

Figure 9.29. Cumulative gas production for case study H

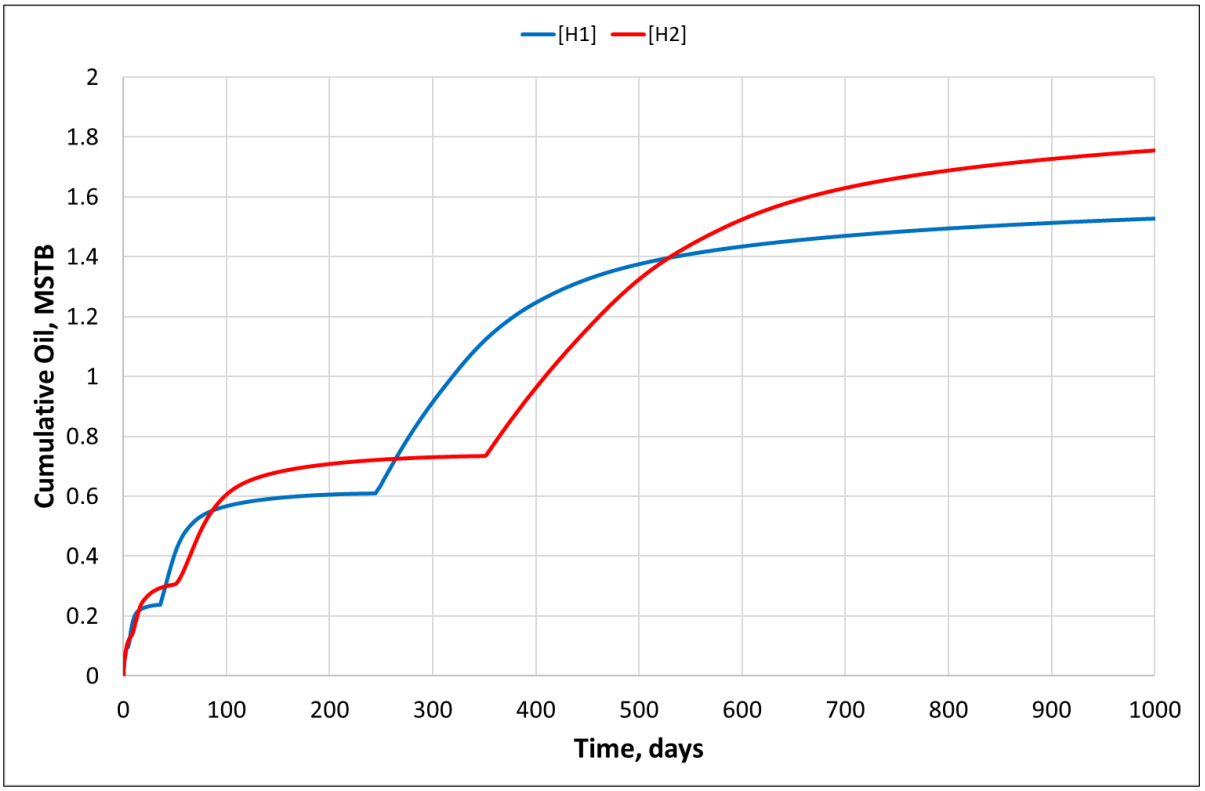

Figure 9.30. Cumulative oil production for case study H

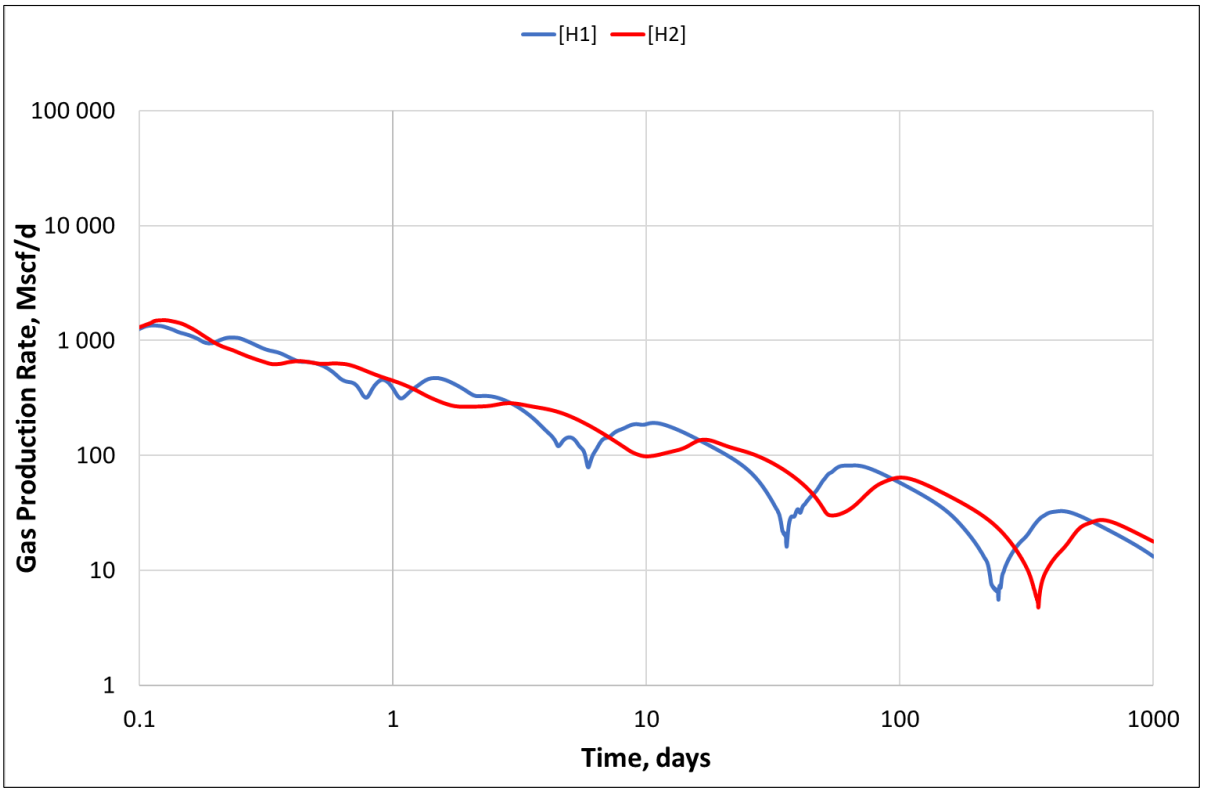

Figure 9.31. Log-log plot for gas production rates for case study H

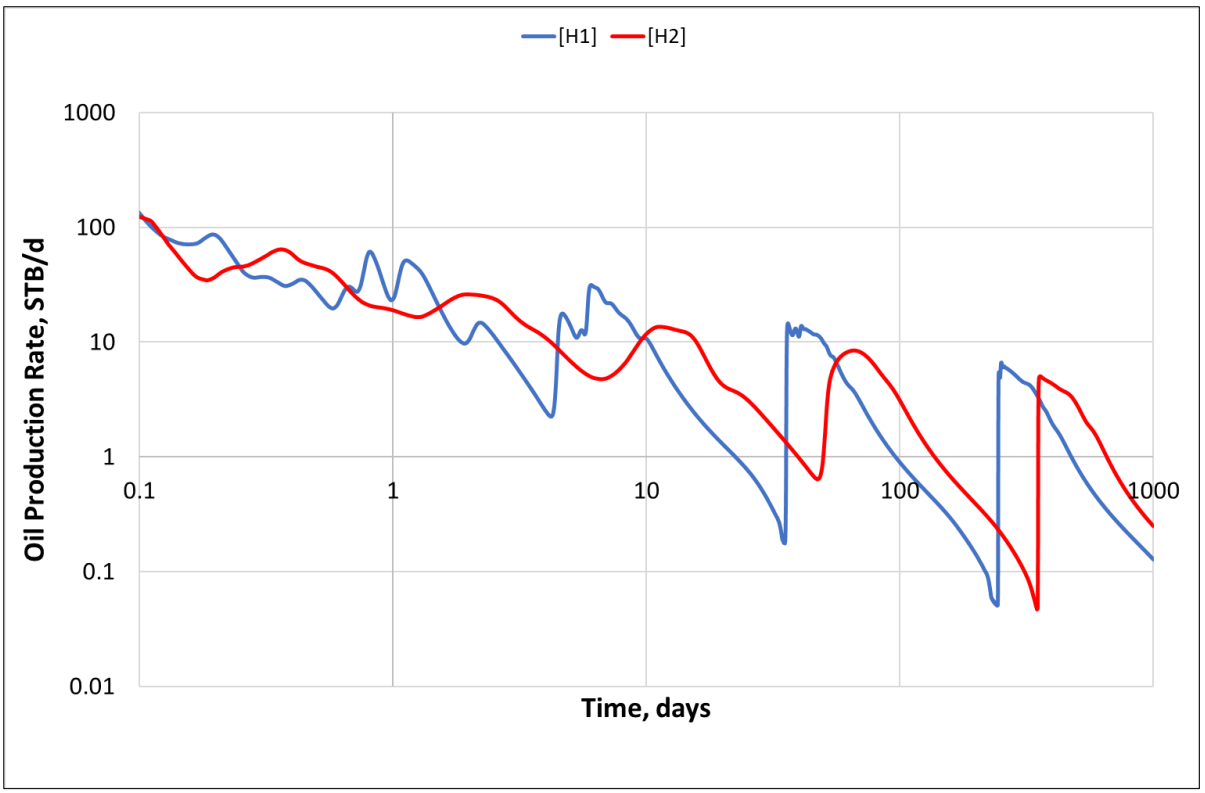

Figure 9.32. Log-log plot for oil production rates for case study H

9.1.9 Case Study I

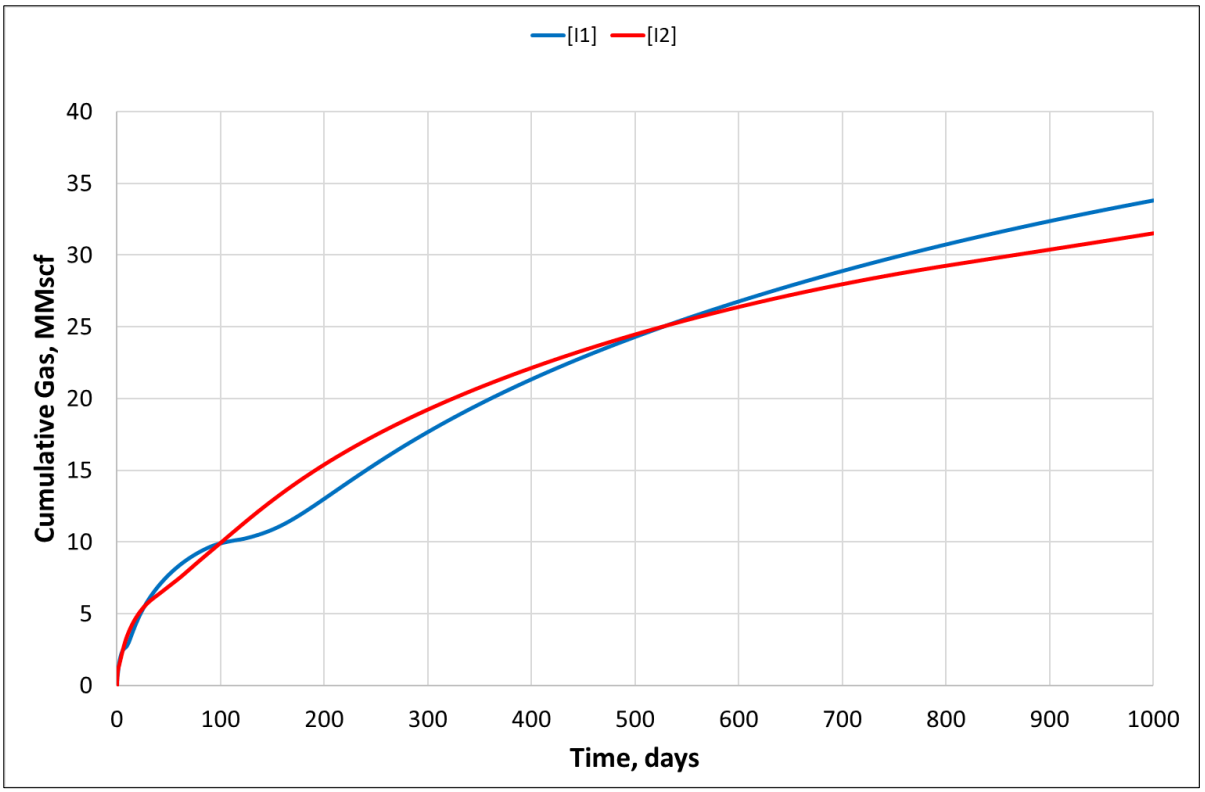

Figure 9.33. Cumulative gas production for case study I

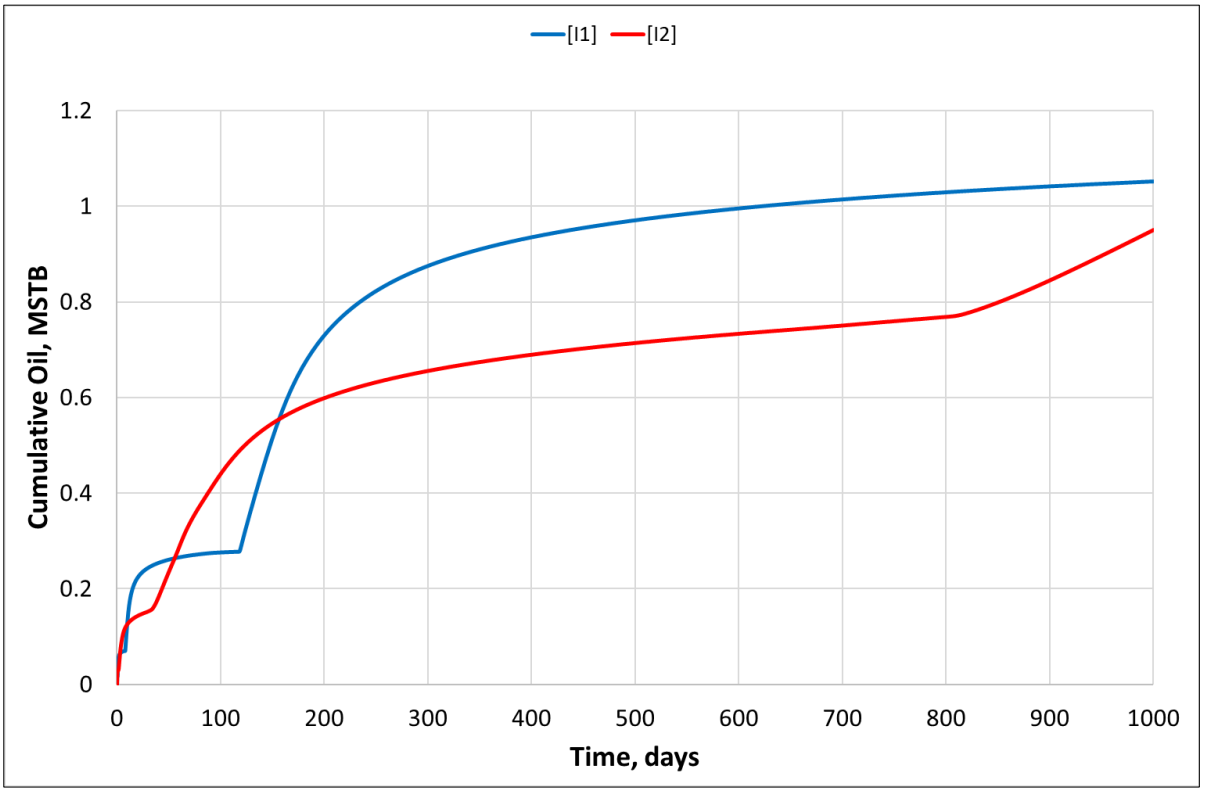

Figure 9.34. Cumulative oil production for case study I

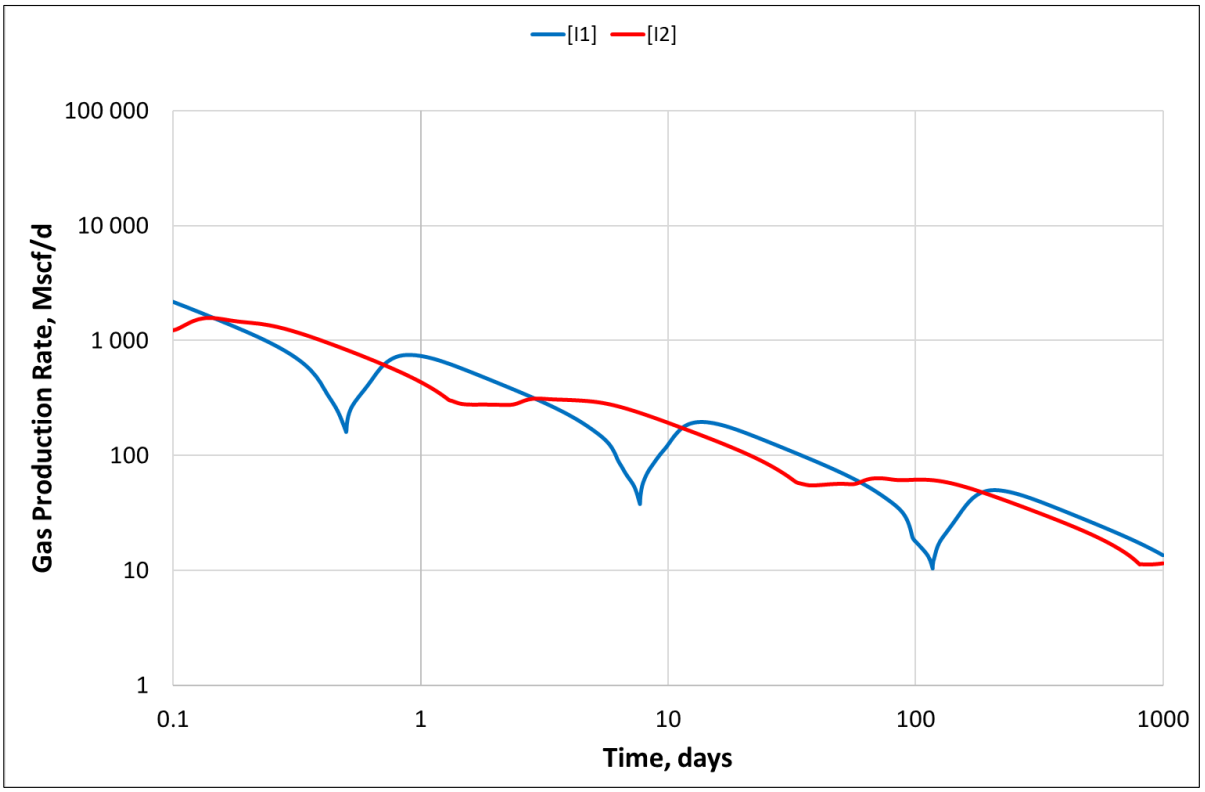

Figure 9.35. Log-log plot for gas production rates for case study I

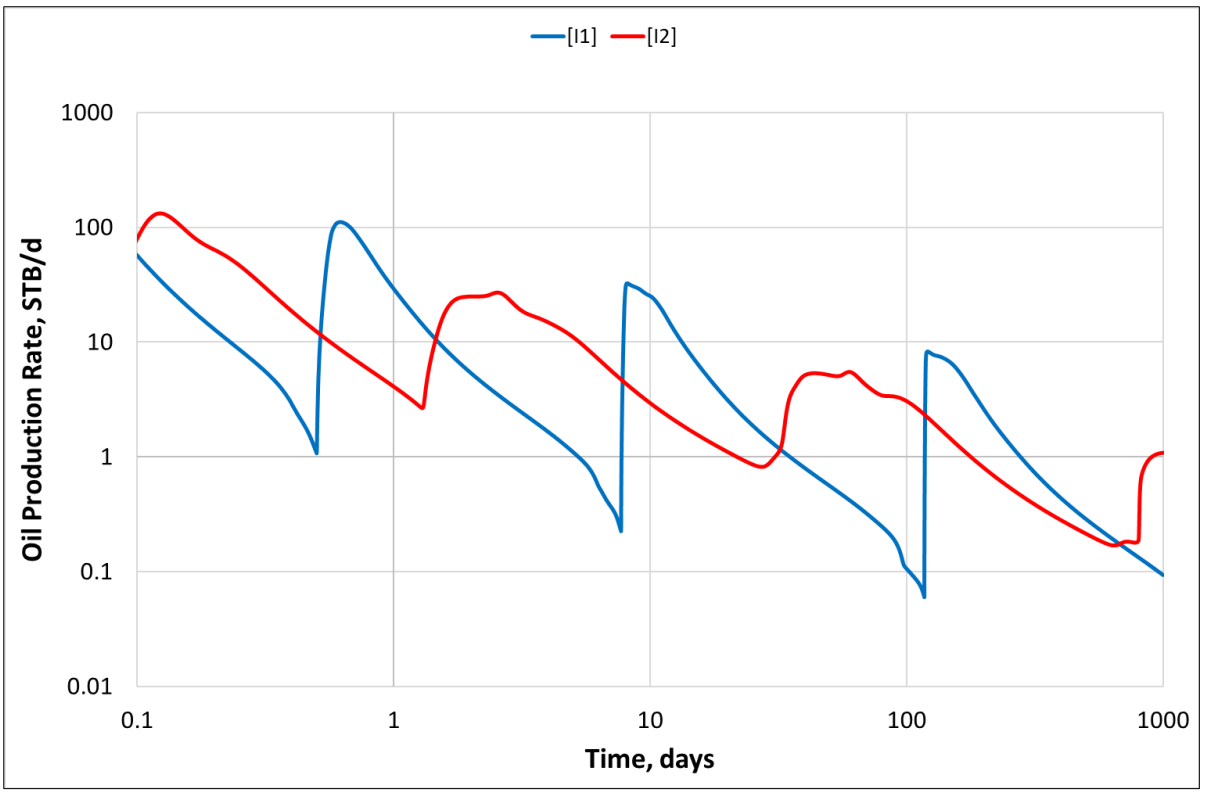

Figure 9.36. Log-log plot for oil production rates for case study I

9.2 Initial Reservoir Fluid Composition

Components	Reservoir Fluid Composition
H_2S	0.0000E+00
N_2	1.6753E-03
CO_2	2.5391E-02
C_1	6.3558E-01
C_2	8.1309E-02
C_3	4.5481E-02
i-C_4	1.0476E-02
n-C_4	1.7867E-02
i-C_5	8.1990E-03
n-C_5	8.7922E-03
C_6	1.2481E-02
C_7	3.1190E-02
C_8	2.6477E-02
C_9	2.0202E-02
C_{10}	1.5827E-02
C_{11}	1.2405E-02
C_{12}	9.7339E-03
C_{13}	7.6482E-03
C_{14}	6.0185E-03
C_{15}	4.7439E-03
C_{16}	3.7459E-03
C_{17}	2.9632E-03
C_{18}	2.3486E-03
C_{19}	1.8651E-03
C_{20}	1.4841E-03
C_{21}	1.1834E-03
C_{22}	9.4551E-04
C_{23}	7.5701E-04
C_{24}	6.0735E-04
C_{25}	4.8827E-04
C_{26+}	2.1123E-03

9.3 EOS Properties

Comp	MW	TC	PC	ZCRIT	SHIFT	AC	PCHOR	OMEGA	OMEGB
H_2S	34.082	672.120	1300.000	0.283	0.102	0.090	80.100	0.427	0.087
N_2	28.014	227.160	492.840	0.292	-0.001	0.037	59.100	0.427	0.087
CO_2	44.010	547.420	1069.500	0.274	0.217	0.225	80.000	0.427	0.087
C_1	16.043	343.010	667.030	0.286	-0.002	0.011	71.000	0.427	0.087
C_2	30.070	549.580	706.620	0.279	0.059	0.099	111.000	0.427	0.087
C_3	44.097	665.690	616.120	0.276	0.091	0.152	151.000	0.427	0.087
i-C_4	58.123	734.130	527.940	0.282	0.110	0.186	188.800	0.427	0.087
n-C_4	58.123	765.220	550.560	0.274	0.110	0.200	191.000	0.427	0.087
i-C_5	72.150	828.700	490.370	0.272	0.098	0.229	227.400	0.427	0.087
n-C_5	72.150	845.460	488.780	0.268	0.119	0.252	231.000	0.427	0.087
C_6	82.422	924.040	489.980	0.249	0.134	0.238	232.810	0.427	0.087
C_7	96.053	990.580	454.180	0.278	0.144	0.274	265.530	0.427	0.087
C_8	108.890	1043.400	421.370	0.271	0.153	0.311	296.330	0.427	0.087
C_9	122.040	1093.500	388.540	0.264	0.170	0.351	327.890	0.427	0.087
C_{10}	134.960	1138.000	360.260	0.258	0.187	0.391	358.900	0.427	0.087
C_{11}	147.800	1178.200	335.580	0.253	0.202	0.431	389.720	0.427	0.087
C_{12}	160.550	1214.900	313.960	0.249	0.217	0.470	420.310	0.427	0.087
C_{13}	173.190	1248.700	294.940	0.245	0.231	0.508	450.670	0.427	0.087
C_{14}	185.740	1279.800	278.130	0.242	0.244	0.546	480.770	0.427	0.087
C_{15}	198.180	1308.700	263.190	0.238	0.256	0.583	510.630	0.427	0.087
C_{16}	210.510	1335.500	249.880	0.236	0.266	0.620	540.220	0.427	0.087
C_{17}	222.730	1360.600	237.950	0.233	0.277	0.655	569.550	0.427	0.087
C_{18}	234.830	1384.100	227.230	0.231	0.286	0.691	598.600	0.427	0.087
C_{19}	246.830	1406.200	217.560	0.229	0.294	0.725	627.390	0.427	0.087
C_{20}	258.710	1427.000	208.810	0.227	0.302	0.759	655.910	0.427	0.087
C_{21}	270.480	1446.700	200.850	0.226	0.309	0.792	684.160	0.427	0.087
C_{22}	282.140	1465.300	193.610	0.224	0.316	0.824	712.140	0.427	0.087
C_{23}	293.690	1483.000	186.980	0.223	0.322	0.856	739.860	0.427	0.087
C_{24}	305.130	1499.800	180.910	0.222	0.327	0.887	767.320	0.427	0.087
C_{25}	316.470	1515.800	175.330	0.221	0.332	0.918	794.520	0.427	0.087
C_{26+}	412.230	1631.400	140.760	0.217	0.360	1.162	1024.300	0.427	0.087

9.4 Binary Interaction Coefficients

0	0	0.08	0.07	0.07	0.06	0.06	0.06	0.06
0.05	0.03	0.03	0.03	0.03	0.03	0.03	0.03	0.03
0.03	0.03	0.03	0.03	0.03	0.03	0.03	0.03	0.03
0.03	0.03	0.03						
0	0.02	0.06	0.08	0.08	0.08	0.08	0.08	0.08
0.08	0.08	0.08	0.08	0.08	0.08	0.08	0.08	0.08
0.08	0.08	0.08	0.08	0.08	0.08	0.08	0.08	0.08
0.08	0.08							
0.12	0.12	0.12	0.12	0.12	0.12	0.12	0.12	0.1
0.1	0.1	0.1	0.1	0.1	0.1	0.1	0.1	0.1
0.1	0.1	0.1	0.1	0.1	0.1	0.1	0.1	0.1
0.1								
0	0	0	0	0	0	0	0	0
0	0	0	0	0	0	0	0	0
0	0	0	0	0	0	0	0	0
0	0	0	0	0	0	0	0	0
0	0	0	0	0	0	0	0	0
0	0	0	0	0	0	0	0	
0	0	0	0	0	0	0	0	0
0	0	0	0	0	0	0	0	0
0	0	0	0	0	0	0		
0	0	0	0	0	0	0	0	0
0	0	0	0	0	0	0	0	0
0	0	0	0	0	0			
0	0	0	0	0	0	0	0	0
0	0	0	0	0	0	0	0	0
0	0	0	0	0				
0	0	0	0	0	0	0	0	0
0	0	0	0	0	0	0	0	0
0	0	0	0					
0	0	0	0	0	0	0	0	0
0	0	0	0	0	0	0	0	0
0	0	0						
0	0	0	0	0	0	0	0	0
0	0	0	0	0	0	0	0	0
0	0							
0	0	0	0	0	0	0	0	0
0	0	0	0	0	0	0	0	0
0								
0	0	0	0	0	0	0	0	0
0	0	0	0	0	0	0	0	0
0	0	0	0	0	0	0	0	0
0	0	0	0	0	0	0	0	
0	0	0	0	0	0	0	0	0
0	0	0	0	0	0	0		
0	0	0	0	0	0	0	0	0
0	0	0	0	0	0			

```
0 0 0 0 0 0 0 0 0
0 0 0 0 0
0 0 0 0 0 0 0 0 0
0 0 0 0
0 0 0 0 0 0 0 0 0
0 0 0
0 0 0 0 0 0 0 0 0
0 0
0 0 0 0 0 0 0 0 0
0
0 0 0 0 0 0 0 0 0
0 0 0 0 0 0 0 0
0 0 0 0 0 0 0
0 0 0 0 0 0
0 0 0 0 0
0 0 0 0
0 0 0
0 0
0
```

9.5 Sensor input files (.dat)

9.5.1 Black oil model input file (.dat)

Note that the input file is for implicit solution. The comments are provided in the model set-up file to switch the solution from implicit to impes solution.

```
TITLE
INCLUDE
Black oil run generated from EOS.
Ultra-tight liquid-rich well performance.
Single fracture segment of total 20 fractures.
ENDTITLE

INCLUDE
Grid-RelPerm.inc
C ------------------------------------------------------------------------
-----------------
C Including black oil table
C ------------------------------------------------------------------------
-----------------
BLACKOIL    1     37    38    SRK
PRESSURES 14.7 100            200            300            400
500            600            700            800            900
1000           1200           1400           1600           1800
2000           2200           2400           2600           2800
3000
3250           3500           3750           4000           4250
4500           4750           5000           5500           6000
7000
8000           9000           10000          12000          14000
16000

RESERVOIR FLUID
INCLUDE
..\comp.inc

SEPARATOR
100   150
14.70 60.0

ENDBLACKOIL

INCLUDE
 ..\eos31.inc

C ------------------------------------------------------------------------
-----------------
C Initialize
C ------------------------------------------------------------------------
-----------------
INITIAL

DEPTH GOR
4625 5000

INCLUDE
well.inc
```

```
C -----------------------------------------------------------------------
-----------------
C Define rate schedules.
C -----------------------------------------------------------------------
-----------------

MAPSPRINT TABLE

C Add CFL 1 for IMPES method
C Comment out IMPLICIT keywork form Grid-RelPerm.inc for impes solution

INCLUDE
..\schedule.inc

END
```

9.5.2 Compositional model input file (.dat)

```
TITLE
INCLUDE
..\Title.inc
ENDTITLE

INCLUDE
..\Grid-RelPerm.inc

INCLUDE
..\eos31.inc

INCLUDE
..\separator.inc

C -----------------------------------------------------------------------
-----------------
C Initialize
C -----------------------------------------------------------------------
-----------------
INITIAL

DEPTH
4625  10000

INCLUDE
..\comp.inc

INCLUDE
..\well.inc

C -----------------------------------------------------------------------
-----------------
C Define rate schedules.
C -----------------------------------------------------------------------
-----------------

INCLUDE
 schedule.inc

END
```

9.6 Include files (.*inc*)

9.6.1 Grid-RelPerm include file (.*inc*)

```
GRID 1001 1 1
PCMULT2 0. 0.
RUN
CPU
IMPLICIT
C Deactivate IMPLICIT keyword for impes method

MAPSPRINT 1 P SO SW KX
MAPSFILE P SW SO SG

C    Bwi cw     denw  visw  cr      pref
MISC 1   3.0E-6 62.4  0.5   4.0E-6  6000

C ------------------------------------------------------------------------
-----------------
C Including grid definition created by SensorGrid
C ------------------------------------------------------------------------
-----------------
INCLUDE
 ..\initial.inc

C ------------------------------------------------------------------------
-----------------
C Relperm
C ------------------------------------------------------------------------
-----------------

KRANALYTICAL 1    ! For matrix
 0.2 0.2 0.2 0.1 ! Swc Sorw Sorg Sgc
 1 1 1           ! krw(Sorw) krg(Swc) kro(Swc)
 2.5 2.5 2.5 2.5  ! nw now ng nog
 -10 10 1. PCGO

 KRANALYTICAL 2   ! For fractures
 0.20 0.2 0.2 0.1 ! Swc Sorw Sorg Sgc
 1 1 1            ! krw(Sorw) krg(Swc) kro(Swc)
 1 1 1 1
 -10 10 1. PCGO   ! pcgo_frac
```

9.6.2 Initial file (.*inc*) for geometric gridding

```
C --------------------------------
C I_CELLS          1001
C J_CELLS          1
C K_CELLS          1
C DEPTH            4500
C SYM_ELEMENTS     2
C FRAC_AREA        37500
C --------------------------------

C ------------------------------------------------------------------------
-----------------
C Cell width along wellbore
C ------------------------------------------------------------------------
-----------------
DELX XVAR
2.43672 2.39713 2.35819 2.31988 2.2822 2.24512 2.20865 2.17277 2.13748
2.10275 2.0686
2.03499 2.00193 1.96941 1.93742 1.90595 1.87499 1.84453 1.81456 1.78509
1.75609
1.72756 1.6995 1.67189 1.64473 1.61801 1.59173 1.56587 1.54043 1.51541
1.49079
1.46657 1.44275 1.41931 1.39626 1.37357 1.35126 1.32931 1.30771 1.28647
1.26557
1.24501 1.22479 1.20489 1.18532 1.16606 1.14712 1.12849 1.11015 1.09212
1.07438
1.05693 1.03976 1.02287 1.00625 0.989903 0.973823 0.958003 0.942441
0.927131 0.91207
0.897253 0.882678 0.868339 0.854233 0.840356 0.826705 0.813275 0.800064
0.787067 0.774281
0.761703 0.749329 0.737157 0.725182 0.713401 0.701812 0.690411 0.679196
0.668162 0.657308
0.64663 0.636126 0.625792 0.615626 0.605626 0.595787 0.586109 0.576588
0.567221 0.558007
0.548942 0.540025 0.531252 0.522622 0.514132 0.50578 0.497564 0.489481
0.48153 0.473707
0.466012 0.458442 0.450994 0.443668 0.436461 0.429371 0.422396 0.415534
0.408784 0.402143
0.39561 0.389184 0.382861 0.376642 0.370523 0.364504 0.358583 0.352758
0.347027 0.34139
0.335844 0.330389 0.325021 0.319742 0.314547 0.309438 0.304411 0.299466
0.294601 0.289815
0.285107 0.280476 0.27592 0.271437 0.267028 0.26269 0.258423 0.254225
0.250095 0.246032
0.242035 0.238104 0.234236 0.230431 0.226687 0.223005 0.219382 0.215818
0.212312 0.208863
0.20547 0.202133 0.198849 0.195619 0.192441 0.189315 0.186239 0.183214
0.180238 0.17731
0.174429 0.171596 0.168808 0.166066 0.163368 0.160715 0.158104 0.155535
0.153009 0.150523
0.148078 0.145672 0.143306 0.140978 0.138688 0.136435 0.134219 0.132038
0.129893 0.127783
0.125707 0.123665 0.121656 0.11968 0.117736 0.115823 0.113942 0.112091
0.11027 0.108479
0.106716 0.104983 0.103277 0.1016 0.0999492 0.0983256 0.0967283 0.095157
0.0936112 0.0920905
0.0905945 0.0891228 0.087675 0.0862508 0.0848496 0.0834713 0.0821153
0.0807814 0.0794691 0.0781781
```

```
0.0769081 0.0756588 0.0744297 0.0732206 0.0720312 0.070861 0.0697099
0.0685775 0.0674635 0.0663675
0.0652894 0.0642288 0.0631854 0.062159 0.0611492 0.0601559 0.0591786
0.0582173 0.0572716 0.0563412
0.055426 0.0545256 0.0536398 0.0527685 0.0519112 0.051068 0.0502384
0.0494223 0.0486194 0.0478296
0.0470526 0.0462882 0.0455363 0.0447966 0.0440689 0.043353 0.0426487
0.0419559 0.0412743 0.0406038
0.0399442 0.0392954 0.038657 0.038029 0.0374113 0.0368035 0.0362057
0.0356175 0.0350389 0.0344697
0.0339098 0.0333589 0.032817 0.0322839 0.0317594 0.0312435 0.030736
0.0302367 0.0297455 0.0292623
0.0287869 0.0283193 0.0278592 0.0274067 0.0269615 0.0265235 0.0260926
0.0256687 0.0252518 0.0248415
0.024438 0.024041 0.0236505 0.0232663 0.0228883 0.0225165 0.0221507
0.0217909 0.0214369 0.0210887
0.0207461 0.0204091 0.0200775 0.0197514 0.0194305 0.0191149 0.0188044
0.0184989 0.0181984 0.0179027
0.0176119 0.0173258 0.0170444 0.0167675 0.0164951 0.0162271 0.0159635
0.0157042 0.0154491 0.0151981
0.0149512 0.0147084 0.0144694 0.0142344 0.0140031 0.0137757 0.0135519
0.0133317 0.0131152 0.0129021
0.0126925 0.0124863 0.0122835 0.0120839 0.0118876 0.0116945 0.0115046
0.0113177 0.0111338 0.0109529
0.010775 0.0106 0.0104278 0.0102584 0.0100917 0.0099278 0.00976653
0.00960787 0.0094518 0.00929825
0.00914721 0.00899861 0.00885243 0.00870862 0.00856715 0.00842798
0.00829107 0.00815639 0.00802389 0.00789354
0.00776531 0.00763917 0.00751507 0.00739299 0.00727289 0.00715474
0.00703852 0.00692418 0.0068117 0.00670104
0.00659218 0.0064851 0.00637975 0.00627611 0.00617416 0.00607386
0.00597519 0.00587812 0.00578263 0.0056887
0.00559629 0.00550537 0.00541594 0.00532796 0.00524141 0.00515626
0.0050725 0.0049901 0.00490904 0.00482929
0.00475084 0.00467366 0.00459774 0.00452305 0.00444957 0.00437729
0.00430618 0.00423623 0.00416741 0.00409972
0.00403312 0.0039676 0.00390315 0.00383974 0.00377737 0.003716 0.00365564
0.00359625 0.00353783 0.00348036
0.00342382 0.0033682 0.00331349 0.00325966 0.00320671 0.00315462
0.00310337 0.00305296 0.00300336 0.00295457
0.00290658 0.00285936 0.00281291 0.00276721 0.00272226 0.00267804
0.00263454 0.00259174 0.00254964 0.00250822
0.00246747 0.00242739 0.00238796 0.00234916 0.002311 0.00227346
0.00223653 0.0022002 0.00216446 0.00212929
0.0020947 0.00206068 0.0020272 0.00199427 0.00196187 0.00193 0.00189865
0.00186781 0.00183747 0.00180762
0.00177825 0.00174936 0.00172095 0.00169299 0.00166549 0.00163843
0.00161182 0.00158563 0.00155987 0.00153453
0.00150961 0.00148508 0.00146096 0.00143723 0.00141388 0.00139091
0.00136831 0.00134609 0.00132422 0.00130271
0.00128155 0.00126073 0.00124025 0.0012201 0.00120028 0.00118078
0.0011616 0.00114273 0.00112417 0.0011059
0.00108794 0.00107027 0.00105288 0.00103578 0.00101895 0.0010024
0.000986113 0.000970094 0.000954335 0.000938832
0.000923581 0.000908578 0.000893818 0.000879298 0.000865014 0.000850962
0.000837139 0.000823539 0.000810161 0.000797
0.000784053 0.000771316 0.000758787 0.00074646 0.000734334 0.000722405
0.00071067 0.000699125 0.000687768
0.0833 0.000687768 0.000699125 0.00071067 0.000722405 0.000734334
0.00074646 0.000758787 0.000771316 0.000784053 0.000797 0.000810161
```

```
0.000823539 0.000837139 0.000850962 0.000865014 0.000879298 0.000893818
0.000908578 0.000923581 0.000938832 0.000954335
0.000970094 0.000986113 0.0010024 0.00101895 0.00103578 0.00105288
0.00107027 0.00108794 0.0011059 0.00112417
0.00114273 0.0011616 0.00118078 0.00120028 0.0012201 0.00124025
0.00126073 0.00128155 0.00130271 0.00132422
0.00134609 0.00136831 0.00139091 0.00141388 0.00143723 0.00146096
0.00148508 0.00150961 0.00153453 0.00155987
0.00158563 0.00161182 0.00163843 0.00166549 0.00169299 0.00172095
0.00174936 0.00177825 0.00180762 0.00183747
0.00186781 0.00189865 0.00193 0.00196187 0.00199427 0.0020272 0.00206068
0.0020947 0.00212929 0.00216446
0.0022002 0.00223653 0.00227346 0.002311 0.00234916 0.00238796 0.00242739
0.00246747 0.00250822 0.00254964
0.00259174 0.00263454 0.00267804 0.00272226 0.00276721 0.00281291
0.00285936 0.00290658 0.00295457 0.00300336
0.00305296 0.00310337 0.00315462 0.00320671 0.00325966 0.00331349
0.0033682 0.00342382 0.00348036 0.00353783
0.00359625 0.00365564 0.003716 0.00377737 0.00383974 0.00390315 0.0039676
0.00403312 0.00409972 0.00416741
0.00423623 0.00430618 0.00437729 0.00444957 0.00452305 0.00459774
0.00467366 0.00475084 0.00482929 0.00490904
0.0049901 0.0050725 0.00515626 0.00524141 0.00532796 0.00541594
0.00550537 0.00559629 0.0056887 0.00578263
0.00587812 0.00597519 0.00607386 0.00617416 0.00627611 0.00637975
0.0064851 0.00659218 0.00670104 0.0068117
0.00692418 0.00703852 0.00715474 0.00727289 0.00739299 0.00751507
0.00763917 0.00776531 0.00789354 0.00802389
0.00815639 0.00829107 0.00842798 0.00856715 0.00870862 0.00885243
0.00899861 0.00914721 0.00929825 0.0094518
0.00960787 0.00976653 0.0099278 0.0100917 0.0102584 0.0104278 0.0106
0.010775 0.0109529 0.0111338
0.0113177 0.0115046 0.0116945 0.0118876 0.0120839 0.0122835 0.0124863
0.0126925 0.0129021 0.0131152
0.0133317 0.0135519 0.0137757 0.0140031 0.0142344 0.0144694 0.0147084
0.0149512 0.0151981 0.0154491
0.0157042 0.0159635 0.0162271 0.0164951 0.0167675 0.0170444 0.0173258
0.0176119 0.0179027 0.0181984
0.0184989 0.0188044 0.0191149 0.0194305 0.0197514 0.0200775 0.0204091
0.0207461 0.0210887 0.0214369
0.0217909 0.0221507 0.0225165 0.0228883 0.0232663 0.0236505 0.024041
0.024438 0.0248415 0.0252518
0.0256687 0.0260926 0.0265235 0.0269615 0.0274067 0.0278592 0.0283193
0.0287869 0.0292623 0.0297455
0.0302367 0.030736 0.0312435 0.0317594 0.0322839 0.032817 0.0333589
0.0339098 0.0344697 0.0350389
0.0356175 0.0362057 0.0368035 0.0374113 0.038029 0.038657 0.0392954
0.0399442 0.0406038 0.0412743
0.0419559 0.0426487 0.043353 0.0440689 0.0447966 0.0455363 0.0462882
0.0470526 0.0478296 0.0486194
0.0494223 0.0502384 0.051068 0.0519112 0.0527685 0.0536398 0.0545256
0.055426 0.0563412 0.0572716
0.0582173 0.0591786 0.0601559 0.0611492 0.062159 0.0631854 0.0642288
0.0652894 0.0663675 0.0674635
0.0685775 0.0697099 0.070861 0.0720312 0.0732206 0.0744297 0.0756588
0.0769081 0.0781781 0.0794691
0.0807814 0.0821153 0.0834713 0.0848496 0.0862508 0.087675 0.0891228
0.0905945 0.0920905 0.0936112
0.095157 0.0967283 0.0983256 0.0999492 0.1016 0.103277 0.104983 0.106716
0.108479 0.11027
```

```
0.112091 0.113942 0.115823 0.117736 0.11968 0.121656 0.123665 0.125707
0.127783 0.129893
0.132038 0.134219 0.136435 0.138688 0.140978 0.143306 0.145672 0.148078
0.150523 0.153009
0.155535 0.158104 0.160715 0.163368 0.166066 0.168808 0.171596 0.174429
0.17731 0.180238
0.183214 0.186239 0.189315 0.192441 0.195619 0.198849 0.202133 0.20547
0.208863 0.212312
0.215818 0.219382 0.223005 0.226687 0.230431 0.234236 0.238104 0.242035
0.246032 0.250095
0.254225 0.258423 0.26269 0.267028 0.271437 0.27592 0.280476 0.285107
0.289815 0.294601
0.299466 0.304411 0.309438 0.314547 0.319742 0.325021 0.330389 0.335844
0.34139 0.347027
0.352758 0.358583 0.364504 0.370523 0.376642 0.382861 0.389184 0.39561
0.402143 0.408784
0.415534 0.422396 0.429371 0.436461 0.443668 0.450994 0.458442 0.466012
0.473707 0.48153
0.489481 0.497564 0.50578 0.514132 0.522622 0.531252 0.540025 0.548942
0.558007 0.567221
0.576588 0.586109 0.595787 0.605626 0.615626 0.625792 0.636126 0.64663
0.657308 0.668162
0.679196 0.690411 0.701812 0.713401 0.725182 0.737157 0.749329 0.761703
0.774281 0.787067
0.800064 0.813275 0.826705 0.840356 0.854233 0.868339 0.882678 0.897253
0.91207 0.927131
0.942441 0.958003 0.973823 0.989903 1.00625 1.02287 1.03976 1.05693
1.07438 1.09212
1.11015 1.12849 1.14712 1.16606 1.18532 1.20489 1.22479 1.24501 1.26557
1.28647
1.30771 1.32931 1.35126 1.37357 1.39626 1.41931 1.44275 1.46657 1.49079
1.51541
1.54043 1.56587 1.59173 1.61801 1.64473 1.67189 1.6995 1.72756 1.75609
1.78509
1.81456 1.84453 1.87499 1.90595 1.93742 1.96941 2.00193 2.03499 2.0686
2.10275
2.13748 2.17277 2.20865 2.24512 2.2822 2.31988 2.35819 2.39713 2.43672

C ------------------------------------------------------------------------
-----------------
C Cell width away from wellbore
C ------------------------------------------------------------------------
-----------------
DELY YVAR
150.002

C ------------------------------------------------------------------------
-----------------
C Porosity
C ------------------------------------------------------------------------
-----------------
POROS CON
 0.05

MOD
501 501 1 1 1 1 = 0.0405319

C ------------------------------------------------------------------------
-----------------
C Rocktype (for relperm curves)
```

```
C ------------------------------------------------------------------------
-----------------
ROCKTYPE CON
 1

MOD
501 501 1 1 1 1 = 2

C ------------------------------------------------------------------------
-----------------
C Permeability
C ------------------------------------------------------------------------
-----------------
KX CON
 0.0001

MOD
501 501 1 1 1 1 = 12004.8

KY EQUALS KX
KZ EQUALS KX

C ------------------------------------------------------------------------
-----------------
C Depth
C ------------------------------------------------------------------------
-----------------
DEPTH CON
 4500

C ------------------------------------------------------------------------
-----------------
C Thickness
C ------------------------------------------------------------------------
-----------------
THICKNESS CON
 250
```

9.6.3 Initial file (.*inc*) for equal-size gridding

```
C ---------------------------------
C I_CELLS          10001
C J_CELLS          1
C K_CELLS          1
C DEPTH            4500
C SYM_ELEMENTS     2
C FRAC_AREA        37500
C ---------------------------------

C ------------------------------------------------------------------------
-----------------
C Cell width along wellbore
C ------------------------------------------------------------------------
-----------------
DELX XVAR
      10001*0.029997
C      Nx    *(Nx*300/Nx)
C Use the formula above when changing the grid cells
C ------------------------------------------------------------------------
C Cell width away from wellbore
C ------------------------------------------------------------------------
DELY YVAR
150.002

C ------------------------------------------------------------------------
-----------------
C Porosity
C ------------------------------------------------------------------------
-----------------
POROS CON
 0.05

C Fracture cell is not 3000 -> needs to be modified for grid cells of
10001 when fracture properties are added

C MOD
C 3000 3000 1 1 1 1 = 0.0405319

C ------------------------------------------------------------------------
-----------------
C Rocktype (for relperm curves)
C ------------------------------------------------------------------------
-----------------
ROCKTYPE CON
 1

C MOD
C 3000 3000 1 1 1 1 = 2

C ------------------------------------------------------------------------
-----------------
C Permeability
C ------------------------------------------------------------------------
-----------------
KX CON
 0.0001

C MOD
```

```
C 3000 3000 1 1 1 1 = 12004.8

KY EQUALS KX
KZ EQUALS KX

C ------------------------------------------------------------------------
-----------------
C Depth
C ------------------------------------------------------------------------
-----------------
DEPTH CON
 4500

C ------------------------------------------------------------------------
-----------------
C Thickness
C ------------------------------------------------------------------------
-----------------
THICKNESS CON
 250
```

9.6.4 Composition include file (.*inc*)

```
C -- Initial Reservoir Composition
C -- Initial Reservoir Composition
0.00000000
0.00167534
0.02539132
0.63558246
0.08130903
0.04548081
0.01047610
0.01786676
0.00819902
0.00879218
0.01248101
0.03118978
0.02647679
0.02020222
0.01582676
0.01240528
0.00973391
0.00764815
0.00601851
0.00474393
0.00374585
0.00296320
0.00234856
0.00186508
0.00148411
0.00118336
0.00094551
0.00075701
0.00060735
0.00048827
0.00211233
```

9.6.5 EOS include file (.*inc*)

```
C Fluid Properties
C ===============================================================================
PVTEOS SRK
250    ! Reservoir temperature (deg F)
CPT          MW           TC           PC           ZCRIT        SHIFT
AC           PCHOR        OMEGA        OMEGB
   H2S        34.082       672.12        1300         0.28292      0.10153
0.09         80.1         0.42748      0.08664
   N2         28.014       227.16        492.84       0.29178      -0.0009
0.037        59.1         0.42748      0.08664
   CO2        44.01        547.42        1069.5       0.27433      0.21749
0.225        80           0.42748      0.08664
   C1         16.043       343.01        667.03       0.2862       -0.00247
0.011        71           0.42748      0.08664
   C2         30.07        549.58        706.62       0.27924      0.05894
0.099        111          0.42748      0.08664
   C3         44.097       665.69        616.12       0.2763       0.09075
0.152        151          0.42748      0.08664
   I-C4       58.123       734.13        527.94       0.28199      0.10952
0.186        188.8        0.42748      0.08664
   N-C4       58.123       765.22        550.56       0.27385      0.11028
0.2          191          0.42748      0.08664
   I-C5       72.15        828.7         490.37       0.27231      0.09773
0.229        227.4        0.42748      0.08664
   N-C5       72.15        845.46        488.78       0.26837      0.11947
0.252        231          0.42748      0.08664
   C6         82.422       924.04        489.98       0.24891      0.13417
0.23825      232.81       0.42748      0.08664
   C7         96.053       990.58        454.18       0.27786      0.14355
0.27411      265.53       0.42748      0.08664
   C8         108.89       1043.4        421.37       0.27121      0.15263
0.31051      296.33       0.42748      0.08664
   C9         122.04       1093.5        388.54       0.26407      0.17011
0.35127      327.89       0.42748      0.08664
   C10        134.96       1138          360.26       0.25826      0.18663
0.39131      358.9        0.42748      0.08664
   C11        147.8        1178.2        335.58       0.25328      0.20229
0.43091      389.72       0.42748      0.08664
   C12        160.55       1214.9        313.96       0.24891      0.21703
0.46995      420.31       0.42748      0.08664
   C13        173.19       1248.7        294.94       0.24504      0.2308
0.50837      450.67       0.42748      0.08664
   C14        185.74       1279.8        278.13       0.24158      0.24362
0.54615      480.77       0.42748      0.08664
   C15        198.18       1308.7        263.19       0.23847      0.25551
0.58326      510.63       0.42748      0.08664
   C16        210.51       1335.5        249.88       0.23569      0.26648
0.61969      540.22       0.42748      0.08664
   C17        222.73       1360.6        237.95       0.2332       0.27659
0.65545      569.55       0.42748      0.08664
   C18        234.83       1384.1        227.23       0.23096      0.28589
0.69052      598.6        0.42748      0.08664
   C19        246.83       1406.2        217.56       0.22896      0.29442
0.72492      627.39       0.42748      0.08664
   C20        258.71       1427          208.81       0.22717      0.30224
0.75865      655.91       0.42748      0.08664
   C21        270.48       1446.7        200.85       0.22558      0.3094
0.79172      684.16       0.42748      0.08664
```

```
   C22        282.14      1465.3      193.61      0.22418     0.31594
0.82413     712.14      0.42748     0.08664
   C23        293.69      1483        186.98      0.22293     0.32191
0.8559      739.86      0.42748     0.08664
   C24        305.13      1499.8      180.91      0.22184     0.32736
0.88704     767.32      0.42748     0.08664
   C25        316.47      1515.8      175.33      0.2209      0.33233
0.91755     794.52      0.42748     0.08664
   C26+       412.23      1631.4      140.76      0.21709     0.36046
1.1619      1024.3      0.42748     0.08664
BIN
0           0           0.08        0.07        0.07        0.06
0.06        0.06        0.06
0.05        0.03        0.03        0.03        0.03        0.03
0.03        0.03        0.03
0.03        0.03        0.03        0.03        0.03        0.03
0.03        0.03        0.03
0.03        0.03        0.03
0           0.02        0.06        0.08        0.08        0.08
0.08        0.08        0.08
0.08        0.08        0.08        0.08        0.08        0.08
0.08        0.08        0.08
0.08        0.08        0.08        0.08        0.08        0.08
0.08        0.08        0.08
0.08        0.08
0.12        0.12        0.12        0.12        0.12        0.12
0.12        0.12        0.1
0.1         0.1         0.1         0.1         0.1         0.1
0.1         0.1         0.1
0.1         0.1         0.1         0.1         0.1         0.1
0.1         0.1         0.1
0.1
0           0           0           0           0           0           0
0           0
0           0           0           0           0           0           0
0           0
0           0           0           0           0           0           0
0           0
0           0           0           0           0           0           0
0           0
0           0           0           0           0           0           0
0           0
0           0           0           0           0           0           0
0
0           0           0           0           0           0           0
0           0
0           0           0           0           0           0           0
0           0
0           0           0           0           0           0           0
0           0           0           0           0           0           0
0           0
0           0           0           0           0           0           0
0           0
0           0           0           0           0           0
0           0           0           0           0           0           0
0           0
0           0           0           0           0           0           0
0           0
0           0           0           0           0
```

0 0 0 0 0 0 0
0 0
0 0 0 0 0 0 0
0 0
0 0 0 0
0 0 0 0 0 0 0
0 0
0 0 0 0 0 0 0
0 0
0 0 0
0 0 0 0 0 0 0
0 0
0 0 0 0 0 0 0
0 0
0 0
0 0 0 0 0 0 0
0 0
0 0 0 0 0 0 0
0 0
0
0 0 0 0 0 0 0
0 0
0 0 0 0 0 0 0
0 0
0 0 0 0 0 0 0
0 0
0 0 0 0 0 0 0
0
0 0 0 0 0 0 0
0 0
0 0 0 0 0 0 0
0 0 0 0 0 0 0
0 0
0 0 0 0 0 0
0 0 0 0 0 0 0
0 0
0 0 0 0 0
0 0 0 0 0 0 0
0 0
0 0 0 0
0 0 0 0 0 0 0
0 0
0 0 0
0 0 0 0 0 0 0
0 0
0 0
0 0 0 0 0 0 0
0
0 0 0 0 0 0 0
0 0
0 0 0 0 0 0 0
0
0 0 0 0 0 0 0
0 0 0 0 0
0 0 0 0 0
0 0 0 0
0 0 0
0 0
0

9.6.6 Well include file (.*inc*)

```
GOC 4625
PINIT 4500

ENDINIT
C -------------------------------------------------------------------------
-----------------
C Include recurrent data generated by SensorGrid (perforations and TZ
modifiers)
C -------------------------------------------------------------------------
-----------------
INCLUDE
..\recurrent.inc

C EXPLICIT WELL
C Add the keyword for explicit well treatment

BHP
 PROD 1000

SKIP
THP
 PROD 100 -2
SKIPEND

WELLTYPE
 PROD MCF

PSM

MAPSFREQ 20
MAPSFILEFREQ 20
DT 0.001
DTMAX 1
```

9.6.7 Recurrent include file with user defined PI (.*inc*)

```
C --------------------------------
C Trans. modification to fractures
C --------------------------------
MODIFY TX 1.0
 500 500 1 1 1 1 * 0.999983
 501 501 1 1 1 1 * 0.999983

C --------------------------------
C Define Wells
C --------------------------------
WELL
        I J  K   PI
 PROD   501 1 1   100
 INJ    501 1 1   100
```

9.6.8 Recurrent include file (.inc) with Surface label

```
C ---------------------------------
C Trans. modification to fractures
C ---------------------------------
MODIFY TX 1.0
 2999 2999 1 1 1 1 * 0.999983
 3000 3000 1 1 1 1 * 0.999983

C ---------------------------------
C Define Wells
C ---------------------------------
WELL SURFACE
        I J  K
 PROD   -3000 1 1
 INJ    -3000 1 1
```

9.6.9 Schedule include file (.inc)

```
WELLTYPE
 PROD MCF
RATE
 PROD  100000 !

DT 0.001
DTMAX 0.001
TIME 0.1
DTMAX 0.01
TIME 1
DTMAX 0.01
TIME 10
DTMAX 0.1
TIME 100
DTMAX 1
TIME 1000
END
```

Rashad Nazaraliyev

NTNU
Norwegian University of
Science and Technology